A NOVEL STRESS ANALYSIS METHOD FOR LAMINATED COMPOSITE STIFFENER WITH ASYMMETRIC Z-SECTION UNDER MECHANICAL AND THERMAL LOADING CONDITIONS

By

SIDHANT SINGH

THESIS

Presented to the Faculty of the Graduate School of

The University of Texas at Arlington in Partial Fulfillment

of the Requirements for the Degree of

MASTER OF SCIENCE IN AEROSPACE ENGINEERING

THE UNIVERSITY OF TEXAS AT ARLINGTON

August 2016

To my dear father, mother and brother

for their love throughout my life

ACKNOWLEDGEMENTS

I would like express my gratitude to Dr. Wen S Chan, my research advisor for his academic and professional guidance, patience, support and encouragement. I learned a lot from him as a person and as a student. I will always admire him for his organized and hardworking personality.

Next, I would like to thank HLAENGINEERS, INC. for giving me the opportunity to work and learn as an intern at the company. I would also like to thank Dr. Dipen Shah for his help and advice which helped me reinforce my fundamentals of FEA and ANSYS™.

Additionally, I would like to appreciate my friends; Abhyudaya, Abhishek, Ashish, Gaurav, Manish and Karan for their friendship and support.

Finally, I sincerely thank and dedicate this work to my Dad - Khel Singh, my lovely Mom - Babita Singh and my Brother - Shourya Singh for their unconditional love, support and sacrifices.

August 07, 2016

ABSTRACT

A NOVEL STRESS ANALYSIS METHOD FOR LAMINATED COMPOSITE STIFFENER WITH ASYMMETRIC Z-SECTION UNDER MECHANICAL AND THERMAL LOADING CONDITIONS.

Sidhant Singh, M.S.

The University of Texas at Arlington, 2016

Supervising Professor: Dr. Wen S Chan

Composites structures are being used as load carrying members in latest aircrafts and performance automobiles, the design validation for such structures can be a time consuming and expensive process, if done by testing. Validation of a structure by analysis saves time and money for a design process and validation by analysis can be done by comparing the analytical solution with the finite element analysis of the structure, which requires availability of analytical expressions for every cross-sectional arrangement of the structural members.

This research focuses on stress analysis of laminated composite stiffener with asymmetric Z-sections, where closed form analytical expressions are developed to determine the sectional properties of composite Z stiffener. The equations for sectional properties such as centroid, equivalent axial stiffness and equivalent bending stiffness are validated by comparing the analytical and finite element analysis results. The effects of different temperature gradients on different sections of the composite Z stiffener are also studied and equations are developed and validated for temperature induced moments in the stiffener. The sectional properties were used to calculate stresses in layer of sub-laminates and are compared with the stresses obtained from finite element analysis of the beam under same conditions. A finite element model is developed on academic version of software ANSYS 16.0 and ANSYS 17.0 classic. The stress and strain results obtained by analytical method shows excellent agreement with the results obtained from finite element analysis.

Table of Contents

Chapter 1 1
INTRODUCTION 1
1.1 Composite Materials Overview 1
1.1.1 Definition 1
1.1.2 Advantages and Disadvantages 1
1.2 Literature Review 3
1.3 Aim of the Research 5
1.4 Outline of Thesis 5
Chapter 2 6
REVIEW OF CONSTITUTIVE EQUATIONS OF COMPOSITE LAMINATED PLATE AND BEAM 6
2.1 Laminate Co-ordinate System 6
2.2 Lamina Constitutive Equation 7
2.2.1 Stress-Strain Relation for 0^0 Lamina 7
2.2.2 Stress-Strain Relation for θ^0 Lamina 8
2.3 Laminate Constitutive Equation: Classical Laminated Plate Theory (CLPT): 9
2.3.1 Displacement Field of Laminate 10
2.3.2 Lamina Stress/Strain Relationship in Laminate Coordinates 11
2.3.3 Force and Moment Resultants of Laminate 12
2.3.4 Constitutive Equation of Laminate 14
2.4 Thermal Loads 16
2.5 Laminated Beam 20
2.5.1 Constitutive Equation of Narrow Laminated Beam under Bending 20
2.5.2 Wide Beam 22
Chapter 3 23
CONSTITUTIVE EQUATIONS OF LAMINATED Z-BEAM 23
3.1 Geometry and Notation of Composite Z-Beam 23
3.2 Constitutive Equation of Beam Structure 24
3.3 Location of Centroid 25
3.3.1 Isotropic Material Centroid 25
3.3.2 Composite Material Centroid 25
3.4 Equivalent Axial Stiffness 27
3.4.1 Constitutive Equation for Sub-laminates 27

3.4.2 Expression for Axial Stiffness 27
3.5 Equivalent Bending Stiffness 29
3.5.1 Expression for Chord Bending Stiffness Dz 29
3.5.2 Expression for Bending Stiffness Dy 34
3.5.3 Stresses in Layers of Flange Sub-laminates 37
3.5.4 Stresses in Layers of Web Sub-laminate 39
3.6 Temperature Effects 40
3.6.1 Temperature Induced Bending Moments 40
3.6.2 Temperature Effects on Isotropic Material Beams 41
3.6.3 Temperature effects on Composite Beam 42
3.6.4 Temperature Induced Bending Moment 43
3.6.5 Stresses in Layers of Sub-laminates by Temperature Induced Moments. 44
Chapter 4 45
FINITE ELEMENT ANALYSIS 45
4.1 Material Properties 45
4.2 Model Geometry and Stacking Sequence 45
4.3 Modeling 46
4.4 Model Validation 49
4.4.1 Axial Stiffness 49
4.4.2 Bending Stiffness 50
4.5 Thermal Model Validation 55
4.5.1 Thermal Model Description 55
4.5.2 Validation of Temperature Induced Moment Model 55
Chapter 5 57
RESULTS AND DISCUSSIONS 57
5.1 Material and Stacking Sequence 57
5.2 Centroid Locations for Results Comparison Cases 59
5.3 Results Comparison for Axial Stiffness 60
5.4 Results Comparison for Bending Stiffness 61
5.5 Results Comparison for Thermal Moments 77
5.5.1 Thermal moment comparison 77
Chapter 6 CONCLUSION AND FUTURE WORK 84
Appendix A 86

METHOD TO CALCULATE RADIUS OF CURVATURE FROM FINITE ELEMENT ANALYSIS 86
Appendix B 89
ANSYS INPUT FILE FOR FINITE ELEMENT MODEL AND ANALYSIS 89
Appendix C 100
MATLAB CODE FOR ANALYTICAL SOLUTION 100
REFERENCES 110

LIST OF ILLUSTRATIONS

Figure Page

Figure 2.1 Local and Global co-ordinate system in lamina 6

Figure 2.2 Composite laminate before and after deformation 10

Figure 2.3 In-plane forces acting on the reference plane (left), the moment and transverse shear forces (right) 12

Figure 2.4 Multidirectional laminate with notation of individual plies 12

Figure 2.5 Deformed shape of narrow vs. wide beam 20

Figure 3.1 Geometry of Z-beam. 24

Figure 3.2 Distances between the reference axes and centroids of the sections. 26

Figure 3.3 Location of section centroids with respect to the beam centroid. 29

Figure 3.4 Local and global co-ordinate systems. 32

Figure 3.5 Temperature induced moments in an isotropic Z beam 40

Figure 3.6 Temperature induced forces and their locations on cross-section of Z-beam 42

Figure 4.1: Meshed and layered asymmetric Z-Beam in ANSYS™ 46

Figure 4.2: Cross-section of the beam showing nodes, centroidal node encircled in red. 47

Figure 4.3: Nodes on both ends connected/coupled to the centroidal node. 48

Figure 4.4: Forces and Boundary conditions applied on centroidal nodes. 51

Figure 4.5: Moment applied by equal and opposite forces. 52

Figure 4.6: Temperature gradients in sections for model validation. 56

LIST OF TABLES

Table Page

Table 4-1 Comparison of axial stiffness calculated from three different methods. 50

Table 4-2 Comparison of bending stiffness obtained from mechanics theory and present method..... 54

Table 4-3 Comparison of bending curvatures obtained from mechanics theory, present method and finite element analysis. 54

Table 4-4 Comparison of moments obtained from FEA and equations for isotropic beam. 56

Table 5-1 Results comparison cases and stacking sequence 58

Table 5-2 Centroid locations for result cases 59

Table 5-3 Axial Stiffness Comparison 60

Table 5-4 Bending Stiffness and curvature values 62

Table 5-5 Bending Stiffness Curvature Comparison for applied $\bar{M}yc$. 63

Table 5-6 Bending Stiffness Curvature Comparison for applied $\bar{M}zc$. 64

Table 5-7 Bending Stiffness Stress Comparison for case 1 – Top Flange 65

Table 5-8 Bending Stiffness Stress Comparison for case 1 – Bottom Flange 66

Table 5-9 Bending Stiffness Stress Comparison for case 1 – Web 67

Table 5-10 Bending Stiffness Stress Comparison for case 2 – Top Flange 68

Table 5-11 Bending Stiffness Stress Comparison for case 2 – Bottom Flange 69

Table 5-12 Bending Stiffness Stress Comparison for case 2 – Web 70

Table 5-13 Bending Stiffness Stress Comparison for case 3– Top Flange 72

Table 5-14 Bending Stiffness Stress Comparison for Case 3– Bottom Flange 73

Table 5-15 Bending Stiffness Stress Comparison for Case 4– Top Flange 74

Table 5-16 Bending Stiffness Stress Comparison for Case 4– Bottom Flange 75

Table 5-17 Bending Stiffness Stress Comparison for case 4 – Web 76

Table 5-18 Result comparison cases for thermal analysis 77

Table 5-19 Thermal moment comparison – Case 1 77

Table 5-20 Thermal Stress Comparison for Case 1 – Top Flange 78

Table 5-21 Thermal Stress Comparison for Case 1 – Bottom Flange 79

Table 5-22 Thermal Stress Comparison for Case 1 – Web 80

Table 5-23 Thermal moment comparison – Case 2 80

Table 5-24 Thermal Stress Comparison for Case 2– Top Flange 81

Table 5-25 Stress Comparison for thermal Case 2 – Bottom Flange 82

Table 5-26 Thermal Stress Comparison for Case 2 – Web 83

LIST OF GRAPHS

Graph Page

Graph 5-1: Comparison of Bending Curvatures for applied moment $\bar{M}yc$. 63

Graph 5-2: Comparison of Bending Curvatures for applied moment $\bar{M}zc$..... 64

Graph 5-3: Comparison of Stresses in layers of top-flange sub-laminate for case 1..... 67

Graph 5-4: Comparison of Stresses in layers of bottom-flange sub-laminate for case 2. 71

Graph 5-5: Comparison stresses in layers of web sub-laminate case 4..... 76

Graph 5-6: Comparison of Stresses in layers of top-flange for thermal case 2. 83

Chapter 1

INTRODUCTION

1.1 Composite Materials Overview

1.1.1 Definition

A structural composite is a material system consisting of two or more phases on a macroscopic scale, whose mechanical performance and properties are designed to be superior to those of the constituent materials acting independently. One phase is stiffer and stronger, used as the reinforcement, whereas the less stiff phase is used as the matrix.

1.1.2 Advantages and Disadvantages

The main advantages of composite materials are: low density, high specific stiffness (modulus to density ratio), and high specific strength (strength to density ratio). The higher specific stiffness and strength are the main reason of selecting composites for aircraft structures. However, there are many other advantages that have been driven into consideration of using composites materials in structural applications: corrosion resistance, long fatigue life, wear resistance, favorable life cycle cost, low thermal expansion, thermal insulation and conductivity, acoustic insulation, and design flexibility.

Some disadvantages of laminated composites are: relative low toughness, low impact resistance, intolerant to out-of-the-plane loads, sensitive to temperature and moisture conditions, requirement of sophisticated nondestructive techniques for detection and monitoring of damage growth, multiple failure modes, and more complex analysis to study them.

Composite material has been widely used these days. Besides using in the aerospace industry about more than 40 years ago, composites are now being used in almost every industry.

Composites find applications in performance motorbikes, bicycles, cars, robotic structures, wind mills, solar panels, aircrafts, spacecraft structures, railcars, rail engines, fishing rods and even used in fabrication of lightweight mobile phone covers.

Composite beams are fabricated as an assembly of flat layers; every layer can have different directional arrangement of the fibers. This enables the designers to alter the physical properties of the beams by varying the layer stacking sequence and fiber orientation angles during designing and fabrication phase, which cannot be achieved by using metals. In composite structural applications, thin-walled composite beam has been used as direct load carrying members and as stiffeners in panel construction. Beams are structural members that carry bending loads and have one dimension (length) larger than the other two dimensions (width and height). The beam requires one dimensional property. However, composites are inherent of two dimensional properties in the fiber and transverse to fiber directions. This property of composite beams also makes it difficult to obtain the analytical solution for designing phase, because unlike metal beams composite beams exhibit different physical properties in every direction and they also vary with layer arrangement as explained previously.

This makes design validation of a composite part an expensive and time consuming process, because the part has to be verified by testing and not by analysis. Testing of every new part raises the time and money involved in the process exponentially, and to avoid this, design and analysis software which use finite element methods are used in the industry as they can analyze complex structures with high accuracy. However, the accuracy of the finite element based solution depends on factors like mesh quality and applied boundary conditions, where an incorrect model will result in meaningless solution. Furthermore, using finite element method for structural analysis is not an efficient method for optimal design process and is also a time consuming process because of structural configuration dependence.

1.2 Literature Review

In engineering analysis, composite beams are often analyzed using smeared property approach for computing their sectional properties. The smeared approach does not consider the effect of un-symmetrical structure in determining the sectional properties. Composite Z-beam is similar to a composite I-beam from analysis point of view, and as there is a lot of research work done on the composite I-beam, research articles related to the I-beam were considered during this research. Craddock and Yen [1] obtained equivalent bending stiffness for symmetric I- beam by using smear property. Lee [2] combined the classical lamination theory with the Vlasov and Gjelsivk theory of thin walled elastic beam to obtain the closed form solution for center of gravity and shear-center of thin walled open sections. The method is applicable to mono symmetric cross-section as well as any arbitrary layup.

Parambil et al.[3] and Sanghavi and Chan [4] developed the closed form solution for finding the ply stresses in the composite I beam under axial, bending and torsion loads applied at the centroid/shear center of the beam. They also determine the equivalent axial and bending stiffness and the centroid location for the composite I beam and validated all the results using the finite element analysis.

Gupta and Rao [5] studied the instability of laminated composite open section beams and also covered a composite Z-beam problem in their study. Chandra and Chopra [6] developed an analytical solution based on Vlasov's theory to study the static structural response of composite I-Beam with elastic couplings subjected to bending and torsional load by neglecting the shear deformation. Barbero et al. [7] in an attempt to predict a design optimization approach for different shapes presented derivation on Mechanics of thin-walled Laminated Beams (MLB) for open and closed sections. They presented the example of laminated I-beam and developed the deflection equation for cantilevered beam by using the laminate smear property. The tip deflection equation incorporated the effects of shear deformation by including a shear correction factor term in the equation. However, the bending stiffness term was direct reciprocal of compliance matrix. Therefore, the bending stiffness only represented the smeared material property of the laminate. Jung and Lee [8] presented a study on the static response and

performed a closed form analysis of thin walled composite I-beams. The analysis included the non-classical effects such as elastic coupling, shell wall thickness, transverse shear deformation, torsion warping, and constrained warping. The closed form solution was derived for both symmetric and asymmetric layup configurations for a cantilever beam subjected to unit bending or torque load at the tip of the beam. In addition, 2D finite element model was developed to validate the results obtained from the closed form solution. They concluded that transverse shear deformation influences the structural behavior of composite beams in terms of slenderness ratio and layup.

Chan and Chou [9] developed a closed form for axial and bending stiffness that included the coupling effect due to both laminate and structural configurations. Later, Chan and his students focused on thin-walled beams for various cross sections. In one of the study, Chan and Dermirhan [10] developed a closed form solution for calculating the bending stiffness of composite tubular beam including fiber variation due the circumference of tube. Their study indicated that the significant difference in evaluating bending stiffness by using the material property of laminate smear method, plate and shell approaches. Later, Rojas and Chan [11] in a study integrated an analysis of laminates including calculation of structural section properties, failure prediction, and analysis of composite laminated beams. Syed and Chan [12] obtained a closed expression for computing centroid location, axial and, bending stiffness as well as shear center of hat-section composite beam. Most recently, Rios [13] presented a unified analysis of stiffener reinforced composite beams. The study presented a general analytical method to study the structural response of composite laminated beams.

1.3 Aim of the Research

The objective of this research is to develop an analytical method to conduct stress analysis of a composite Z-beam with uneven flanges and with an arbitrary layup under mechanical and thermal loads. The research covers closed form expressions of sectional properties such as centroid, axial and bending stiffness of the Z-beam as well as ply stresses. Finite element analysis is also conducted to validate the developed analytical expressions.

1.4 Outline of Thesis

Chapter 2 briefly reviews stress/strain relationship in lamina and laminate and Classical Lamination Theory (CLT) which depicts the constitutive equations of laminated plates. Extension of laminated plate theory to laminated beam is included accompanying to the introduction of the concept of narrow and wide beams.

Chapter 3 explains the geometry of the composite Z-beam with unsymmetrical Z cross section and covers the derivations of the analytical equations developed to calculate the sectional properties of a composite beam with Z cross-section.

Chapter 4 describes the development of finite element model including meshing, boundary condition, and applied loads.

Chapter 5 includes the validation of analytical methods by comparing with FEM results. The result of sectional properties such as centroid, shear center, axial and bending stiffness is presented in this chapter.

Chapter 6 concludes of the research and explains the future work of the research.

Chapter 2

REVIEW OF CONSTITUTIVE EQUATIONS OF COMPOSITE LAMINATED PLATE AND BEAM

The chapter reviews the stress/strain relationship of lamina and laminates under mechanical and thermal loads. The Classical Laminated Plate Theory (CLPT) is briefly introduced. Extension of this theory to analyze laminated beam is also illustrated. In this process, the structural characteristic of wide beam versus narrow beam is presented. This chapter presented all of the fundamental equations used for the analysis of composite Z-Beam. These fundamental equations were taken from Ref. [14].

2.1 Laminate Co-ordinate System

A laminate is made up of perfectly bonded layers of lamina with different fiber orientation and is usually loaded in one plane. Two co-ordinate systems as shown in Figure 2.1 are used to describe the properties of the lamina.

- 1-2-3 co-ordinates refer to the lamina's local co-ordinate system, where 1 is the fiber direction, 2 is the transverse direction and 3 is perpendicular to the ply plane.
- x-y-z co-ordinate system are the global co-ordinate system and are selected at the mid-plane of laminates.

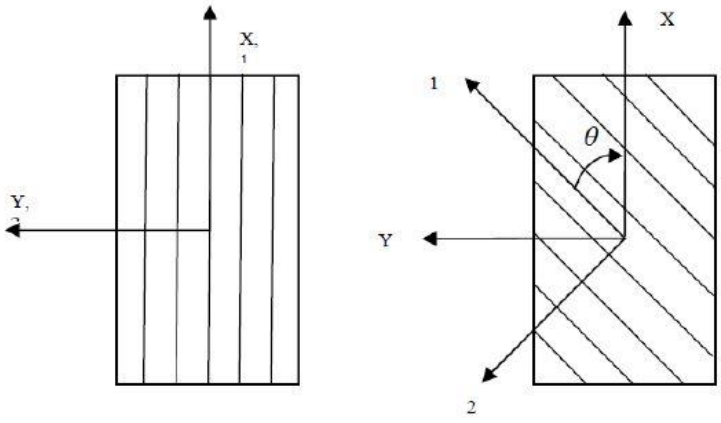

Figure 2.1 Local and Global co-ordinate system in lamina

2.2 Lamina Constitutive Equation

2.2.1 Stress-Strain Relation for 0^0 Lamina

Since composite lamina is thin, a state of plane stress is assumed for the analysis purpose.

$$\sigma_3 = \tau_{13} = \tau_{23} = 0 \tag{2.1}$$

Therefore, orthotropic stress strain relation can be written in matrix form for a composite lamina. The strain-stress relation is given below.

$$[\varepsilon]_{1-2} = [S]_{1-2}[\sigma]_{1-2} \tag{2.2}$$

$$\begin{bmatrix} \varepsilon_1 \\ \varepsilon_2 \\ \gamma_{12} \end{bmatrix} = \begin{bmatrix} S_{11} & S_{12} & 0 \\ S_{12} & S_{22} & 0 \\ 0 & 0 & S_{66} \end{bmatrix} \begin{bmatrix} \sigma_1 \\ \sigma_2 \\ \tau_{12} \end{bmatrix} \tag{2.3}$$

And the stress-strain relationship is

$$\begin{bmatrix} \sigma_1 \\ \sigma_2 \\ \tau_{12} \end{bmatrix} = \begin{bmatrix} Q_{11} & Q_{12} & 0 \\ Q_{12} & Q_{22} & 0 \\ 0 & 0 & Q_{66} \end{bmatrix} \begin{bmatrix} \varepsilon_1 \\ \varepsilon_2 \\ \gamma_{12} \end{bmatrix} \tag{2.4}$$

Where,

$\varepsilon_1 and\ \varepsilon_2$ are strains in the 1 and 2 directions, respectively

γ_{12} is shear strain in 1-2 plane

$[S]_{1-2}$ is compliance matrix of the order 3 x 3 in 1-2 co-ordinate system

$[Q]_{1-2}$ is stiffness matrix of the order 3 x 3 in 1-2 co-ordinate system

$$S_{11} = \frac{1}{E_1};\ S_{22} = \frac{1}{E_2};\ S_{12} = -\frac{\upsilon_{12}}{E_1} = -\frac{\upsilon_{21}}{E_2};\ S_{66} = \frac{1}{G_{12}}$$

$$Q_{11} = \frac{E_1}{1-\upsilon_{12}\upsilon_{21}};\quad Q_{22} = \frac{E_2}{1-\upsilon_{12}\upsilon_{21}} \tag{2.5}$$

$$Q_{12} = \frac{\upsilon_{21}E_1}{1-\upsilon_{12}\upsilon_{21}} = \frac{\upsilon_{12}E_2}{1-\upsilon_{12}\upsilon_{21}};\ Q_{66} = G_{12}$$

where $E_1, E_2, \upsilon_{12}, and\ G_{12}$ are four independent material constants.

2.2.2 Stress-Strain Relation for θ^0 Lamina

The laminate global(x-y) co-ordinate system is not coincident with the laminas local (1-2) co-ordinate system. A relation between the stress and strain components in local (1-2) system and global(x-y) system is given in this section.

The compliance matrices for x-y co-ordinate system and 1-2 co-ordinate system are related as:

$$[\bar{S}]_{x-y} = [T_\varepsilon(-\theta)][S]_{1-2}[T_\sigma(\theta)] = [T_\sigma(\theta)]^T[S]_{1-2}[T_\sigma(\theta)] \quad (2.6)$$

The stiffness matrices for x-y co-ordinate system and 1-2 co-ordinate system are related as:

$$[\bar{Q}]_{x-y} = [T_\sigma(-\theta)][Q]_{1-2}[T_\varepsilon(\theta)] = [T_\varepsilon(\theta)]^T[S]_{1-2}[T_\varepsilon(\theta)] \quad (2.7)$$

Where,

$[\bar{S}]_{x-y}$ is compliance matrix for x-y co-ordinate system

$[\bar{Q}]_{x-y}$ is reduced stiffness matrix for x-y co-ordinate system

The matrices $[T_\varepsilon(\theta)]$ and $[T_\sigma(\theta)]$ are the transformation matrices for strain and stress, respectively and are given as.

$$[T_\varepsilon(\theta)] = \begin{bmatrix} m^2 & n^2 & mn \\ n^2 & m^2 & -mn \\ -2mn & 2mn & m^2 - n^2 \end{bmatrix} \quad (2.8)$$

$$[T_\sigma(\theta)] = \begin{bmatrix} m^2 & n^2 & 2mn \\ n^2 & m^2 & -2mn \\ -mn & mn & m^2 - n^2 \end{bmatrix} \quad (2.9)$$

where $m = cos\theta$; $n = sin\theta$,and θ is fiber orientation with respect to the x-axis

Hence, the stress-strain relationship for angled ply with θ degree fiber orientation in x-y coordinate system is,

$$\begin{bmatrix}\sigma_x\\ \sigma_y\\ \tau_{xy}\end{bmatrix} = \begin{bmatrix}\bar{Q}_{11} & \bar{Q}_{12} & \bar{Q}_{16}\\ \bar{Q}_{12} & \bar{Q}_{22} & \bar{Q}_{26}\\ \bar{Q}_{16} & \bar{Q}_{26} & \bar{Q}_{66}\end{bmatrix}\begin{bmatrix}\varepsilon_x\\ \varepsilon_y\\ \gamma_{xy}\end{bmatrix} \quad (2.10)$$

Or

$$[\sigma]_{x-y} = \left[\bar{\mathrm{Q}}\right]_{x-y}[\varepsilon]_{x-y} \quad (2.11)$$

2.3 Laminate Constitutive Equation: Classical Laminated Plate Theory (CLPT):

Classical lamination theory is commonly used to analyze the behavior of laminated composite to evaluate stresses and strains in individual plies in the laminate. The theory explained in this section also incorporates the effects of temperature.

Following are the assumptions for the classical lamination theory:

1. Each Layer of the laminate is quasi-homogeneous and orthotropic.
2. The laminate is thin with its lateral dimensions much larger than its thickness and is loaded in its plane only, i.e., the laminate and its layer (except for their edges) are in a state of plane stress.
3. All displacements are small compared with the thickness of the laminate.
4. Displacements are continuous throughout the laminate.
5. In-plane displacements vary linearly through the thickness of the laminate, i.e., u and v displacements in the x and y directions are linear functions of z.
6. Transverse shear strain γ_{xz} and γ_{yz} are negligible. This assumption and the preceding one imply that straight lines normal to the middle surface remain straight and normal to that surface after deformation.
7. Strain-displacement and stress-strain relations are linear.
8. Normal distances from the middle surface remain constant, i.e., the transverse normal strain ε_z is negligible.

2.3.1 Displacement Field of Laminate

The reference plane of laminated plate is located at the mid-plane of the plate as shown in the above figure. The mid plane displacements are assumed to be

$$u_0 = u_0(x,y);\ v_0 = v_0(x,y);\ w_0 = w_0(x,y) \tag{2.12}$$

The displacements at any point shown in Figure 2.2 are given as

$$u(x,y,z) = u_0 - z\frac{\partial w_0}{\partial x}\ ; v(x,y,z) = v_0 - z\frac{\partial w_0}{\partial y} \tag{2.13}$$

Where z is the co-ordinate variable of a general point of the cross section. For small displacements, the classical strain-displacement relations of elasticity yields,

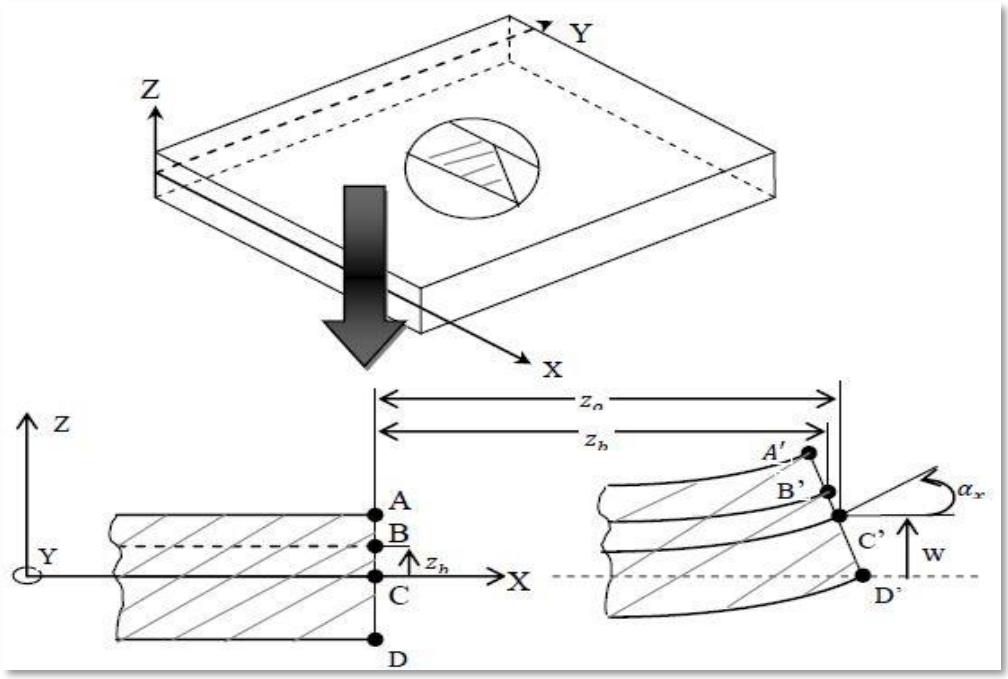

Figure 2.2 Composite laminate before and after deformation

$$\varepsilon_x = \frac{\partial u}{\partial x} = \frac{\partial u_0}{\partial x} - z\frac{\partial^2 w}{\partial x^2}$$
$$\varepsilon_y = \frac{\partial v}{\partial y} = \frac{\partial v_0}{\partial y} - z\frac{\partial^2 w}{\partial y^2} \quad (2.14)$$
$$\gamma_{xy} = \frac{\partial u}{\partial y} + \frac{\partial v}{\partial x} = \frac{\partial u_0}{\partial y} + \frac{\partial v_0}{\partial x} - 2z\frac{\partial^2 w}{\partial x \partial y}$$

The strain components on the reference plane are expressed as:

$$\varepsilon_x^0 = \frac{\partial u_0}{\partial x}\ ;\ \varepsilon_y^0 = \frac{\partial v_0}{\partial y};\ \gamma_{xy}^0 = \frac{\partial u_0}{\partial y} + \frac{\partial v_0}{\partial x} \quad (2.15)$$

The curvatures of the laminate are given as:

$$\kappa_x = -\frac{\partial^2 w}{\partial x^2}\ ;\ \kappa_y = -\frac{\partial^2 w}{\partial y^2}\ ;\ \kappa_{xy} = -2\frac{\partial^2 w}{\partial x \partial y} \quad (2.16)$$

2.3.2 Lamina Stress/Strain Relationship in Laminate Coordinates

The strains in the k[th] layer can be related to mid-plane strains and curvatures as shown below:

$$[\varepsilon_{x-y}]_K = [\varepsilon^0] + z_k[K]$$
$$\begin{bmatrix}\varepsilon_x \\ \varepsilon_y \\ \gamma_{xy}\end{bmatrix}_k = \begin{bmatrix}\varepsilon_x^0 \\ \varepsilon_y^0 \\ \gamma_{xy}^0\end{bmatrix} + z_k\begin{bmatrix}\kappa_x \\ \kappa_y \\ \kappa_{xy}\end{bmatrix} \quad (2.17)$$

The stresses of the k[th] layer in the laminate can be written as:

$$[\sigma_{x-y}]_{k^{th}} = \left[\bar{Q}_{x-y}\right]_{k^{th}}[\varepsilon_{x-y}]_{k^{th}} \quad (2.18)$$

Which can also be written as,

$$[\sigma_{x-y}]_{k^{th}} = \left[\bar{Q}_{x-y}\right]_{k^{th}}([\varepsilon^0{}_{x-y}] + z_{k^{th}}[\kappa_{x-y}]) \quad (2.19)$$

2.3.3 Force and Moment Resultants of Laminate

The following figures will be used to explain the equations in this section.

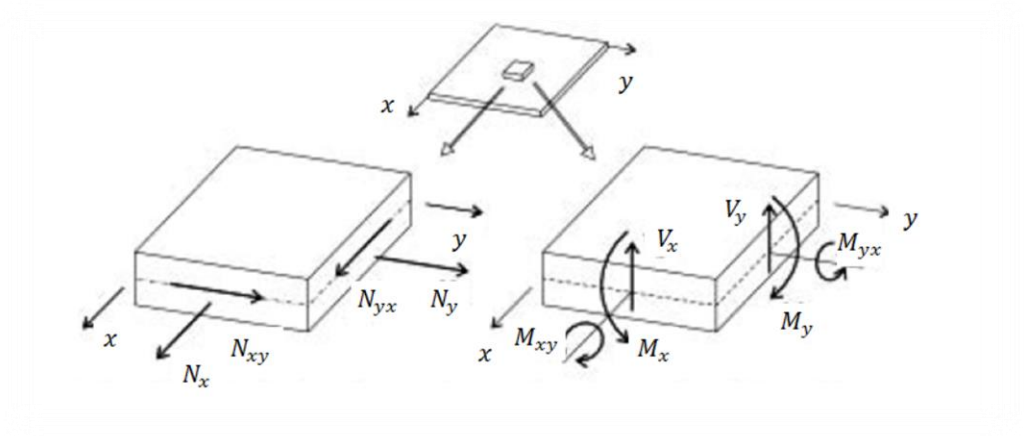

Figure 2.3 In-plane forces acting on the reference plane (left), the moment and transverse shear forces (right)

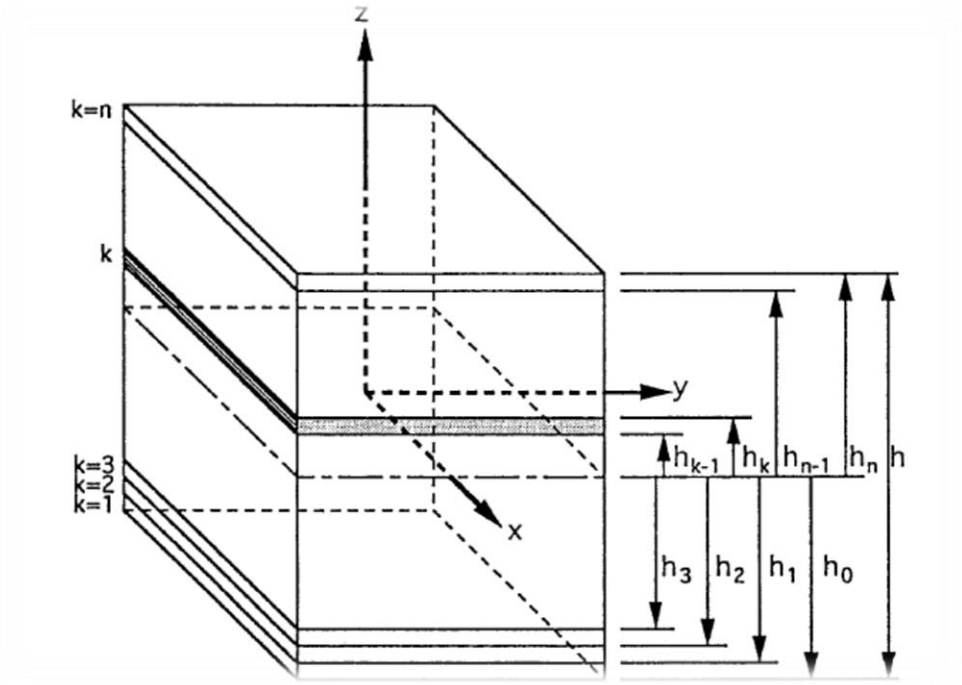

Figure 2.4 Multidirectional laminate with notation of individual plies

The sum of forces and moments in each layer shown in Figs. 2.4 and 2.5 is given as:

$$\begin{bmatrix} N_x \\ N_y \\ N_{xy} \end{bmatrix} = \sum_{k=1}^{n} \int_{h_{k-1}}^{h_k} \begin{bmatrix} \sigma_x \\ \sigma_y \\ \tau_{xy} \end{bmatrix}_k dz \ (\frac{lb}{in}) \tag{2.20}$$

$$\begin{bmatrix} M_x \\ M_y \\ M_{xy} \end{bmatrix} = \sum_{k=1}^{n} \int_{h_{k-1}}^{h_k} \begin{bmatrix} \sigma_x \\ \sigma_y \\ \tau_{xy} \end{bmatrix}_k z dz \ (\frac{lb.in}{in}) \tag{2.21}$$

Where,

z = the co-ordinate variable of a point on laminate cross section

t = layer thickness

N_x , N_y = normal forces per unit length

N_{xy} = shear forces per unit length

M_x , M_y = bending moments per unit length

M_{xy} = twisting moments per unit length

2.3.4 Constitutive Equation of Laminate

Substituting Eq. 2.19 into Eq. 2-20 and 2-21, we obtain Eq. 2-22.

$$\begin{bmatrix} N \\ M \end{bmatrix} = \begin{bmatrix} A & B \\ B & D \end{bmatrix} \begin{bmatrix} \varepsilon^0 \\ k \end{bmatrix} \tag{2.22}$$

$$\begin{bmatrix} N_x \\ N_y \\ N_{xy} \\ M_x \\ M_y \\ M_{xy} \end{bmatrix} = \begin{bmatrix} A_{11} & A_{12} & A_{16} & B_{11} & B_{12} & B_{16} \\ A_{12} & A_{22} & A_{26} & B_{12} & B_{22} & B_{26} \\ A_{16} & A_{26} & A_{66} & B_{16} & B_{26} & B_{66} \\ B_{11} & B_{12} & B_{16} & D_{11} & D_{12} & D_{16} \\ B_{12} & B_{22} & B_{26} & D_{12} & D_{22} & D_{26} \\ B_{16} & B_{26} & B_{66} & D_{16} & D_{26} & D_{66} \end{bmatrix} \begin{bmatrix} \varepsilon_x^0 \\ \varepsilon_y^0 \\ \gamma_{xy}^0 \\ \kappa_x \\ \kappa_y \\ \kappa_{xy} \end{bmatrix} \tag{2.23}$$

$$\begin{aligned} [A] &= \sum_{k=1}^{n} \left[\overline{\mathrm{Q}}_{x-y}\right]_{k^{th}} (h_k - h_{k-1}) \\ [B] &= \frac{1}{2} \sum_{k=1}^{n} \left[\overline{\mathrm{Q}}_{x-y}\right]_{k^{th}} (h_k^2 - h_{k-1}^2) \\ [D] &= \frac{1}{3} \sum_{k=1}^{n} \left[\overline{\mathrm{Q}}_{x-y}\right]_{k^{th}} (h_k^3 - h_{k-1}^3) \end{aligned} \tag{2.24}$$

Inverting Eq. 2.22, we have

$$\begin{bmatrix} \varepsilon^0 \\ k \end{bmatrix} = \begin{bmatrix} a & b \\ b^T & d \end{bmatrix} \begin{bmatrix} N \\ M \end{bmatrix} \tag{2.25}$$

Where,

$$\begin{bmatrix} a & b \\ b^T & d \end{bmatrix} = \begin{bmatrix} A & B \\ B & D \end{bmatrix}^{-1} \tag{2.26}$$

It should be noted that b matrix may or may not be symmetric.

[A] matrix is called in-plane extensional stiffness matrix because it directly relates in-plane strains $(\varepsilon_x^0, \varepsilon_y^0, \gamma_{xy}^0)$ to in-plane forces per unit width (N_x, N_y, N_{xy}) . A_{11} and A_{22} are called the axial extension stiffness, A_{12} is the stiffness due to Poisson's ratio effect, A_{16} and A_{26} are the stiffness due to shear coupling, and A_{66} is the shear stiffness.

[B] matrix is known as extensional-bending coupling stiffness matrix. This matrix relates in-plane strains to bending moments and curvatures to in-plane forces. This coupling effect does not exist for isotropic materials. Thus, if Bij≠0, in-plane forces produce flexural and twisting deformation in addition to in-plane deformation; moments as well produce extensional and shear deformation of the middle surface in addition to flexural and twisting deformation. B_{11} and B_{22} are the coupling stiffness due to direct curvature, B_{12} is the coupling stiffness due to Poisson's ratio effect, B_{16} and B_{26} are the extension-twisting coupling stiffness or shear bending coupling stiffness, and B_{66} is the shear-twisting coupling stiffness.

[D] matrix is the bending stiffness matrix because it relates curvatures $(\kappa_x, \kappa_y, \kappa_{xy})$ to bending moments per unit width (M_x, M_y, M_{xy}) . D_{11} and D_{22} are the bending stiffness, D_{12} is the bending stiffness due to Poisson's ratio effect, D_{16} and D_{26} are the bending-twisting coupling, and D_{66} is the torsional stiffness.

2.4 Thermal Loads

The behavior of composite changes under different environmental conditions such as different temperature and moisture contents. The change of the structural behavior due to these effects depends on coefficient of thermal expansion (CTE) and coefficient of moisture expansion (CHE). It has been observed that the characteristics of the change of structural response due to temperature is similar to the change due to the moisture. Hence, the equations used for evaluating the structure response due to temperature can also be used for that due to the moisture.

For an orthotropic material thermal strain is written as the equation shown below.

$$\varepsilon_i^T = \alpha_i \, \Delta T \tag{2.27}$$

Where

α_i is the coefficient of thermal expansion.

i = 1,2,3 represents normal component of thermal strain

ΔT is the temperature gradient.

It is noted that no shear strains are induced when an orthotropic material is experienced in temperature environment. This gives

$$\gamma_{12}^T = \gamma_{13}^T = \gamma_{23}^T = 0 \tag{2.28}$$

For a ply under both mechanical and thermal loads, the total ply strain can be expressed as

$$\varepsilon_1 = \frac{1}{E_1}[\sigma_1 - \nu_{12}\sigma_2] + \alpha_1 \, \Delta T$$

$$\varepsilon_2 = \frac{1}{E_2}[\sigma_2 - \nu_{21}\sigma_1] + \alpha_2 \, \Delta T \tag{2.29}$$

$$\gamma_{12} = \frac{\tau_{12}}{G_{12}}$$

Where

ε_1 and ε_2 are strains in local 1 and 2 directions respectively

σ_1 and σ_2 are stresses in corresponding local directions of ply

E_1 and E_2 are modulus in their respective local directions

α_1 and α_2 are CTE's in corresponding local directions of ply

The above equation can be written in the matrix form as.

$$\begin{bmatrix} \varepsilon_1 \\ \varepsilon_2 \\ \gamma_{12} \end{bmatrix}_{total} = [S_{1-2}] \begin{bmatrix} \sigma_1 \\ \sigma_2 \\ \tau_{12} \end{bmatrix} + \begin{bmatrix} \alpha_1 \\ \alpha_2 \\ 0 \end{bmatrix} \Delta T \tag{2.30}$$

Using equation 2.7 for axes transformation, strain in x-y co-ordinate system are given as

$$\left[\varepsilon_{x-y}\right]_K = [T_\varepsilon(-\theta)]_K \, [\varepsilon_{1-2}]_K \tag{2.31}$$

Where

$\left[\varepsilon_{x-y}\right]_K$ are the strains in K_{th} layer in global(x-y) co-ordinate system.

$[\varepsilon_{1-2}]_K$ are the strains in K_{th} layer in local(1-2) co-ordinate system.

The transformation of thermal strains from local to global co-ordinate system is given by following equation.

$$\left[\alpha_{x-y}\right]_K = [T_\varepsilon(-\theta)]_K \, [\alpha_{1-2}]_K \tag{2.32}$$

Total strains in global co-ordinate system including the thermal strains can be written as.

$$\left[\varepsilon_{x-y}\right]_{K,total} = \left[\bar{S}_{x-y}\right]_K \left[\sigma_{x-y}\right]_K + \left[\alpha_{x-y}\right]_K \Delta T \tag{2.33}$$

Where

$$\left[\bar{S}_{x-y}\right] = [T_\sigma(\theta)]^T [S_{1-2}][T_\sigma(\theta)] \tag{2.34}$$

Rearranging Equation 2.33

$$\left[\sigma_{x-y}\right]_K = \left[\overline{Q}_{x-y}\right]_K \{\left[\varepsilon_{x-y}\right]_{K,total} - \left[\alpha_{x-y}\right]_K \Delta T\} \quad (2.35)$$

Expanding the global strains $\left[\varepsilon_{x-y}\right]$, by using Equation 2.17 and rewriting Equation 2.33.

$$\left[\sigma_{x-y}\right]_K = [Q]_K \{[\varepsilon^0] + z[\kappa] - \left[\alpha_{x-y}\right]_K \Delta T\} \quad (2.36)$$

By summing up the forces from the ply stresses, we get the following equation.

$$[N] = \sum_{K=1}^{n} \int_{h_{k-1}}^{h_k} \left[\sigma_{x-y}\right]_K dz = \left\{\sum_{K=1}^{n} \int_{h_{k-1}}^{h_k} [\bar{Q}]_K \, dz\right\} \left[\varepsilon^0\right] + \left\{\sum_{K=1}^{n} \int_{h_{k-1}}^{h_k} [\bar{Q}]_K \, z dz\right\} [\kappa] - \left\{\sum_{K=1}^{n} \int_{h_{k-1}}^{h_k} [\bar{Q}]_K \left[\alpha_{x-y}\right]_K dz\right\} \Delta T \quad (2.37)$$

From Equation 2.22, the above equation can be written as.

$$[N] = [A]\left[\varepsilon^0\right] + [B][\kappa] - [N^T] \quad (2.38)$$

Where

$[N]$ is the total force matrix.

[A] gives in-plane extensional stiffness matrix.

[B] is extensional-bending coupling stiffness matrix.

$[\kappa]$ represents the mid-plane curvatures.

$\left[\varepsilon^0\right]$ is the mid-plane strain matrix.

$[N^T]$ is the force due to temperature, and is given by the expression below.

$$[N^T] = \left\{ \sum_{K=1}^{n} \int_{h_{k-1}}^{h_k} [\bar{Q}]_K \left[\alpha_{x-y}\right]_K dz \right\} \Delta T \tag{2.39}$$

The moment induced because of temperature can be obtained similarly and is given by the following expression.

$$[M^T] = \left\{ \sum_{K=1}^{n} \int_{h_{k-1}}^{h_k} [\bar{Q}]_K \left[\alpha_{x-y}\right]_K z dz \right\} \Delta T \tag{2.40}$$

The Equation 2.22, of the force and moment matrices obtained in the lamination theory can be modified to include the temperature induced forces and moments.

Now, the total force and moment matrices are given as.

$$\begin{aligned} [\bar{N}] &= [A]\left[\varepsilon^0\right] + [B][\kappa] \\ [\bar{M}] &= [B]\left[\varepsilon^0\right] + [D][\kappa] \end{aligned} \tag{2.41}$$

Where

$$\begin{aligned} [\bar{N}] &= [N] + [N^T] \\ [\bar{M}] &= [M] + [M^T] \end{aligned} \tag{2.42}$$

Where

$[\bar{N}]$ is the total force matrix, which includes thermal and mechanical forces.

$[\bar{M}]$ is the total moment matrix, which includes thermal and mechanical moments.

Equation 2.41 describes the laminate constitutive equation of laminate under mechanical and thermal load environment. If the moisture environment is present, additional moisture induced load can be superimposed into the above equation. The expression of the moisture induced load will be identical to the thermal induced load except replacing the α-matrix by the β-matrix.

It should be noted that the above equation is valid for the composite material properties remain constants under the environmental condition.

2.5 Laminated Beam

The foundation of beam analysis is based upon the one-dimensional moment-curvature relationship along the longitudinal axis of the beam under bending. This approach used for laminated composite beam is not different from the isotropic beam. However, evaluation of this relationship depends on the sectional properties which possess a unique behavior that is different from the isotropic beam. These properties are not only dependent of geometry of the cross-section but also of the composite material property and their stacking sequence of laminate as well.

Analysis of a beam structure which is one-dimensional problem requires for inputting one dimensional structural property in its constitutive equation. However, composite material is inherent with two-dimensional property. Hence, an equivalent one-dimensional property of composite beam is needed. The equivalent one-dimensional property is dependent of the structural response of the deformed beam and the structural response of the beam is dependent on the ratio of the width to height of the beam cross-section. The following describes those behaviors.

2.5.1 Constitutive Equation of Narrow Laminated Beam under Bending

Figure 2.6 shows a sketch of structural response of a beam under bending. As shown in the figure, if the width to height ratio of the cross section is small (namely "narrow beam", the lateral curvature is induced due to the effect of Poisson's ratio. Conversely, the induced lateral curvature is negligible except at the neighborhood of the laminate edge (namely "wide beam"), if the width to height ratio is large. Hence, the response of structure beam exhibits $M_y \neq 0$ and $K_y = 0$ for a wide beam and $M_y = 0$ and $K_y \neq 0$ for a narrow beam.

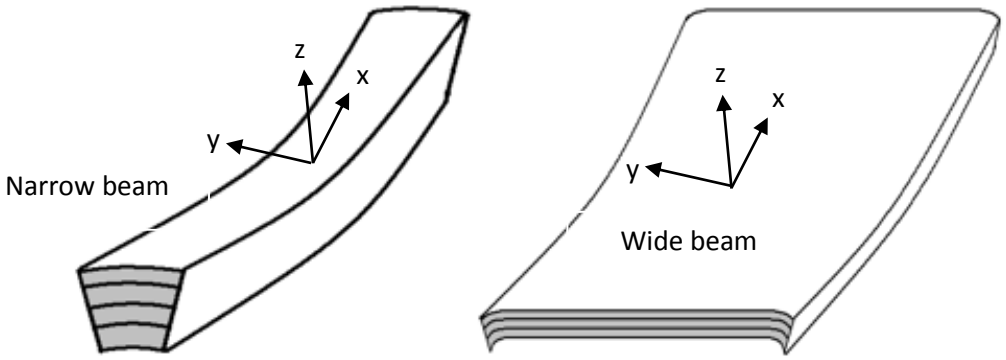

Figure 2.5 Deformed shape of narrow vs. wide beam

Moreover, if the width of the flange laminate is much smaller than the height (depth) of the beam. The flange will have refrain from its twisting. With this in mind, a further assumption of zero K_{xy} is enforced in deriving the beam's constitutive equation.

$$N_x \neq 0, N_y = 0,\ N_{xy} = 0, \qquad M_x \neq 0, M_y = 0, M_{xy} \neq 0$$
$$\varepsilon_x^0 \neq 0, \varepsilon_y^0 \neq 0, \gamma_{xy}^0 \neq 0, K_x \neq 0, K_y \neq 0, K_{xy} = 0 \tag{2.43}$$

With the above assumption, the constitutive equation for a narrow beam can be written as a pseudo-one dimensional relationship below [3]:

$$\begin{pmatrix} \varepsilon_x^o \\ K_x \end{pmatrix} = \begin{pmatrix} a_{11} & b_{11} \\ b_{11} & d_{11} \end{pmatrix} \begin{pmatrix} N_x \\ M_x \end{pmatrix}$$
$$\begin{pmatrix} N_x \\ M_x \end{pmatrix} = \begin{pmatrix} A_1^* & B_1^* \\ B_1^* & D_1^* \end{pmatrix} \begin{pmatrix} \varepsilon_x^o \\ K_x \end{pmatrix} \begin{bmatrix} \varepsilon_x^o \\ K_x \end{bmatrix} \tag{2.44}$$

And

$$\begin{bmatrix} A_1^* & B_1^* \\ B_1^* & D_1^* \end{bmatrix} = \begin{bmatrix} a^* & b^* \\ b^* & d^* \end{bmatrix}^{-1} \tag{2.45}$$

Where,

$$a^* = a_{11} - \frac{b_{16}^2}{d_{66}},\ b^* = b_{11} - \frac{b_{16} d_{16}}{d_{66}}$$
$$d^* = d_{11} - \frac{d_{16}^2}{d_{66}} \tag{2.46}$$

ε_x^0 and κ_x are the mid-plane strain and curvature along the longitudinal axis of the beam, A_1^*, B_1^*, and D_1^* refer to the axial, coupling and bending stiffness and a^*, b^* and d^* are the compliance, coupling and flexibility components of narrow laminate, respectively. The matrices of a, b and d are the conventional laminated plate properties.

2.5.2 Wide Beam

Opposite to a narrow beam, wide beam acting essentially as a plate does not show distortion of the cross-section except at the outer edges (See Fig. 2.5). As a result of this, its curvatures κ_y and κ_{xy} are restrained.

Substituting $\varepsilon_y^o = \gamma_{xy}^o = \kappa_y = \kappa_{xy} = 0$ in laminate constitutive equation, we obtain,

$$\begin{bmatrix} N_x \\ M_x \end{bmatrix} = \begin{bmatrix} A_{11} & B_{11} \\ B_{11} & D_{11} \end{bmatrix} \begin{bmatrix} \varepsilon_x^o \\ K_x \end{bmatrix} \tag{2.47}$$

It should remind that the non-zero terms, N_y, N_{xy}, M_y, and M_{xy}, are induced due to strains and curvatures restrained. Rearranging the above equation, we relate the axial force per unit width to the corresponding axial strain and the bending moment to the corresponding curvature, directly. We obtain

$$N_x = \left(A_{11} - \frac{B_{11}^2}{D_{11}} \right) \cdot \varepsilon_x^0 \quad \text{and} \quad M_x = \left(D_{11} - \frac{B_{11}^2}{A_{11}} \right) \cdot \kappa_x \tag{2.48}$$

Chapter 3

CONSTITUTIVE EQUATIONS OF LAMINATED Z-BEAM

This chapter covers derivations of the analytical equations to determine the sectional properties of Z-beam. The laminate constitutive equation of narrow beam, Eq. (2-44) is selected because of it's the width and the height ratio of the beam. The closed-form expression of sectional property such as centroid, axial and bending stiffness are included. Equations for calculating the ply stresses of Z-beam under mechanical and thermal load are also presented.

3.1 Geometry and Notation of Composite Z-Beam

Figure 3.1 shows the geometry of the Z-beam, which is divided into three parts (laminates), the top and bottom flanges and the web laminates, which are denoted by f1, f2 and w, respectively. W and h are designated for the width and thickness of the corresponding laminate. It is noted that the height and width of the web are actually the width and thickness of the web laminate, respectively. Hence, W_w and h_w represent the width and thickness of the web laminate. W_{f1} and $W_{f2,}$ and h_{f1} and h_{f2} represent the width and thickness of the top and bottom flange laminates, respectively.

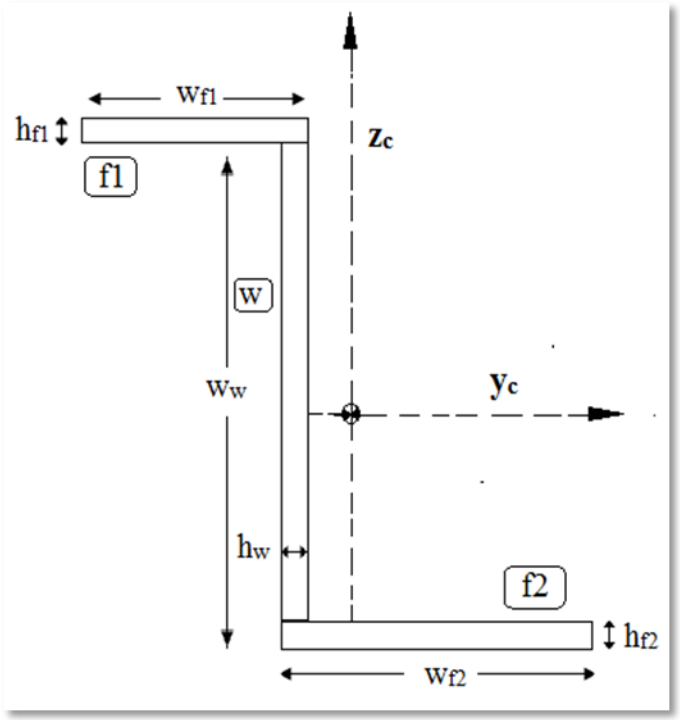

Figure 3.1 Geometry of Z-beam.

3.2 Constitutive Equation of Beam Structure

For a beam under axial load in the x-direction and beam bending, $\bar{M}_y$ and chord bending, $\bar{M}_z$ with respect to z-axis at its centroid the characteristic equation of beam under loads can be written as:

$$\begin{bmatrix} \bar{N}_x \\ \bar{M}_y \\ \bar{M}_z \end{bmatrix} = \begin{bmatrix} \overline{EA} & 0 & 0 \\ 0 & \bar{D}_y & \bar{D}_{yz} \\ 0 & \bar{D}_{yz} & \bar{D}_z \end{bmatrix} \begin{bmatrix} \varepsilon_x^c \\ \kappa_y^c \\ \kappa_z^c \end{bmatrix} \tag{3.1}$$

Where $\overline{EA}$, $\bar{D}_y$, $\bar{D}_z, and\ \bar{D}_{xz}$ are the corresponding axial and bending stiffness and the corresponding axial strain at the mid-plane of i-th laminate can be expressed as.

$$\varepsilon_{x,i}^o = \varepsilon_x^c + z_{i,c}\kappa_y^c + y_{i,c}\kappa_z^c \tag{3.2}$$

Where, $z_{i,c}$ and $y_{i,c}$ are the distance from the midpoint of i-th laminate to the centroid location.

3.3 Location of Centroid

The location of the centroid for a given cross-section is the point where the induced moment is balanced when an axial load in applied or vice versa. Hence, the centroid of a cross-section area refers to the geometric center of the area only if the material is symmetrically distributed in the entire area. Moreover, the centroid is a location on the cross-section of a beam where the structural response due to axial and bending loads is decoupled. This states that if an axial load is applied at the centroid, it will result in axial strain only. Conversely, if bending moment is applied at the centroid, the beam exhibits curvature deformation with no axial strain.

3.3.1 Isotropic Material Centroid

For Isotropic materials, the centroid depends only on geometrical parameters. The equations to determine the centroid location for isotropic materials are described below.

$$y_c = \frac{\sum y_i A_i}{\sum A_i} \quad \text{and} \quad z_c = \frac{\sum z_i A_i}{\sum A_i} \tag{3.3}$$

Where y_c and z_c are the distance from the reference coordinates to the location of the centroid of the entire cross-section. y_i and z_i the centroid location of each element *i,* and A_i is the cross-section area of element *i*.

3.3.2 Composite Material Centroid

The centroid for a composite section can be calculated by taking summation of the moments of axial loads acting on the centroids of each laminate and equating them to the total axial force acting on the centroid of the whole structure. With aid of Equation 2.44 and zero curvature at its centroid, we obtain the centroid of the asymmetric composite Z-beam given as.

$$\bar{z}_c = \frac{\sum_{i=1}^{3} w_i N_{x,i} z_{c,i}}{\sum_{i=1}^{3} w_i N_{x,i}} = \frac{w_{f1} A^*_{1,f1} z_{c,f1} + w_{f2} A^*_{1,f2} z_{c,f2} + w_w A^*_{1,w} z_{c,w}}{w_{f1} A^*_{1,f1} + w_{f2} A^*_{1,f2} + w_w A^*_{1,w}} \tag{3.4}$$

$$\bar{y}_c = \frac{w_{f1} A^*_{1,f1} y_{c,f1} + w_{f2} A^*_{1,f2} y_{c,f2} + w_w A^*_{1,w} y_{c,w}}{w_{f1} A^*_{1,f1} + w_{f2} A^*_{1,f2} + w_w A^*_{1,w}} \tag{3.5}$$

Where, $z_{c,f1}$, $z_{c,w}$, $z_{c,f2}$, $y_{c,f1}$, $y_{c,w}$, $y_{c,f2}$ are y and z distances from the reference z_r and y_r axis to the centroid of each section namely, web (w), flange 1 (f1) and flange 2 (f2), and are shown in Figure 3-2.

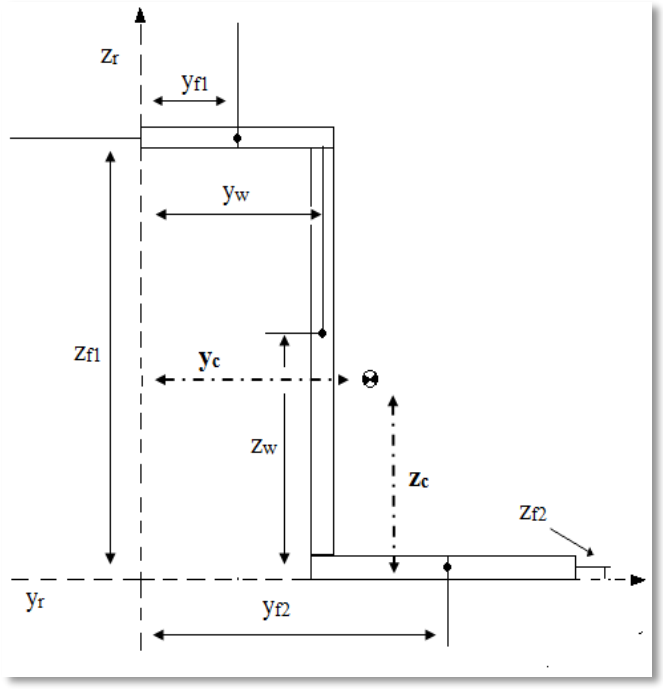

Figure 3.2 Distances between the reference axes and centroids of the sections.

3.4 Equivalent Axial Stiffness

3.4.1 Constitutive Equation for Sub-laminates

To determine the axial stiffness, the constitutive equations without the thermal loads are considered. Hence, constitutive equation of sub-laminates can be obtained from the narrow beam section, Equation 2.44 through 2.46. The equations representing flange sub-laminates *fi,* are given as.

$$\begin{aligned} N_{x,fi} &= A^*_{1,fi}\varepsilon^0_{x,f1} + B^*_{1,fi}\kappa_{x,fi} \\ M_{x,fi} &= B^*_{1,fi}\varepsilon^0_{x,f1} + D^*_{1,fi}\kappa_{x,fi} \end{aligned} \tag{3.6}$$

Where *i* refers to the different sections of the beam, and *i*=1 denotes top flange and *i*=2 denotes bottom flange. Also, $\varepsilon^{\circ}_{x,fi}$ and $\kappa_{x,fi}$ represent the respective mid-plane strains and curvatures of the sub-laminates. Constitutive equations for web are similar, and *w* is used in subscript instead of *fi.*

$$\begin{aligned} N_{xw} &= A^*_w\varepsilon^{\circ}_{x,w} + B^*_w\kappa_{x,w} \\ M_{xw} &= B^*_w\varepsilon^{\circ}_{x,w} + D^*_w\kappa_{x,w} \end{aligned} \tag{3.7}$$

If the web is of symmetric layup, then B^*_w would be zero.

3.4.2 Expression for Axial Stiffness

For a structure made of isotropic material, the force and strain relationship is given as.

$$\bar{N}_x = (EA)\varepsilon_x \tag{3.8}$$

Where,

$\bar{N}_x$ is total applied force on the structure.

EA is the axial stiffness of the structure.

The total axial force on composite Z-beam is given by the following expression.

$$\bar{N}_x = w_{f1}N_{x,f1} + w_{f2}N_{x,f2} + w_wN_{x,w} \tag{3.9}$$

Where,

$N_{x,f1}, N_{x,f2}, and\ N_{x,w}$ are the axial forces per unit width of sub-laminates, f1, f2, and w along X-direction. $\bar{N}_x$ is total force acting in X-direction,

Substituting the constitutive Equations 3.6 and 3.7 in the total force Equation 3.9, the following is obtained.

$$\begin{aligned}\bar{N}_x = w_{f1}(A^*_{1,f1}\mathring{\varepsilon}_{x,f1} + B^*_{1,f1}\kappa_{x,f1}) + w_{f2}(A^*_{1,f2}\mathring{\varepsilon}_{x,f2} + B^*_{1,f2}\kappa_{x,f2}) \\ + w_w(A^*_w\mathring{\varepsilon}_{x,w} + B^*_w\kappa_{x,w})\end{aligned} \tag{3.10}$$

Now, as the laminates are bonded, the strains for all laminates will be equal along the x-axis.

$$\mathring{\varepsilon}_{x,f1} = \mathring{\varepsilon}_{x,f1} = \mathring{\varepsilon}_{x,w} = \varepsilon_x \tag{3.11}$$

Also, if axial force is applied at the centroid, no curvatures will be present.

$$\kappa_{x,f1} = \kappa_{x,f2} = \kappa_{x,w} = 0 \tag{3.12}$$

When conditions from Equations 3.11 and 3.12 are applied on Equation 3.10, following expression is obtained.

$$\bar{N}_x = [w_{f1}(A^*_{1,f1}) + w_{f2}(A^*_{1,f2}) + w_w(A^*_w)]\varepsilon_x \tag{3.13}$$

Comparing Equation 3.13 and 3.8, the expression for axial stiffness is given as.

$$\bar{A}_x = [w_{f1}(A^*_{1,f1}) + w_{f2}(A^*_{1,f2}) + w_w(A^*_w)] \tag{3.14}$$

3.5 Equivalent Bending Stiffness

3.5.1 Expression for Chord Bending Stiffness $\bar{D}_z$

To obtain the bending stiffness of asymmetric composite Z-beam along y axis, a moment $\bar{M}_z^c$ is applied at the centroid. With no axial strain existence, $\bar{M}_z^c$ gives following relationship:

$$\bar{M}_z^c = \bar{D}_{yz}\kappa_y^c + \bar{D}_z\kappa_z^c \tag{3.15}$$

Where,

$\bar{M}_z^c$ = sum of the moment components of each sub-laminate pointing to the z-direction.

$\bar{D}_z = EI_{zz}$ = equivalent bending stiffness of z-beam about z-axis.

κ_z^c = curvature of the beam about z-axis and κ_y^c is curvature of the beam about y-axis.

The total moment for the beam, $\bar{M}_z^c$ referring to Fig. 3.3 is given by following equation;

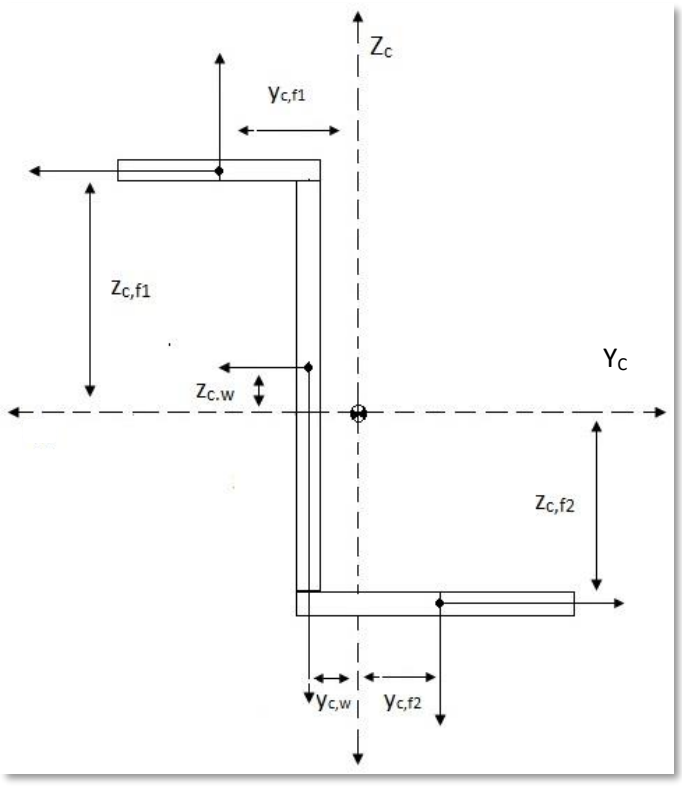

Figure 3.3 Location of section centroids with respect to the beam centroid.

Moment by top flange f1, is given as

$$\bar{M}_{z,f1} = \int_{-y_{c,f1}-\, w_{f1}/2}^{-y_{c,f1}+\, w_{f1}/2} \left(y * \, N_{x,f1}\right) dy \tag{3.16}$$

Moment by bottom flange f2, is given as

$$\bar{M}_{z,f2} = \int_{y_{c,f2}-\, w_{f2}/2}^{y_{c,f2}+\, w_{f2}/2} \left(y * \, N_{x,f2}\right) dy \tag{3.17}$$

Moment by web w, is given as

$$\bar{M}_{z,w} = \, w_w \, M_{x,w} + \, w_w \, N_{x,w} y_{c,w} \tag{3.18}$$

Where, $y_{c,f1}$, $y_{c,f2}$, $y_{c,w}$ and $z_{c,f1}$, $z_{c,f2}$, $z_{c,w}$ are the locations of the centroids of section from the centroidal axes of the beam and are shown in Figure 3.3.

When the beam is subjected to bending, the mid-plane strains can be adjusted to:

$$\varepsilon_x = \, \overset{0}{\varepsilon_x} + \, y_c \, \kappa_z^c + \, z_c \, \kappa_y^c \tag{3.19}$$

Since the bending moment, $\bar{M}_{z,f1}$ is applied at the centroid, no axial strains will be induced. Also, the local co-ordinate system of flange sub-laminates align with the centroidal co-ordinate system. The centroidal co-ordinate system can be referred as the global co-ordinate system of the beam.

The structure is perfectly bonded, hence curvatures will be equal, following conditions are obtained for top flange.

$$\begin{aligned} \overset{0}{\varepsilon_x} &= 0 \\ \kappa_{y,f1} &= \, \kappa_z^c \\ \kappa_{x,f1} &= \, \kappa_y^c \end{aligned} \tag{3.20}$$

By applying Equation 3.19 in Equation 3.6, the constitutive equation for the force on top flange can be written as.

$$N_{x,f1} = \, A_{1,f1}^* * \left(y_{c,f1} \, \kappa_z^c + z_{c,f1} \, \kappa_y^c\right) + \, B_{1,f1}^* * \, \kappa_y^c \tag{3.21}$$

Substituting Equation 3.21 in the moment Equation 3.16 for top flange, the following expression is obtained.

$$\bar{M}_{z,f1} = \int_{-y_{c,f1}-\, w_{f1}/2}^{-y_{c,f1}+\, w_{f1}/2} \left(y_{c,f1} * \left(A^*_{1,f1} * \left(y_{c,f1}\, \kappa^c_z + z_{c,f1}\ \kappa^c_y\right) + B^*_{1,fi} * \kappa^c_y\right)\right) dy \tag{3.22}$$

The above integral gives following expression for moment by top flange.

$$\bar{\mathrm{M}}_{z,f1} = \left\{A^*_{1,f1}\left[y^2_{c,f1}\, w_{f1} + \left(\frac{w^3_{f1}}{12}\right)\right]\kappa^c_z\right\} + \left\{\left(A^*_{1,f1}\, w_{f1}\, y_{c,f1}\, z_{c,f1} + B^*_{1,f1}\, w_{f1}\, y_{c,f1}\right)\kappa^c_y\right\} \tag{3.23}$$

Following the same procedure, the equation for moment by bottom flange is given as.

$$\bar{\mathrm{M}}_{z,f2} = \left\{A^*_{1,f2}\left[y^2_{c,f2}\, w_{f2} + \left(\frac{w^3_{f2}}{12}\right)\right]\kappa^c_z\right\} + \left\{\left(A^*_{1,f2}\, w_{f2}\, y_{c,f2}\, z_{c,f2} + B^*_{1,f2}\, w_{f2}\, y_{c,f2}\right)\kappa^c_y\right\} \tag{3.24}$$

Unlike the flanges, the local co-ordinate system of the web is different form the global co-ordinate system of the beam, which results in following expression mid plane strains of web.

$$\varepsilon_{x,w} = \overset{0}{\varepsilon_x} + y_{c,w}\, \kappa^c_z + z_{c,w}\, \kappa^c_y \tag{3.25}$$

Where,

$$\begin{aligned} \overset{0}{\varepsilon_x} &= 0 \\ \kappa_{x,w} &= \kappa^c_z \\ \kappa_{y,w} &= \kappa^c_y \end{aligned} \tag{3.26}$$

In the local co-ordinate system of web, the curvature in x direction of the web laminate corresponds to the curvature about z direction of the beam's global co-ordinate system and the curvature in y direction of the web laminate corresponds to the curvature about y direction of the beam's global co-ordinate system. The local and global co-ordinate systems are shown in

Figure 3.4 below, where x, y, and z represent global axes and x', y', and z' represents the local axes.

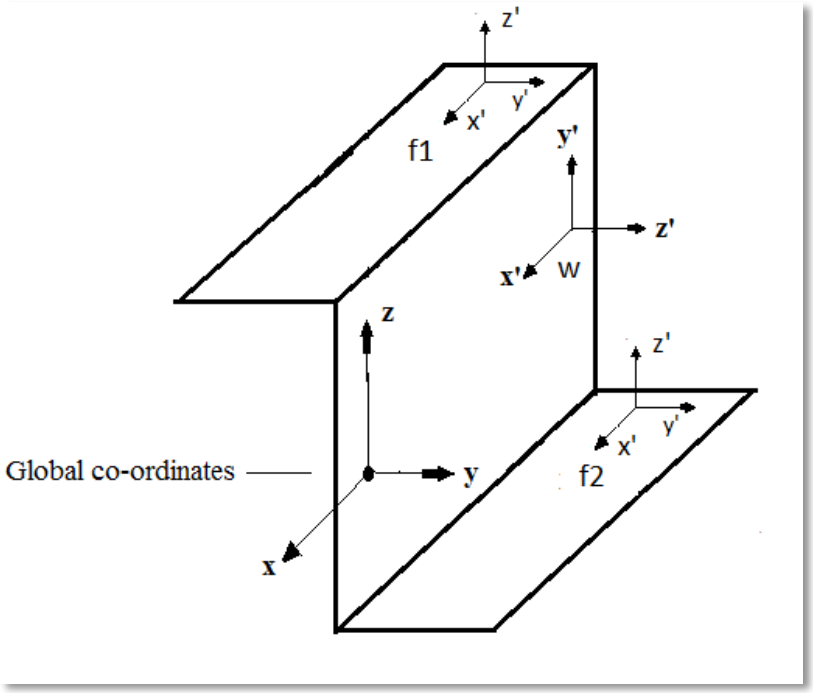

Figure 3.4 Local and global co-ordinate systems.

From Equations 3.7 and 3.25 the constitutive equations of web for force and moment along x-axis are given as.

$$N_{xw} = A_w^* \left[\left(z_{c,w} \ \kappa_y^c \right) + \left(y_{c,w} \ \kappa_z^c \right) \right] + B_w^* \ \kappa_z^c \tag{3.27}$$

$$M_{xw} = B_w^* \left[\left(z_{c,w} \ \kappa_y^c \right) + \left(y_{c,w} \ \kappa_z^c \right) \right] + D_w^* \ \kappa_z^c \tag{3.28}$$

Substituting Equations 3.27 and 3.28 in moment Equation 3.18, we get:

$$\begin{aligned} \bar{M}_{z,w} = \ & w_w \left(B_w^* \left[\left(z_{c,w} \ \kappa_y^c \right) + \left(y_{c,w} \ \kappa_z^c \right) \right] + D_w^* \ \kappa_z^c \right) \\ & + w_w \left(A_w^* \left[\left(z_{c,w} \ \kappa_y^c \right) + \left(y_{c,w} \ \kappa_z^c \right) \right] + B_w^* \ \kappa_z^c \right) y_{c,w} \end{aligned} \tag{3.29}$$

Rearranging the above equation.

$$\begin{aligned} \bar{M}_{z,w} = \ & \left[D_w^* \ w_w + A_w^* \ y_{c,w}^2 \ w_w + 2 \ B_w^* \ y_{c,w} \ w_w \right] \ \kappa_z^c \\ & + \left[B_w^* \ w_w \ z_{c,w} + A_w^* \ w_w \ z_{c,w} \ y_{c,w} \right] \ \kappa_y^c \end{aligned} \tag{3.30}$$

Combining Equations 3.30, 3.23, and 3.24, the equation for the total moment is obtained, which is given as.

$$\begin{aligned}\bar{M}_z^c = &\left\{\left[A_{1,f1}^* \left[y_{c,f1}^2\, w_{f1} + \left(\frac{w_{f1}^3}{12}\right)\right]\right] + \left[A_{1,f2}^* \left[y_{c,f2}^2\, w_{f2} + \left(\frac{w_{f2}^3}{12}\right)\right]\right] + \left[D_w^*\, w_w \;+\; A_w^*\, y_{c,w}^2\, w_w \;+\; 2\, B_w^*\, y_{c,w}\, w_w\right]\right\} \kappa_z^c + \\ &\left\{\left(A_{1,f1}^*\, w_{f1}\, y_{c,f1}\, z_{c,f1} + B_{1,f1}^*\, w_{f1}\, y_{c,f1}\right) + \left(A_{1,f2}^*\, w_{f2}\, y_{c,f2}\, z_{c,f2} + B_{1,f2}^*\, w_{f2}\, y_{c,f2}\right) + \left(B_w^*\, w_w\, z_{c,w} + A_w^*\, w_w\, z_{c,w}\; y_{c,w}\right)\right\} \kappa_y^c\end{aligned} \tag{3.31}$$

By comparing Equation 3.31 and Equation 3.15, expressions for bending stiffness $\bar{D}_z$ and $\bar{D}_{yz}$ can be obtained.

$$\begin{aligned}\bar{D}_z = &\left\{\left[A_{1,f1}^* \left[y_{c,f1}^2\, w_{f1} + \left(\frac{w_{f1}^3}{12}\right)\right]\right] \right. \\ &+ \left[A_{1,f2}^* \left[y_{c,f2}^2\, w_{f2} + \left(\frac{w_{f2}^3}{12}\right)\right]\right] \\ &\left. + \left[D_w^*\, w_w \;+\; A_w^*\, y_{c,w}^2\, w_w \;+\; 2\, B_w^*\, y_{c,w}\, w_w\right]\right\}\end{aligned} \tag{3.32}$$

$$\begin{aligned}\bar{D}_{yz} = &\left\{\left(A_{1,f1}^* w_{f1}\, y_{c,f1}\, z_{c,f1} + B_{1,f1}^*\, w_{f1}\, y_{c,f1}\right)\right. \\ &+ \left(A_{1,f2}^*\, w_{f2}\, y_{c,f2}\, z_{c,f2} + B_{1,f2}^*\, w_{f2}\, y_{c,f2}\right) \\ &\left. + \left(B_w^*\, w_w\, z_{c,w} + A_w^*\, w_w\, z_{c,w}\; y_{c,w}\right)\right\}\end{aligned} \tag{3.33}$$

The bending stiffness of composite Z-Beam can be obtained from above equations, the equations provides bending stiffness about z-direction of the beam $\bar{D}_z$ and y-z directional coupled bending stiffness $\bar{D}_{yz}$.

3.5.2 Expression for Bending Stiffness $\bar{D}_y$

To obtain the bending stiffness of asymmetric composite Z-beam about y-axis, a moment $\bar{M}_y^c$ is applied at the centroid. Mechanics theory gives following relationship:

$$\bar{M}_y^c = \bar{D}_y \kappa_y^c + \bar{D}_{yz} \kappa_z^c \tag{3.34}$$

Where,

$\bar{M}_y^c$ is sum of the total moment components of each sub-laminate

$\bar{D}_y = EI_{yy}$ = equivalent bending stiffness of *Z*-beam about y-axis.

κ_z^c is curvature of the beam about z-axis and κ_y^c is curvature of the beam about y-axis.

Since $\bar{D}_{yz}$ has been obtained in the previous case, we focus to obtain the term of $\bar{D}_y$ which is corresponding to κ_y^c. Hence, in the following derivation, we will ignore the term of $\bar{D}_{yz}$.

Hence, Equation 3.35 will be rewritten as

$$\bar{\bar{M}}_y^c = \bar{D}_y \kappa_y^c \tag{3.35}$$

Where $\bar{\bar{M}}_y^c$ is part of moment caused by κ_y^c.

The equations for moments by top and bottom flanges are given below. The web has different co-ordinate system and its equations for moment are described later in this section.

$$\bar{\bar{M}}_y^c = \bar{\bar{M}}_{y,f} + \bar{\bar{M}}_{y,w} \tag{3.36}$$

Where,

$\bar{\bar{M}}_{y,f}$ is the total moment about global y-direction, by top and bottom flanges.

$\bar{\bar{M}}_{y,w}$ = total moment about global y-direction, by web caused by κ_y^c.

First, obtaining the expression for $\bar{\bar{M}}_{y,f}$, which can be done by multiplying the local moments and forces of the flanges with their respective sectional widths to get the total

local/sectional forces and moments. Shifting the local forces and moments to the global centroid, following expression is obtained.

$$\bar{\bar{\mathrm{M}}}_{y,f} = w_{f1}\,\mathrm{M}_{x,f1} + w_{f1}\,N_{x,f1}\,z_{c,f1} + w_{f2}\,\mathrm{M}_{x,f2} + w_{f2}\,N_{x,f2}\,z_{c,f2} \tag{3.37}$$

Adjusting the mid-plane strains and curvatures, to read curvature about y-axis only.

$$\varepsilon_x = \overset{0}{\varepsilon_x} + z_c\,\kappa_y^c \tag{3.38}$$

For top flange, the above equation becomes.

$$\varepsilon_{x,f1} = \overset{0}{\varepsilon_x} + z_{c,f1}\,\kappa_{x,f1} \tag{3.39}$$

The structure is perfectly bonded, and the moment is applied at the centroid, which results in following conditions.

$$\begin{aligned} \overset{0}{\varepsilon_x} &= 0 \\ \kappa_{x,f1} &= \kappa_y^c \end{aligned} \tag{3.40}$$

By implementing above conditions in Equation 3.38, strains for top and bottom flanges are given as.

$$\begin{aligned} \varepsilon_{x,f1} &= z_{c,f1}\kappa_y^c \\ \varepsilon_{x,f2} &= z_{c,f2}\kappa_y^c \end{aligned} \tag{3.41}$$

The constitutive equations of the flanges are given as.

$$N_{x,fi} = A^*_{1,fi}\,z_{c,fi}\,\kappa_y^c + B^*_{1,fi}\,\kappa_y^c \tag{3.42}$$

$$M_{x,fi} = B^*_{1,fi}\,z_{c,fi}\,\kappa_y^c + D^*_{1,fi}\,\kappa_y^c \tag{3.43}$$

Where, i= 1 and 2, represents top and bottom flanges, respectively.

Inserting Equation 3.42 and 3.43 in Equation 3.37, the expression for $\bar{\mathrm{M}}_{y,f}$ is obtained.

$$\begin{aligned} \bar{\bar{\mathrm{M}}}_{y,f} = w_{f1}\left[B^*_{1,f1}\,z_{c,f1}\kappa_y^c + D^*_{1,f1}\,\kappa_y^c\right] + w_{f1}\left[A^*_{1,f1}z_{c,f1}\kappa_y^c + B^*_{1,f1}\,\kappa_y^c\right] z_{f1} + \\ w_{f2}\left[B^*_{1,f2}z_{c,f2}\kappa_y^c + D^*_{1,f2}\,\kappa_y^c\right] + w_{f2}\left[A^*_{1,f2}z_{c,f2}\kappa_y^c + B^*_{1,f2}\,\kappa_y^c\right] z_{f2} \end{aligned} \tag{3.44}$$

$$\bar{\bar{\mathrm{M}}}_{y,f} = \left[w_{f1}B^*_{1,f1}z_{c,f1} + w_{f1}D^*_{1,f1} + w_{f1}A^*_{1,f1}z^2_{c,f1} + w_{f1}B^*_{1,f1}z_{c,f1} + w_{f2}\,B^*_{1,f2}\,z_{c,f2} + w_{f2}\,D^*_{1,f2} + w_{f2}\,A^*_{1,f2}\,z^2_{c,f2} + w_{f2}B^*_{1,f2}\,z_{c,f2}\right]\kappa^c_y \quad (3.45)$$

Now, obtaining the expression for $\bar{\bar{\mathrm{M}}}_{y,w}$.

The web has a different co-ordinate system, the global κ^c_y is web's local $\kappa_{y,w}$.

Integrating axial force of the web to obtain the moment along the x-direction and shifting the moment to centroid of the Z-beam.

$$\bar{\bar{\mathrm{M}}}_{y,w} = \int_{\frac{w_w}{2} - z_{c,w}}^{z_{c,w} + w_w/2} \{z * N_{x,w}\}\, dz \quad (3.46)$$

Reading only κ^c_y which is local $\kappa_{y,w}$, and considering that the web is of symmetric layup and the beam is perfectly bonded.

$$\begin{aligned} B^*_{1,w} &= 0 \\ \kappa_{x,w} &= \kappa^c_z \\ \kappa_{y,w} &= \kappa^c_y \end{aligned} \quad (3.47)$$

Applying above conditions in Equation 3.7, the constitutive equations for the web are given as.

$$\begin{aligned} N_{xw} &= A^*_{1,w}\left[z_{c,w}\,\kappa^c_y\right] + B^*_{1,w}\,\kappa^c_z \\ M_{xw} &= B^*_{1,w}\left[z_{c,w}\,\kappa_{y,w}\right] + D^*_{1,w}\kappa^c_z \end{aligned} \quad (3.48)$$

Reading curvature κ^c_y and inserting Equation 3.48 in Equation 3.46, and expanding the integral, the following expression is obtained.

$$\bar{\bar{\mathrm{M}}}_{y,w} = A^*_{1,w}\left[z^2_{c,w}\,w_w + \left(\frac{w^3_w}{12}\right)\right]\,\kappa^c_y \quad (3.49)$$

Combining Equation 3.49, 3.45 and inserting them in Equation 3.36, the equation for the total moment about y-direction is obtained, which is given as.

$$\bar{\bar{M}}_y^c = \Big[w_{f1}\, D_{1,f1}^* + w_{f1}\, A_{1,f1}^*\, z_{c,f1}^2 + 2\, w_{f1}\, B_{1,f1}^*\, z_{c,f1} + w_{f2}\, D_{1,f2}^* + w_{f2}\, A_{1,f2}^*\, z_{c,f2}^2 + 2\, w_{f2}\, B_{1,f2}^*\, z_{c,f2} + A_{1,w}^* \left[z_{c,w}^2\, w_w + \left(\frac{w_w^3}{12} \right) \right] \Big] \kappa_y^c \tag{3.50}$$

By comparing Equation 3.50 and Equation 3.35, expressions for bending stiffness $\bar{D}_y$ can be obtained.

$$\bar{D}_y = \Big[w_{f1}\, D_{1,f1}^* + w_{f1}\, A_{1,f1}^*\, z_{c,f1}^2 + 2\, w_{f1}\, B_{1,f1}^*\, z_{c,f1} + w_{f2}\, D_{1,f2}^* + w_{f2}\, A_{1,f2}^*\, z_{c,f2}^2 + 2\, w_{f2}\, B_{1,f2}^*\, z_{c,f2} + A_{1,w}^* \left[z_{c,w}^2\, w_w + \left(\frac{w_w^3}{12} \right) \right] \Big] \tag{3.51}$$

3.5.3 Stresses in Layers of Flange Sub-laminates

The approach of finding mid-plane strain and curvature and then using lamination theory equations to find stresses in the layers was followed to find the stresses. Individual forces in the Laminates were obtained by using curvatures of the beam under bending load.

Applying moments at the centroid of Z-beam, and considering following equations.

$$\begin{aligned} \bar{\mathrm{M}}_y^c &= \bar{D}_y \kappa_y^c + \bar{D}_{yz} \kappa_z^c \\ \bar{\mathrm{M}}_z^c &= \bar{D}_{yz} \kappa_y^c + \bar{D}_z \kappa_z^c \end{aligned} \tag{3.52}$$

Rearranging above equations, the equations for curvatures κ_y^c and κ_z^c can be obtained.

$$\begin{aligned} \kappa_y^c &= \frac{\bar{\mathrm{M}}_y^c \bar{D}_z - \bar{\mathrm{M}}_z^c \bar{D}_{yz}}{\bar{D}_y \bar{D}_z - \bar{D}_{yz}^{\,2}} \\ \kappa_z^c &= \frac{\bar{\mathrm{M}}_z^c \bar{D}_y - \bar{\mathrm{M}}_y^c \bar{D}_{yz}}{\bar{D}_y \bar{D}_z - \bar{D}_{yz}^{\,2}} \end{aligned} \tag{3.53}$$

The stresses are extracted by applying a moment $\bar{M}_y^c$ at the centroid of the beam, therefore modifying the above equations for curvatures.

$$\kappa_y^c = \frac{\bar{M}_y^c \bar{D}_z}{\bar{D}_y \bar{D}_z - \bar{D}_{yz}^{\ 2}}$$
$$\kappa_z^c = \frac{-\bar{M}_y^c \bar{D}_{yz}}{\bar{D}_y \bar{D}_z - \bar{D}_{yz}^{\ 2}} \tag{3.54}$$

Equation 3.53 and 3.54 can be used to obtain the curvature values, when a moment about y-direction is applied at the beam centroid.

Considering the fact that the moment is applied at the centroid and the conditions in Equation 3.40, the strains for top flange can be written as.

$$\varepsilon_{x,f1} = z_{c,f1}\ \kappa_y^c + y_{c,f1}\ \kappa_z^c \tag{3.55}$$

The axial force and moment in top flange is given by the constitutive equations for top flange as.

$$N_{x,f1} = A_{1,f1}^* * \left(z_{c,f1}\ \kappa_y^c + y_{c,f1}\ \kappa_z^c\right) + B_{1,f1}^* * \kappa_y^c$$
$$M_{x,f1} = B_{1,f1}^* \left(z_{c,f1}\ \kappa_y^c + y_{c,f1}\ \kappa_z^c\right) + D_{1,f1}^* * \kappa_y^c \tag{3.56}$$

The force and moment obtained from Equations 3.60 and 3.61 can be used to calculate the stress values in all layers of top flange sub-laminate from lamination theory.

The relation between mid-plane strains and forces on a composite laminate can be written in matrix from as.

$$\begin{bmatrix} \varepsilon_x^0 \\ \varepsilon_y^0 \\ \gamma_{xy}^0 \\ \kappa_x \\ \kappa_y \\ \kappa_{xy} \end{bmatrix}_{f1} = \begin{bmatrix} a_{11} & b_{11} & b_{16} \\ a_{12} & b_{12} & b_{26} \\ a_{16} & b_{16} & b_{66} \\ b_{11} & d_{11} & d_{16} \\ b_{12} & d_{12} & d_{26} \\ b_{16} & d_{16} & d_{66} \end{bmatrix}_{f1} \begin{bmatrix} N_{x,f1} \\ M_{x,f1} \\ M_{xy,f1} \end{bmatrix} \tag{3.57}$$

The strains in k[th] layer of top flange sub-laminate can be calculated as.

$$[\varepsilon_{f1}]_k = \left[\varepsilon^{^0}\right]_{f1} + z_k[\kappa]_{f1} \tag{3.58}$$

Where, z_k is the position of k[th] layer from the mid-plane of sub-laminate f1 (top flange).

$$\begin{bmatrix} \varepsilon_{x,f1} \\ \varepsilon_{y,f1} \\ \varepsilon_{xy,f1} \end{bmatrix}_k = \begin{bmatrix} \varepsilon^0_{x,f1} \\ \varepsilon^0_{y,f1} \\ \gamma^0_{xy,f1} \end{bmatrix} + z_k \begin{bmatrix} \kappa_{x,f1} \\ \kappa_{y,f1} \\ \kappa_{xy,f1} \end{bmatrix} \tag{3.59}$$

Stress in global directions of k[th] layer of top flange sub-laminate can be calculated from laminations theory by using following equation.

$$[\sigma_{x-y_{f1}}]_k = [\bar{Q}]_k\,[\varepsilon_{f1}]_k \tag{3.60}$$

The above method can also be used to extract stress values from bottom flange sub-laminate, as both flanges have same orientation with respect to global co-ordinates.

3.5.4 Stresses in Layers of Web Sub-laminate

The strains for web laminate under bending load from moment $\bar{M}_y^c$ are given as.

$$\varepsilon_{x,w} = \varepsilon_x^{^0} + z_{c,w}\ \kappa_y^c + y_{c,w}\ \kappa_z^c \tag{3.61}$$

Where,

$$\varepsilon_x^{^0} = 0 \tag{3.62}$$
$$\kappa_{y,w} = \kappa_y^c \quad \text{and } \kappa_{x,w} = \kappa_z^c$$

The force and moment in web is given by the constitutive equations for web as.

$$N_{x,w} = A^*_{1,w} * \left(z_{c,w}\,\kappa_{x,w} + y_{c,w}\,\kappa_{z,w}\right) + B^*_{1,w} * \kappa_z^c \tag{3.63}$$

$$M_{x,w} = B^*_{1,w}\,(z_{c,w}\,\kappa_{x,w} + y_{c,w}\,\kappa_{z,w}) + D^*_{1,w} * \kappa_z^c \tag{3.64}$$

The force and moment obtained from Equation 3.63 and 3.64 can be used to calculate the stress values in all layers of web sub-laminate from lamination theory, by using Equation 3.57 through Equation 3.60.

3.6 Temperature Effects

3.6.1 Temperature Induced Bending Moments

When the cross section of the beam is exposed to a temperature change, and different sections are exposed to different temperature gradients, a normal force and moments about the centroid are generated. The figure below shows, temperature induced moments on an isotropic material, asymmetric beam of Z cross-section. When top flange is exposed to a positive temperature gradient, and Web and Bottom flange experience zero temperature gradient, the top flange will experience a normal force N_t which will tend to move out of the plane of paper and as the sections are joined, it will generate moments $M_{x,t,c}$ and $M_{y,t,c}$ about the centroid of the beam.

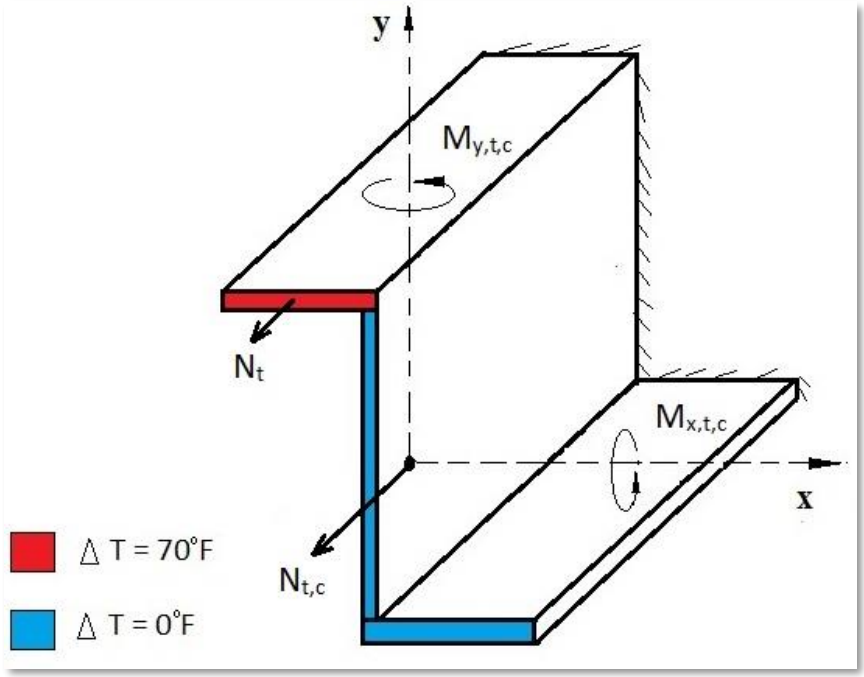

Figure 3.5 Temperature induced moments in an isotropic Z beam

The beam shown in above figure is an asymmetric isotropic beam of Z cross-section and the centroidal axes of this beam are different from the centroidal axes of the composite laminated Z-beam, this means that the moment directions shown in Figure 3.5 do not reflect moment directions of the composite Z-beam.

3.6.2 Temperature Effects on Isotropic Material Beams

The beams in aircraft are generally thin walled and do not necessarily have axes of symmetry, also they are subjected to temperature gradient while in service. Depending on the location and purpose on the beam in the structure, the beam experiences different temperate gradients on different sections like in case of a Z-Beam, web, top and bottom flange experiencing different temperature gradients causing each component have their own normal force and moments, and as explained previously.

The effects of temperature on such beams have been determined for isotropic beam cross-sections. The equations for the moment and force resultants due to temperature gradients on an isotropic beam an arbitrary cross section are given below [15].

$$N_{x,t,c} = \sum E\ \alpha\ \Delta T\ A_i \tag{3.65}$$

$$M_{x,t,c} = \sum E\ \alpha\ \Delta T\ \bar{y}_i\ A_i \tag{3.66}$$

$$M_{y,t,c} = \sum E\ \alpha\ \Delta T\ \bar{x}_i\ A_i \tag{3.67}$$

Where,

$N_{x,t,c}$ is the normal force resultant.

$M_{x,t,c}$ and $M_{y,t,c}$ are the moment resultants about the centroidal x and y directions respectively.

A_i is the cross-sectional areas of the components.

$\bar{x}_i$ and $\bar{y}_i$ are the coordinates of its centroid.

The above equations are summation equations, as the cross-section of the structure is divided into different sections and temperature effects on each section are evaluated separately and summarized. The temperature induced normal forces and moments can be used to obtain stresses, and the stresses can be added to the mechanical stresses for the analysis of structure and the beam.

3.6.3 Temperature effects on Composite Beam

The thermal behavior of the composite laminates is different from the thermal behavior of the isotropic materials, as discussed in the thermal section of Chapter 2, each ply has its own coefficient of thermal expansion. This section covers the equations for the moments generated by the different temperature gradients on different sections of the laminated Z-Beam.

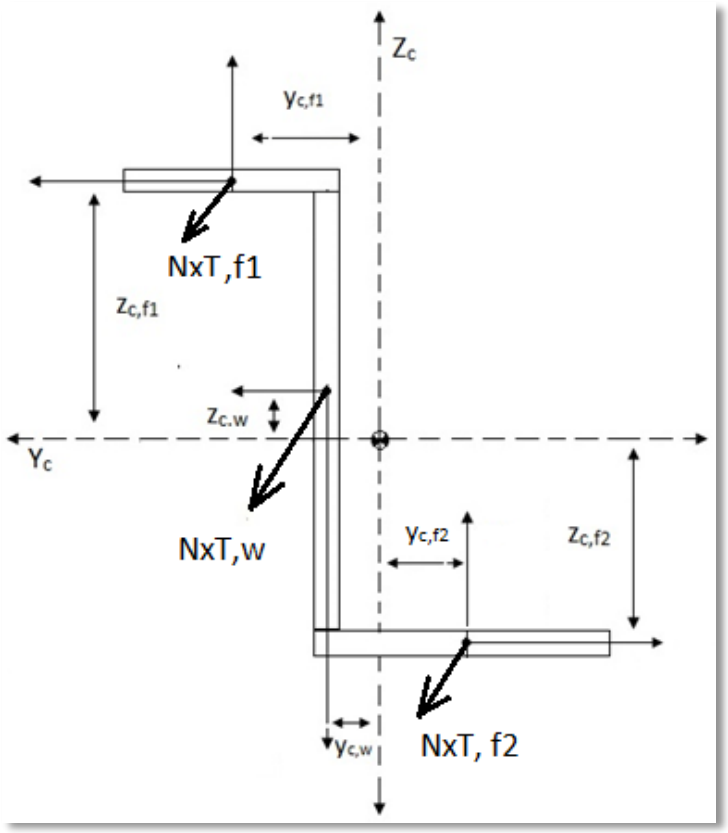

Figure 3.6 Temperature induced forces and their locations on cross-section of Z-beam

The above figure shows normal forces generated in the sections of composite Z-beam, where script T represents the forces and moments because of temperature gradient, all other notations remain same as before. For example $N_{x,f1}^{T}$ represents normal force due to temperature gradient, along x-direction of top flange sub-laminate.

3.6.4 Temperature Induced Bending Moment

To calculate the moments generated about the centroid because of temperature gradients on composite Z-beam, normal forces generated because of temperature are used to derive the expression for induced moments.

Temperature change also generates moments in composite laminates, but for balanced and symmetric laminates those moments are zero. So for a balanced and symmetric laminate, which is the desired laminate setup for thermal applications of composites, the resultant thermal moments about the centroid are induced by the normal forces generated in the sections because of temperature gradient.

Moment about z-axis of Z-beam can be given by following expression.

$$M_z^{cT} = M_{z,f1}^{cT} + M_{z,f2}^{cT} + M_{z,w}^{cT} \tag{3.68}$$

Where,

M_z^{cT} = Moment induced about z-axis of Z-beam by normal thermal forces.

Subscripts f1, f2, and w refers to top flange, bottom flange, and web respectively.

Now, evaluating moments generated by two flanges and web separately.

Moment about z-axis of the centroid, induced by top flange:

$$M_{z,f1}^{cT} = \int_{-y_{c,f1}-w_{f1}/2}^{-y_{c,f1}+w_{f1}/2} \{y * N_{x,f1}^{T}\}\, dy \tag{3.69}$$

Moment about z-axis of the centroid, induced by bottom flange:

$$M_{z,f1}^{cT} = \int_{y_{c,f2}-w_{f2}/2}^{y_{c,f2}+w_{f2}/2} \{y * N_{x,f1}^{T}\}\, dy \tag{3.70}$$

Moment about z-axis of the centroid, induced by web:

$$M_{z,w}^{cT} = w_w * N_{x,w}^{T} * y_{c,w} \tag{3.71}$$

Where,

$y_{c,f1}$ and $y_{c,f2}$ are distances from centroid of the beam to the centroids of top and bottom flanges respectively.

$N_{x,i}^{T}$ is the force in x-direction induced by the temperature change, which was explained in section 2.2.3 of Chapter 2, expression for which is given by Equation 2.39.

Expanding the integrals in Equation 3.72 through 3.74, and inserting them in Equation 3.71, the total moment M_z^{cT} is given by following expression.

$$M_z^{cT} = -(N_{x,f1}^{T} * y_{f1} * w_{f1}) + (N_{x,f2}^{T} * y_{f2} * w_{f2}) + (N_{x,w}^{T} * y_w * w_w) \tag{3.72}$$

Similar method can be followed to obtain the equation for M_y^{cT}, which is shown below.

$$M_y^{cT} = -(N_{x,f1}^{T} * z_{f1} * w_{f1}) + (N_{x,f2}^{T} * z_{f2} * w_{f2}) + (N_{x,w}^{T} * z_w * w_w) \tag{3.73}$$

3.6.5 Stresses in Layers of Sub-laminates by Temperature Induced Moments.

The temperature induced moments M_y^{cT} and M_z^{cT} are experienced simultaneously by the beam, considering Equations 3.52 through 3.54, and inserting temperature induced moments in place of respective mechanical moments, the curvatures can be given by following expressions.

$$\kappa_y^c = \frac{M_y^{cT}\bar{D}_z - M_z^{cT}\bar{D}_{yz}}{\bar{D}_y\bar{D}_z - \bar{D}_{yz}^{\,2}} \tag{3.74}$$

$$\kappa_z^c = \frac{M_y^{cT}\bar{D}_y - M_y^{cT}\bar{D}_{yz}}{\bar{D}_y\bar{D}_z - \bar{D}_{yz}^{\,2}} \tag{3.75}$$

The stresses in layers of sub-laminates can be calculated by following the exact procedure explained in the previous section.

Chapter 4
FINITE ELEMENT ANALYSIS

This chapter explains finite element modeling of the composite Z-Beam in detail. Validation of the model, applied boundary conditions and extraction of the results is covered in this chapter. Modeling of the composite Z-Beam was done in ANSYS™ Classic (APDL) version 16 and 17.

4.1 Material Properties

The material used for the composite laminate was 0.005" thick AS4/3501-6 graphite/epoxy laminate, unidirectional layer orthotropic properties for which are given as.

$E_1 = 19.3 * 10^6$ psi	$E_2 = 1.62 * 10^6$ psi	$E_1 = 1.62 * 10^6$ psi
$\nu_{12} = 0.288$	$\nu_{23} = 0.288$	$\nu_{13} = 0.288$
$G_{12} = 1.02 * 10^6$ psi	$G_{23} = 1.02 * 10^6$ psi	$G_{13} = 1.02 * 10^6$ psi
$\alpha_1 = 2.0 * 10^{-6}$ in/in/^{0}F	$\alpha_2 = 15 * 10^{-6}$ in/in/^{0}F	$\alpha_3 = 15 * 10^{-6}$ in/in/^{0}F

Where E_1, E_2, and E_3 are the Young's moduli, and α_1, α_2, α_3 are co-efficient of thermal expansion of the composite lamina in lamina's local coordinates. G_{12}, G_{23}, G_{13} are the shear moduli, ν_{12} , ν_{23}, and ν_{13} are Poisson's ratio with respect to the 1-2, 2-3 and 1-3 planes, respectively.

4.2 Model Geometry and Stacking Sequence

The composite Z-Beam was asymmetric, the web had a width of 1", the top flange was 0.5" wide and bottom flange was 0.7" wide. The stacking sequence for the web laminate was 4 ply $[\pm 45]_S$ laminate, which was kept same throughout the study. The stacking sequence for the top and bottom flanges were identical initially, which was an 8 ply $[\pm 45/\ 0/\ 90\ ]_S$ laminate, each ply was 0.005" thick. The dimensions of the model beam were parameterized, to consider cases of different dimensions, if required.

4.3 Modeling

The composite beam was modeled in ANSYS™ Classic (APDL) version 16 and 17, a SOLID185, layered structural solid element was used to model the beam. The element is a 3D block element with eight nodes and three degrees of freedom per node.

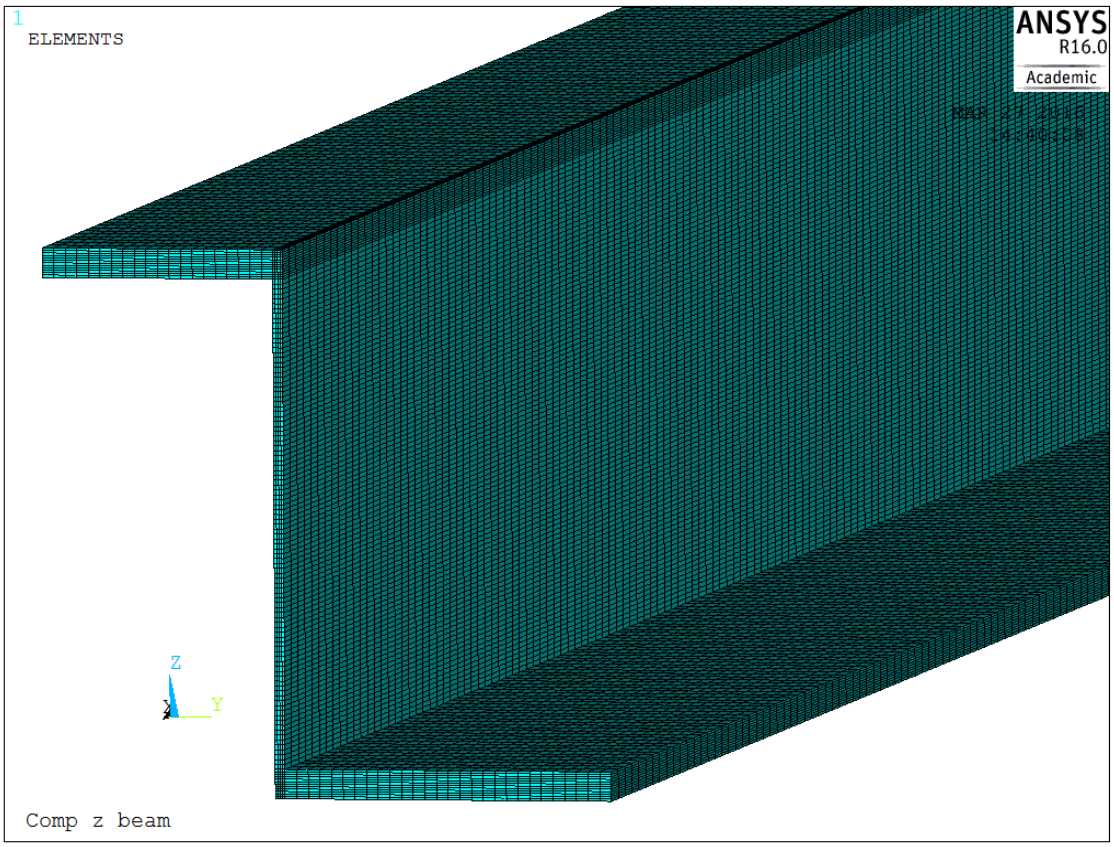

Figure 4.1: Meshed *and* layered asymmetric Z-Beam in ANSYS™.

The SOLID185 is a structural layered solid element, the element can be assigned different layers and each layer can be assigned different properties like fiber orientation, co-ordinate system etc. The cross section of the Z-beam was modeled as three different volumes for web, top and bottom flange, each of which was assigned their specific stacking sequences separately. The meshing was done manually to obtain an efficient mesh, which would provide accurate solution by not consuming much processing power and time. To better explain the application of forces and boundary conditions, the two ends of the beam were named, the end at zero length

(l=0) was named as *origin end*, and the end where forces and moments were applied was named *force end*. These names will be used further in this document.

The length of the beam was 10”, this length was selected by considering the cross-sectional dimensions of the beam to minimize any interference of the results by the applied boundary conditions. As the beam was asymmetric, its centroid did not lie on the cross section, it was a point outside the cross-section. Location of centroid varied depending on the ply layup and material properties, so the location of the centroid was also parameterized in the model.

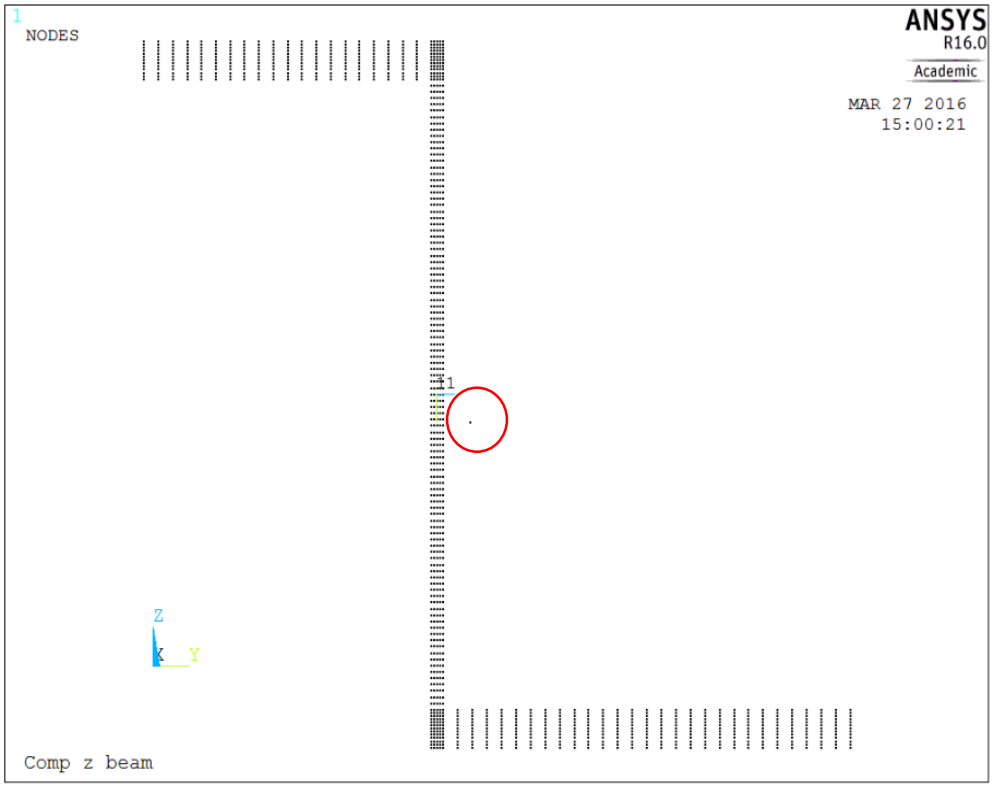

Figure 4.2: Cross-section of the beam showing nodes, centroidal node encircled in red.

The study required application of loads on the centroid to obtain the axial and bending properties of the beam. In order to ensure uniform longitudinal cross-sectional deformation along x-axis under the influence of finite tension load applied at the centroidal node a multi-point constraint was generated about the centroidal node. The multi-point constraint is used to couple degrees of freedom of a set of nodes (Slave nodes) to a parent node (Pilot node), this feature also served as a connection to transmit the loads between the centroidal node and nodes on the

beam cross-section, as centroid was not connected to the beam initially. The multi-point constraint connected the centroidal node and the nodes on the end of cross-section by generating constraint equations that mathematically relates nodes on the cross-section. The constraint equations generated are based on small deflection theory.

The centroidal node was created at both ends of the beam and the nodes along the free edges of the beam were identified before issuing the command. Multiple rigid lines were formed to link the slave nodes (nodes on the edges) to the pilot node (centroidal node).

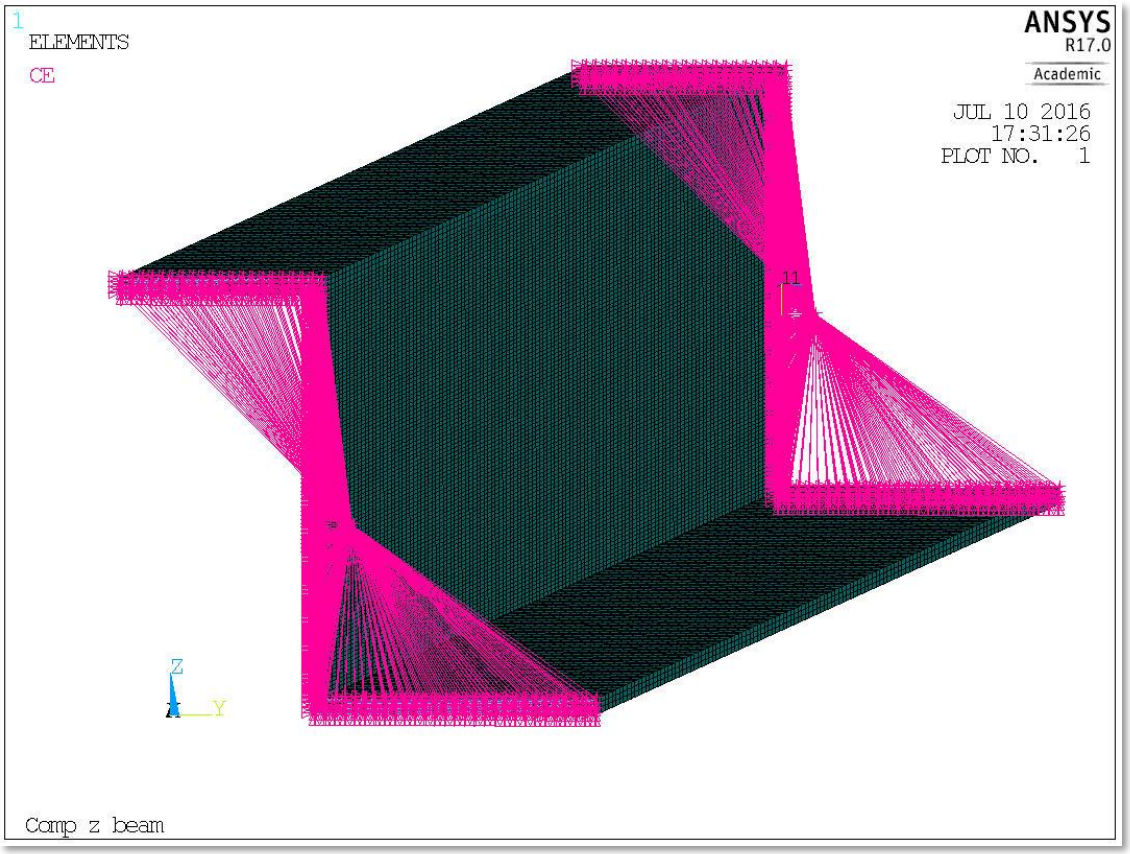

Figure 4.3: Nodes on both ends connected/coupled to the centroidal node.

The loads were applied to the centroidal node on the force end and the boundary conditions on origin end were applied on the centroidal node at that end.

4.4 Model Validation

4.4.1 Axial Stiffness

The finite element model was validated by changing the material to isotropic while maintaining same model size, geometry, element orientation, and comparing the beam properties obtained by different methods.

Material of the model was changed from an orthotropic to isotropic material, aluminum was chosen for this validation, and properties of aluminum are given as.

$$E = E_1 = E_2 = E_3 = 1.02 * 10^7 psi$$

$$v = v_{12} = v_{23} = v_{13} = 0.30$$

$$G = G_{12} = G_{12} = G_{12} = \frac{E}{2(1+v)} = 3.7 * 10^6 psi$$

$$\alpha_1 = \alpha_2 = \alpha_3 = \alpha = 13.1 * 10^{-6} \text{ in/in}/^0F$$

The properties compared were axial and bending curvatures of the beam, and were obtained from Mechanics theory, current method and Finite Element methods.

Mechanics method and present method were covered in Chapter 3, Equation 3.6 and Equation 3.12 were used to obtain the values of axial stiffness A_x from mechanics' method and current method, respectively.

Axial stiffness of the beam was obtained from the finite element analysis by applying a force of 1 lb on the centroid in x-direction and axial deflection (U_x) was observed.

Following equation was used to calculate the axial stiffness of the beam.

$$A_x = \frac{FL}{2(U_{x\ at\ x=L/2})} \tag{4.1}$$

Where,

A_x is axial stiffness of the beam.

F is force applied on the centroid.

L is length of the beam.

U_x is the displacement in x direction.

To minimize the distortion of the results by boundary conditions or the applied load, the results were read halfway through the length of the beam, at L/2.

Table 4-1 Comparison of axial stiffness calculated from three different methods.

Length L (in)	Load F (lb)	Mechanics Eqn. 3.6 $A_{x,m}$ (lb)	Present method (Eq. 3.12) $A_{x,e}$ (lb)	FEM $A_{x,fe}$ (lb)	Difference % $A_{x,m}$- $A_{x,fe}$	Difference % $A_{x,e}$- $A_{x,fe}$
10	1	68000	67980	69787	2.5	0.02

4.4.2 Bending Stiffness

To obtain the bending stiffness and bending curvatures, a bending moment should be applied at the centroid of the beam and to ensure effective transfer of the bending effect to the cross-section of the beam, some more modeling was performed at force end of the beam. The conditions on the origin end, where boundary conditions would be applied were not changed.

A small circular beam was modeled at the centroid location at force end and the small beam was meshed in such a way that the middle node of the beam was a point lying on the centroid location of the force end. The circular beam was 0.02” in length in global x-direction, with its middle point on centroid, the beam ran parallel to the web of the Z beam, and the local co-ordinate system of the small beam was aligned with the global co-ordinate system of the Z-Beam.

The circular beam had total three nodes along its length, mid node being at the centroid. Middle node of the circular beam was coupled to all the nodes on the force end of the Z beam by using multi-point constraint explained earlier in section 4.3.

In order to apply the moments at the centroid of the Z beam, two equal and opposite forces were applied on the nodes at two opposite ends of the circular beam, simulating a moment. To avoid distortions in moment application because of local deformations in circular beam, properties of the circular beam were adjusted considering its length and material to minimize the deformation of the circular beam in the process.

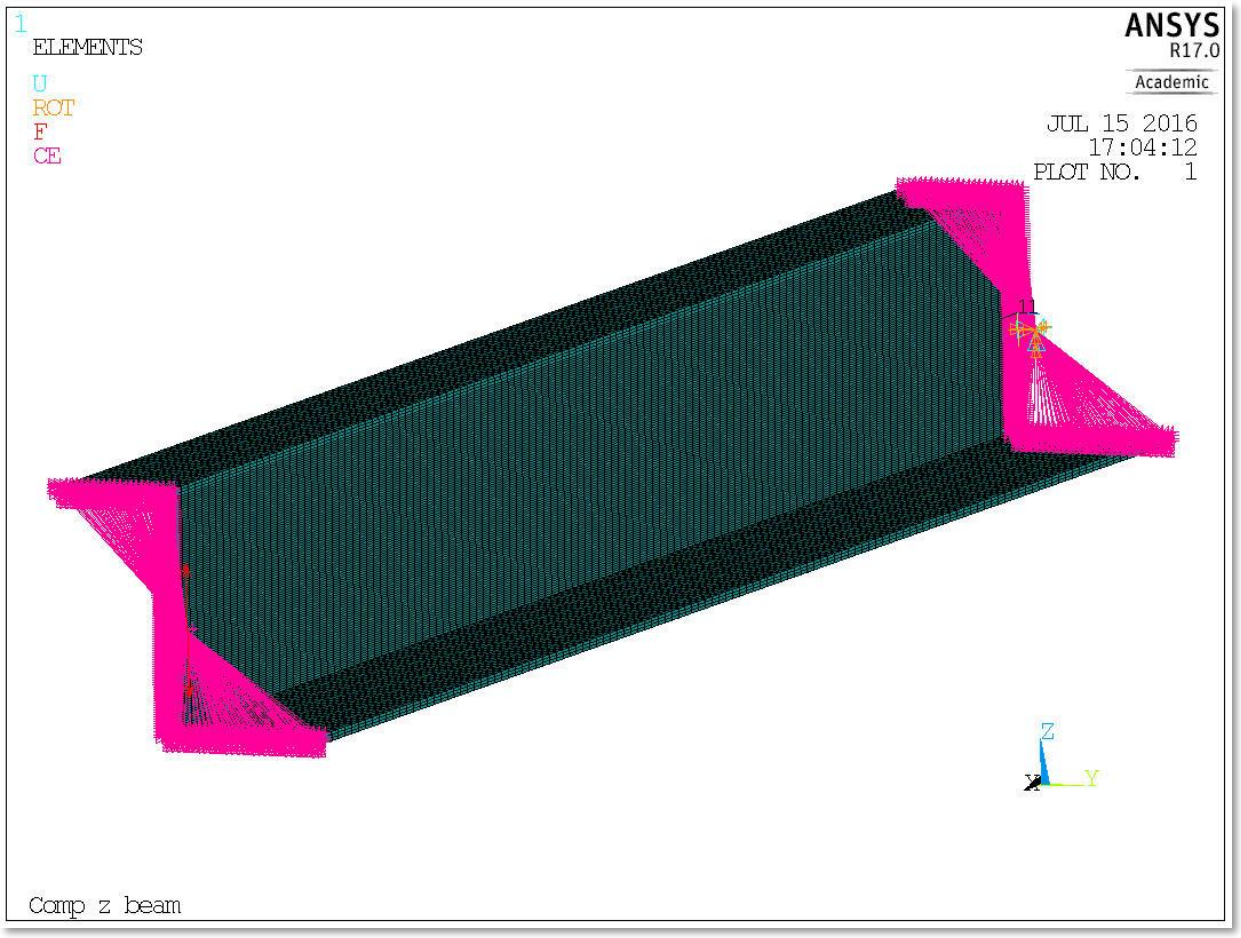

Figure 4.4: Forces and boundary conditions applied on centroidal nodes.

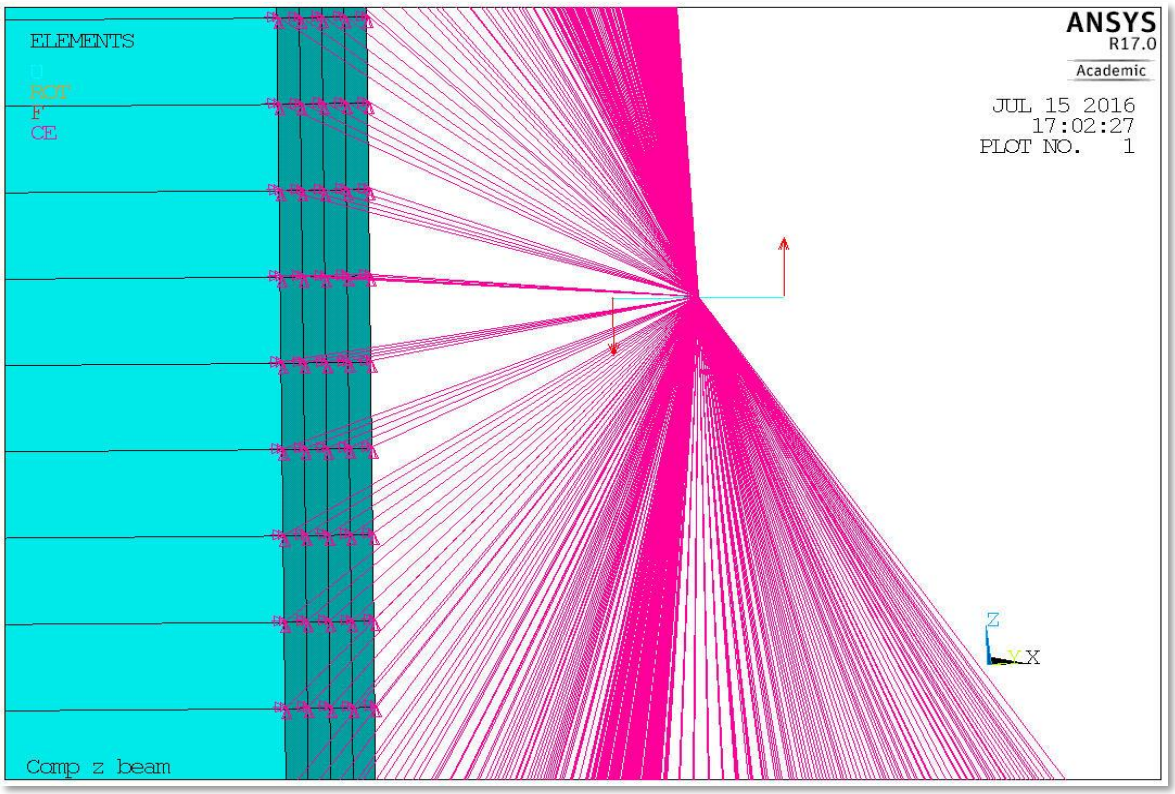

Figure 4.5: Moment applied by equal and opposite forces.

To apply a moment on the centroidal node, which was at the center of the circular beam and was coupled to the slave nodes at the force end of the beam, two equal and opposite forces were applied on the end nodes of the circular beam as shown in the figure above. The circular beam was 0.02" long and forces of magnitude 5 lb were applied at the two ends of the circular beam, generating a concentrated moment of 0.1 lb-in at the centroid of the beam.

Both moments $\bar{M}_y^c$ and $\bar{M}_z^c$ had same magnitude of 0.1 lb-in and were applied in the same manner as described above, the direction of forces were changed, magnitude was kept same.

The beam was showing significant curvatures in both x and y directions, upon application of moment on the centroid, regardless of the moment applied (Mz or My) because of coupling, as D_{yz} was non-zero. Thus the values of $\bar{D}_y$, $\bar{D}_z$, and $\bar{D}_{yz}$ could not be obtained directly from the available equations.

Hence, to verify the model, curvatures κ_y^c and κ_z^c of the beam were obtained from the finite element analysis were compared with the curvatures obtained from developed equations, which were assigned isotropic material properties.

The values of bending stiffness of the isotropic beam were obtained from current method and were used to calculate the curvature values. Equation 3.53 and Equation 3.54 were modified, as only one moment was applied at a time.

$$\kappa_y^c = \frac{\bar{M}_y^c \bar{D}_y}{\bar{D}_y \bar{D}_z - \bar{D}_{yz}^{\,2}} \tag{4.2}$$

$$\kappa_z^c = \frac{-\bar{M}_y^c \bar{D}_{xy}}{\bar{D}_y \bar{D}_z - \bar{D}_{yz}^{\,2}} \tag{4.3}$$

$$\kappa_y^c = \frac{-\bar{M}_z^c \bar{D}_{xy}}{\bar{D}_y \bar{D}_z - \bar{D}_{yz}^{\,2}} \tag{4.4}$$

$$\kappa_z^c = \frac{\bar{M}_z^c \bar{D}_x}{\bar{D}_y \bar{D}_z - \bar{D}_{yz}^{\,2}} \tag{4.5}$$

The above equations give values of both curvatures κ_y^c and κ_z^c, for applied bending moment $\bar{M}_y^c$ or $\bar{M}_z^c$.

The method to obtain the curvatures from the finite element analysis is explained in Appendix A [16].

Table 4-2 Comparison of bending stiffness obtained from mechanics theory and present method.

Isometric Bending Stiffness			
Property	Method		% Difference
	Mechanics	Present Method	
$\overline{D}_y$ (lb-in^2)	143980	143979	0.0
$\overline{D}_z$ (lb-in^2)	56218	56218	0.0
$\overline{D}_{yz}$ (lb-in^2)	-71576	-71575	0.0

Table 4-3 Comparison of bending curvatures obtained from mechanics theory, present method and finite element analysis.

	Bending curvature - $\bar{M}_y^c = 0.1$			
Property	Method			% Difference Eqn. vs FEA
	Mechanics	Present Method	FEA	
κ_y^c (1/in)	1.892E-06	1.892E-06	1.882E-06	-0.531
κ_z^c (1/in)	2.41E-06	2.411E-06	2.388E-06	-0.963

	Bending curvature - $\bar{M}_z^c = 0.1$			
Property	Method			% Difference Eqn. vs FEA
	Mechanics	Present Method	FEA	
κ_y^c (1/in)	2.41E-06	2.411E-06	2.39E-06	-0.879
κ_z^c (1/in)	4.846E-06	4.846E-06	4.823E-06	-0.477

4.5 Thermal Model Validation

To validate the developed equations for the temperature induced moments on Z-beam, a finite element thermal analysis was to be performed on the laminated Z-beam. To validate the finite element thermal techniques, a finite element thermal analysis was performed on the isotropic Z-beam model.

4.5.1 Thermal Model Description

Thermal model was similar to the developed and validated finite element model, but with some minor modifications. It had different boundary conditions and results extraction techniques. The model was connected to its centroids on both ends by multi point constraints, the slave nodes on both ends of the beam shared boundary conditions with the master nodes, which were centroidal nodes.

All degrees of freedom were constrained for the centroidal node on the origin end of the beam, and only y and z directional displacements were constrained for the centroid at the force end of the Z-beam.

Temperature gradients on sections will generate forces and moments in the beam and as force end of the beam cannot displace in z and y directions, the beam can elongate in x-direction, hence, the moments were captured as reaction moments at the origin end centroidal node.

4.5.2 Validation of Temperature Induced Moment Model

The finite element thermal model was validated by comparing the temperature induced moments for an isotropic Z-beam of identical cross-sectional geometry. The moments obtained from the isotropic Equations 3.69 and 3.70 were compared against the moments obtained from the isotropic finite element model.

To validate the thermal model, top flange of the Z beam was subjected to a temperature gradient of 70 degree Fahrenheit, with web and bottom flange experiencing zero change in temperature.

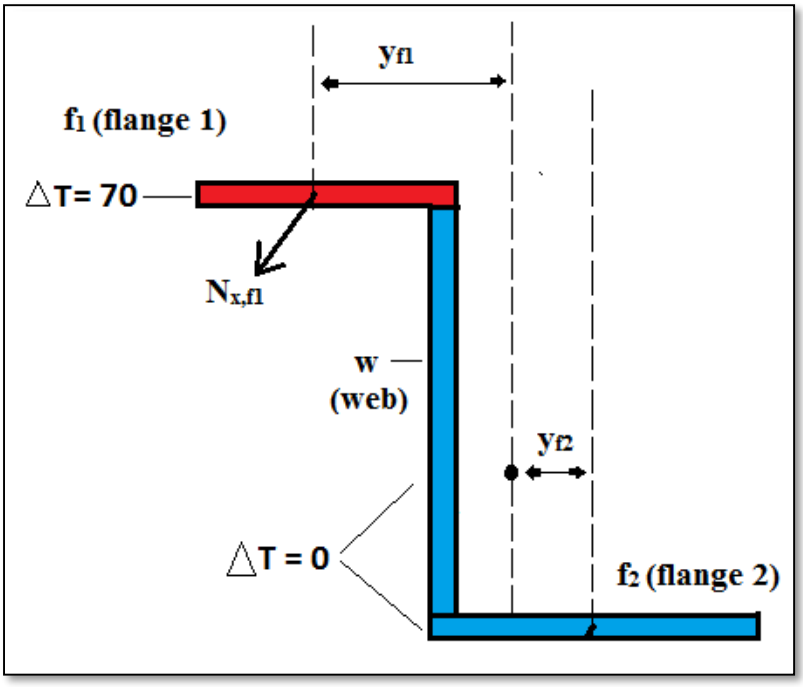

Figure 4.6: Temperature gradients in sections for model validation.

Table 4-4 Comparison of moments obtained from FEA and equations for isotropic beam.

Property	Unit	FEA (M_y^{cT})	Present Method (M_y^{cT})	% Diff.	FEA (M_z^{cT})	Present Method (M_z^{cT})	% Diff.
Moment	lb-in	108.2	106.6	1.4	-59.4	-56.8	4.3

Chapter 5

RESULTS AND DISCUSSIONS

This chapter covers detailed validation of the results for the analytical equations developed in Chapter 3. The results were compared for different layer arrangements.

5.1 Material and Stacking Sequence

The material with following properties was used to obtain the results throughout the study. The composite laminate was 0.005" thick AS4/3501-6 graphite/epoxy laminate, unidirectional layer orthotropic properties for which are given as.

$E_1 = 19.3 * 10^6$ psi	$E_2 = 1.62 * 10^6$ psi	$E_1 = 1.62 * 10^6$ psi
$\nu_{12} = 0.288$	$\nu_{23} = 0.288$	$\nu_{13} = 0.288$
$G_{12} = 1.02 * 10^6$ psi	$G_{23} = 1.02 * 10^6$ psi	$G_{13} = 1.02 * 10^6$ psi
$\alpha_1 = 2.0 * 10^{-6}$ in/in/^{0}F	$\alpha_2 = 15 * 10^{-6}$ in/in/^{0}F	$\alpha_3 = 15 * 10^{-6}$ in/in/^{0}F

Where E_1, E_1, and E_1 are the Young's moduli of the composite lamina along the material coordinates. G_{12}, G_{12}, G_{12} and are the Shear moduli and ν_{12} , ν_{23}, and ν_{13} are Poisson's ratio with respect to the 1-2, 2-3 and 1-3 planes, respectively.

Different layer arrangements were considered for the results comparison. In this section each layer arrangement will be given a case number which will be used in results comparison tables.

The cross-sectional geometry of the beam depended on the stacking sequence and number of plies used, that effected the height of the sections. The width of sections was not altered for any of the cases. The web was 1 inches wide, top flange was 0.5 inches wide and the bottom flange was 0.7 inches wide.

The cases are listen in the table on next page.

Table 5-1 Results comparison cases and stacking sequence

Case	Description	Layup for Top Flange (0.5 in wide)	Layup for Bottom Flange (0.7 in wide)	Layup for Web
1	Balanced and Symmetric	$[\pm 45/\ 0/\ 90\ ]_S$	$[\pm 45/\ 0/\ 90\ ]_S$	$[\pm 45]_S$
2	Balanced and Symmetric	$[\pm 45/\ 0/\ 90\ ]_S$	$[\pm 45/\ 0_2/\ 90\ ]_S$	$[\pm 45]_S$
3	Balanced and Asymmetric	$[\pm 45/0/90/0/90/\pm 45]_T$	$[\pm 45/0/90/0/90/\pm 45]_T$	$[\pm 45]_S$
4	Unbalanced and Asymmetric	$[\pm 45/\text{-}60/15/30/0/\pm 45]_T$	$[\pm 45/\text{-}60/15/30/0/\pm 45]_T$	$[\pm 45]_S$

The stacking sequences for the cases listed in table 5.1 were determined by understanding the role of stacking sequence on the practical manufacturing of laminated beam of Z-Section. The arrangement and its respective modeling was carefully examined and the web was kept symmetric for all the cases, which is desirable for the practical application of Z-Beam.

5.2 Centroid Locations for Results Comparison Cases

The centroid of a composite beam or laminate depends on the geometry, stacking sequence and ply orientation, unlike isotropic materials. The centroid locations of isotropic case and for all the cases listed above are listed in the following table. The centroid locations are according to the Figure 3.2 in chapter 3.

Table 5-2 Centroid locations for result cases

Case	Description	Centroid $\bar{z}_c$ (in)	Centroid $\bar{y}_c$ (in)
1	Balanced and Symmetric	0.466	0.573
2	Balanced and Symmetric	0.369	0.633
3	Balanced and Asymmetric	0.466	0.573
4	Unbalanced and Asymmetric	0.467	0.572

5.3 Results Comparison for Axial Stiffness

The results for axial stiffness from finite element analysis were compared with the results obtained from developed equations. The results comparison for all the cases is provided in the following table.

Table 5-3 Axial Stiffness Comparison

Case	Property	Unit	Present Method	FEA	% Difference
1	$\bar{A}_x$	(In-lb)/in	4.436E5	4.424E5	-0.251
2	$\bar{A}_x$	(In-lb)/in	5.787E5	5.779E5	-0.125
3	$\bar{A}_x$	(In-lb)/in	4.430E5	4.423E5	-0.161
4	$\bar{A}_x$	(In-lb)/in	4.222E5	4.223E5	0.026

5.4 Results Comparison for Bending Stiffness

The results for bending stiffness comparison are listed in this section. As described in section 4.4.2 of Chapter 4, curvatures and stresses from finite element analysis were compared with the curvature and stresses obtained from the developed equations. The bending curvatures were obtained by applying both moments $\bar{M}_y^c$ and $\bar{M}_z^c$, the moments were applied by applying two equal and opposite forces of 5 lb in magnitude and both forces were applied at 0.01" from the centroid, hence the magnitude of both applied moments is 0.1 lb-in.

The values of bending stiffness were obtained from the developed equations, bending stiffness values were used to obtain the curvature values by using Equation 4.5 thru 4.8. The curvature values were obtained by applying only one moment and keeping other moment as zero. Both moments were applied by one by one and curvature values were obtained from both moments were compared with the curvature values obtained from finite element analysis. The equations to obtain the curvature are listed below.

All the stresses were obtained by applying moment $\bar{M}_y^c$ of magnitude 0.1 lb-in at the centroid.

Result comparison tables are listed from next page onwards.

Table 5-4 Bending Stiffness and curvature values

Bending Stiffness Values – Current Method							
Case #	Property	Unit	Value	Curvatures – Present Method			
				$\bar{M}_y^c = 0.1$ lb-in		$\bar{M}_z^c = 0.1$ lb-in	
				κ_y^c (1/in)	κ_z^c (1/in)	κ_y^c (1/in)	κ_z^c (1/in)
1	$\bar{D}_y$	(lb-in^2)	1.047e+05	2.951e-06	3.771e-06	3.771e-06	7.123e-06
	$\bar{D}_z$	(lb-in^2)	4.339e+04				
	$\bar{D}_{yz}$	(lb-in^2)	-5.544e+04				
2	$\bar{D}_y$	(lb-in^2)	1.057e+05	2.929e-06	3.761e-06	3.761e-06	7.135e-06
	$\bar{D}_z$	(lb-in^2)	4.339e+04				
	$\bar{D}_{yz}$	(lb-in^2)	-5.573e+04				
3	$\bar{D}_y$	(lb-in^2)	1.046e+05	2.954e-06	3.774e-06	3.774e-06	7.131e-06
	$\bar{D}_z$	(lb-in^2)	4.332e+04				
	$\bar{D}_{yz}$	(lb-in^2)	-5.536e+04				
4	$\bar{D}_y$	(lb-in^2)	9.908e+04	3.002e-06	3.805e-06	3.805e-06	7.266e-06
	$\bar{D}_z$	(lb-in^2)	4.094e+04				
	$\bar{D}_{yz}$	(lb-in^2)	-5.189e+04				

Table 5-5 Bending Stiffness Curvature Comparison for applied M_y^c.

Bending curvature - $\bar{M}_y^c = 0.1$					
Case	Property	Unit	Present Method	FEA	% Difference
1	κ_y^c	(1/in)	2.951E-06	2.953E-06	0.07
	κ_z^c	(1/in)	3.771E-06	3.777E-06	0.16
2	κ_y^c	(1/in)	2.928E-06	2.93E-06	0.07
	κ_z^c	(1/in)	3.761E-06	3.768E-06	0.19
3	κ_y^c	(1/in)	2.953E-06	2.955E-06	0.07
	κ_z^c	(1/in)	3.774E-06	3.746E-06	-0.75
4	κ_y^c	(1/in)	3.0022e-06	3.11E-06	2.99
	κ_z^c	(1/in)	3.8054e-06	3.874E-06	1.29

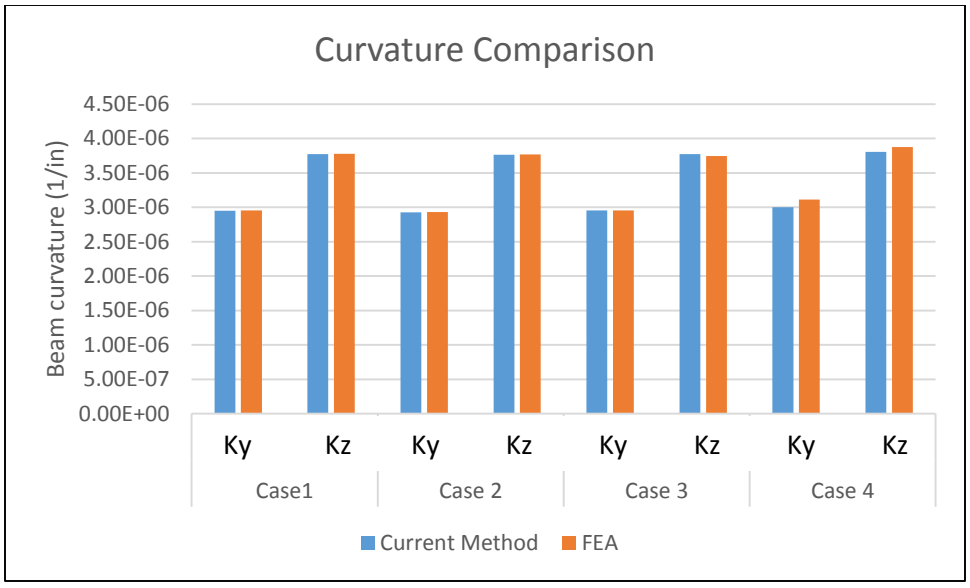

Graph 5-1: Comparison of Bending Curvatures for applied moment M_y^c.

Table 5-6 Bending Stiffness Curvature Comparison for applied M_z^c.

Bending curvature - $\bar{M}_z^c = 0.1$					
Case	Property	Unit	Present Method	FEA	% Difference
1	κ_y^c	(1/in)	3.771E-06	3.788E-06	0.45
	κ_z^c	(1/in)	7.123E-06	7.098E-06	-0.35
2	κ_y^c	(1/in)	3.761E-06	3.758E-06	-0.08
	κ_z^c	(1/in)	7.135E-06	7.142E-06	0.10
3	κ_y^c	(1/in)	3.774E-06	3.748E-06	-0.69
	κ_z^c	(1/in)	7.131E-06	7.099E-06	-0.45
4	κ_y^c	(1/in)	3.8054e-06	3.962E-06	3.48
	κ_z^c	(1/in)	7.2660e-06	7.394E-06	1.20

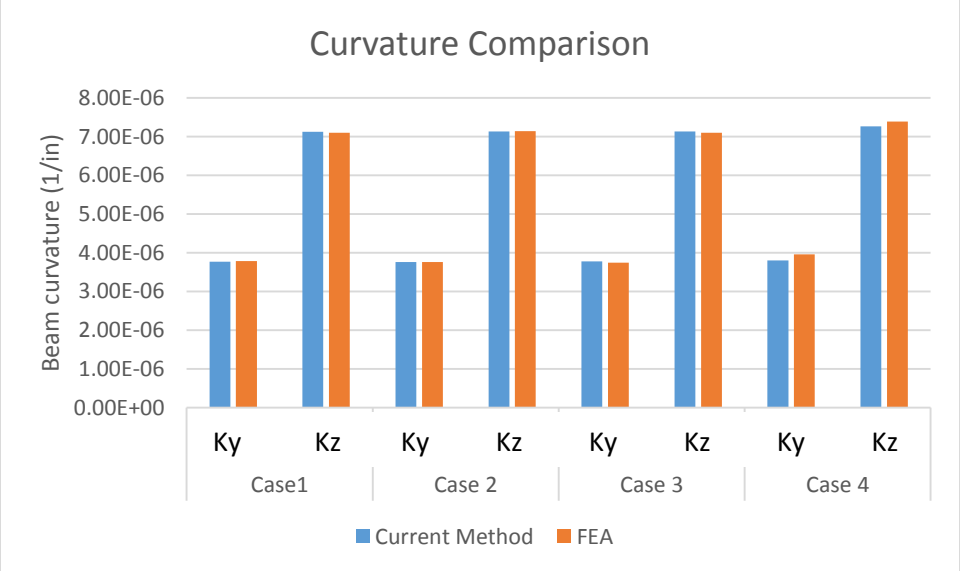

Graph 5-2: Comparison of Bending Curvatures for applied moment M_z^c.

Table 5-7 Bending Stiffness Stress Comparison for case 1 – Top Flange

Case 1- Balance and Symmetric – Top Flange $[\pm 45/\ 0/\ 90\ ]_S$						
Ply #	Ply orientation	Property	Unit	Present Method	FEA	% Difference
1	+45	σ_x	lb/in^2	2.973	2.998	0.83
		σ_y	lb/in^2	1.376	1.402	1.85
		τ_{xy}	lb/in^2	1.752	1.821	3.79
2	-45	σ_x	lb/in^2	2.966	2.985	0.64
		σ_y	lb/in^2	1.418	1.561	9.16
		τ_{xy}	lb/in^2	-1.782	-1.825	2.36
3	0	σ_x	lb/in^2	10.842	11.552	6.15
		σ_y	lb/in^2	-0.025	-0.027	7.41
		τ_{xy}	lb/in^2	-0.003	-0.003	0.00
4	90	σ_x	lb/in^2	0.818	0.854	4.22
		σ_y	lb/in^2	-2.921	-2.857	-2.24
		τ_{xy}	lb/in^2	-0.002	-0.002	0.00
5	90	σ_x	lb/in^2	0.778	0.801	2.87
		σ_y	lb/in^2	-2.576	-2.652	2.87
		τ_{xy}	lb/in^2	0.002	0.002	0.00
6	0	σ_x	lb/in^2	9.702	10.341	6.18
		σ_y	lb/in^2	0.009	0.01	10.00
		τ_{xy}	lb/in^2	0.003	0.003	0.00
7	-45	σ_x	lb/in^2	2.591	2.681	3.36
		σ_y	lb/in^2	1.338	1.412	5.24
		τ_{xy}	lb/in^2	-1.585	-1.621	2.22
8	+45	σ_x	lb/in^2	2.584	2.642	2.20
		σ_y	lb/in^2	1.381	1.4	1.36
		τ_{xy}	lb/in^2	1.614	1.7	5.06

Table 5-8 Bending Stiffness Stress Comparison for case 1 – Bottom Flange

Case 1- Balance and Symmetric – Bottom Flange $[\pm 45/\ 0/\ 90\ ]_S$						
Ply #	Ply orientation	Property	Unit	Present Method	FEA	% Difference
1	+45	σ_x	lb/in^2	-1.63	-1.58	-3.2
		σ_y	lb/in^2	-0.908	-0.879	-3.3
		τ_{xy}	lb/in^2	-1.037	-1.021	-1.6
2	-45	σ_x	lb/in^2	-1.637	-1.587	-3.2
		σ_y	lb/in^2	-0.865	-0.845	-2.4
		τ_{xy}	lb/in^2	1.007	1.001	-0.6
3	0	σ_x	lb/in^2	-6.177	-5.841	-5.8
		σ_y	lb/in^2	-0.011	-0.01	-10.0
		τ_{xy}	lb/in^2	-0.003	-0.003	0.0
4	90	σ_x	lb/in^2	-0.504	-0.512	1.6
		σ_y	lb/in^2	1.632	1.717	5.0
		τ_{xy}	lb/in^2	-0.002	-0.002	0.0
5	90	σ_x	lb/in^2	-0.544	-0.556	2.2
		σ_y	lb/in^2	1.978	1.998	1.0
		τ_{xy}	lb/in^2	0.002	0.002	0.0
6	0	σ_x	lb/in^2	-7.316	-7.21	-1.5
		σ_y	lb/in^2	0.022	0.024	8.3
		τ_{xy}	lb/in^2	0.003	0.003	0.0
7	-45	σ_x	lb/in^2	-2.012	-1.981	-1.6
		σ_y	lb/in^2	-0.945	-0.931	-1.5
		τ_{xy}	lb/in^2	1.204	1.187	-1.4
8	+45	σ_x	lb/in^2	-2.019	-1.987	-1.6
		σ_y	lb/in^2	-0.903	-0.874	-3.3
		τ_{xy}	lb/in^2	-1.175	-1.112	-3.2

Table 5-9 Bending Stiffness Stress Comparison for case 1 – Web

Case 1- Balance and Symmetric – Web $[\pm 45]_S$						
Ply #	Ply orientation	Property	Unit	Current Method	FEA	% Difference
1	+45	σ_x	lb/in^2	-0.244	-0.256	4.69
		σ_y	lb/in^2	-0.011	-0.012	8.33
		τ_{xy}	lb/in^2	-0.118	-0.121	1.67
2	-45	σ_x	lb/in^2	-0.244	-0.254	3.94
		σ_y	lb/in^2	0.041	0.042	4.76
		τ_{xy}	lb/in^2	0.075	0.078	3.85
3	-45	σ_x	lb/in^2	-0.516	-0.528	2.27
		σ_y	lb/in^2	-0.080	-0.083	0.00
		τ_{xy}	lb/in^2	0.256	0.268	4.48
4	+45	σ_x	lb/in^2	-0.380	-0.412	5.00
		σ_y	lb/in^2	0.006	0.006	0.00
		τ_{xy}	lb/in^2	-0.144	-0.145	0.69

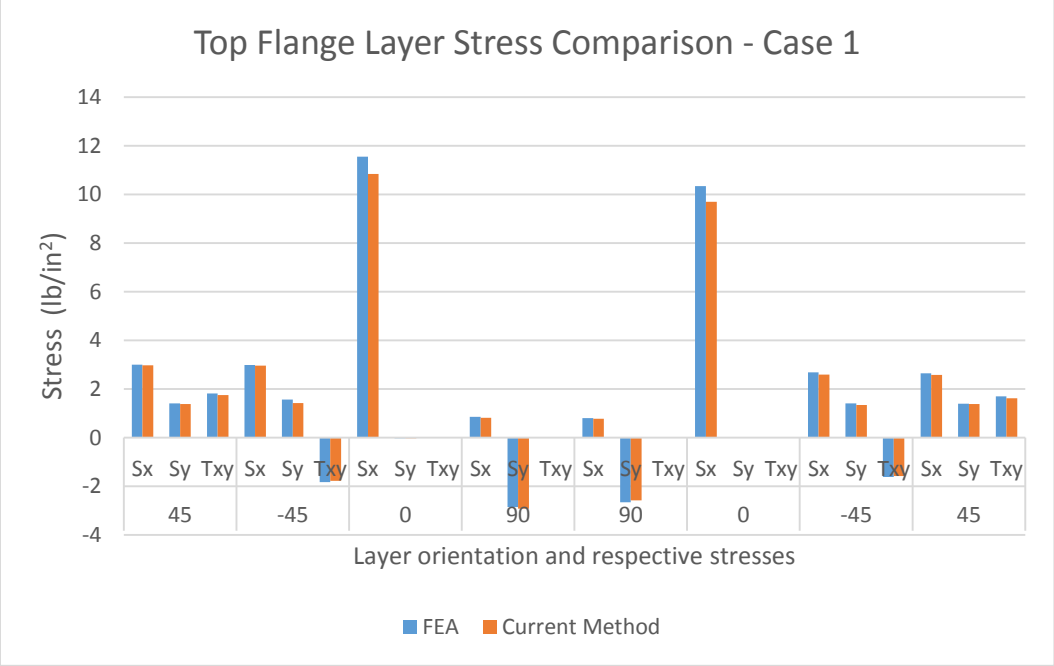

Graph 5-3: Comparison of Stresses in layers of top-flange sub-laminate for case 1.

Table 5-10 Bending Stiffness Stress Comparison for case 2 – Top Flange

Case 2- Balance and Symmetric – Top Flange $[\pm 45/\ 0/\ 90\ ]_S$						
Ply #	Ply orientation	Property	Unit	Present Method	FEA	% Difference
1	+45	σ_x	lb/in^2	2.956	2.998	1.40
		σ_y	lb/in^2	1.368	1.421	3.73
		τ_{xy}	lb/in^2	1.743	1.766	1.30
2	-45	σ_x	lb/in^2	2.949	3.102	4.93
		σ_y	lb/in^2	1.411	1.621	11.88
		τ_{xy}	lb/in^2	-1.772	-1.821	2.69
3	0	σ_x	lb/in^2	10.78	11.312	4.69
		σ_y	lb/in^2	-0.024	-0.026	7.69
		τ_{xy}	lb/in^2	-0.003	-0.003	0.00
4	90	σ_x	lb/in^2	0.813	0.854	4.80
		σ_y	lb/in^2	-2.905	-3.113	6.68
		τ_{xy}	lb/in^2	-0.002	-0.002	0.00
5	90	σ_x	lb/in^2	0.773	0.785	1.53
		σ_y	lb/in^2	-2.562	-2.654	3.47
		τ_{xy}	lb/in^2	0.002	0.0019	-5.26
6	0	σ_x	lb/in^2	9.649	10.21	5.49
		σ_y	lb/in^2	0.009	0.01	10.00
		τ_{xy}	lb/in^2	0.003	0.003	0.00
7	-45	σ_x	lb/in^2	2.577	2.687	4.09
		σ_y	lb/in^2	1.331	1.432	7.05
		τ_{xy}	lb/in^2	-1.576	-1.658	4.95
8	+45	σ_x	lb/in^2	2.570	2.741	6.20
		σ_y	lb/in^2	1.373	1.412	2.62
		τ_{xy}	lb/in^2	1.606	1.721	6.68

Table 5-11 Bending Stiffness Stress Comparison for case 2 – Bottom Flange

Case 2- Balance and Symmetric – Bottom Flange $[\pm 45/\ 0_2/\ 90/\ ]_S$						
Ply #	Ply orientation	Property	Unit	Present Method	FEA	% Difference
1	+45	σ_x	lb/in^2	-1.579	-1.545	-2.20
		σ_y	lb/in^2	-0.904	-0.876	-3.20
		τ_{xy}	lb/in^2	-1.014	-0.987	-2.74
2	-45	σ_x	lb/in^2	-1.589	-1.521	-4.47
		σ_y	lb/in^2	-0.865	-0.845	-2.37
		τ_{xy}	lb/in^2	0.988	0.953	-3.67
3	0	σ_x	lb/in^2	-5.901	-5.754	-2.55
		σ_y	lb/in^2	-0.021	-0.021	0.00
		τ_{xy}	lb/in^2	-0.003	-0.003	0.00
4	0	σ_x	lb/in^2	-6.182	-5.897	-4.83
		σ_y	lb/in^2	-0.012	-0.011	-9.09
		τ_{xy}	lb/in^2	-0.002	-0.002	0.00
5	90	σ_x	lb/in^2	-0.504	-0.478	-5.44
		σ_y	lb/in^2	1.628	1.597	-1.94
		τ_{xy}	lb/in^2	-0.001	-0.001	0.00
6	0	σ_x	lb/in^2	-7.307	-7.212	-1.35
		σ_y	lb/in^2	0.022	0.020	-10.00
		τ_{xy}	lb/in^2	0.002	0.002	0.00
7	0	σ_x	lb/in^2	-7.588	-7.325	-3.59
		σ_y	lb/in^2	0.03	0.028	-7.14
		τ_{xy}	lb/in^2	0.003	0.003	0.00
8	90	σ_x	lb/in^2	-0.544	-0.531	-8.80
		σ_y	lb/in^2	1.976	1.887	-4.72

		τ_{xy}	lb/in^2	0.001	0.001	0.00
9	-45	σ_x	lb/in^2	-2.061	-1.985	-3.83
		σ_y	lb/in^2	-0.947	-0.911	-3.95
		τ_{xy}	lb/in^2	1.224	1.184	-3.73
10	+45	σ_x	lb/in^2	-2.071	-1.998	-3.65
		σ_y	lb/in^2	-0.907	-0.925	-0.78
		τ_{xy}	lb/in^2	-1.198	-1.098	-9.11

Table 5-12 Bending Stiffness Stress Comparison for case 2 – Web

Case 2- Balance and Symmetric – Web $[\pm 45]_S$						
Ply #	Ply orientation	Property	Unit	Current Method	FEA	% Difference
1	+45	σ_x	lb/in^2	-0.223	-0.211	-5.69
		σ_y	lb/in^2	-0.011	-0.011	0.00
		τ_{xy}	lb/in^2	-0.110	-0.106	-3.77
2	-45	σ_x	lb/in^2	-0.223	-0.208	-7.21
		σ_y	lb/in^2	0.04	0.038	-5.26
		τ_{xy}	lb/in^2	0.067	0.065	-3.08
3	-45	σ_x	lb/in^2	-0.493	-0.472	-4.45
		σ_y	lb/in^2	-0.079	-0.072	-9.72
		τ_{xy}	lb/in^2	0.246	0.229	-7.42
4	+45	σ_x	lb/in^2	-0.357	-0.345	-3.48
		σ_y	lb/in^2	0.006	0.006	0.00
		τ_{xy}	lb/in^2	-0.135	-0.125	-8.00

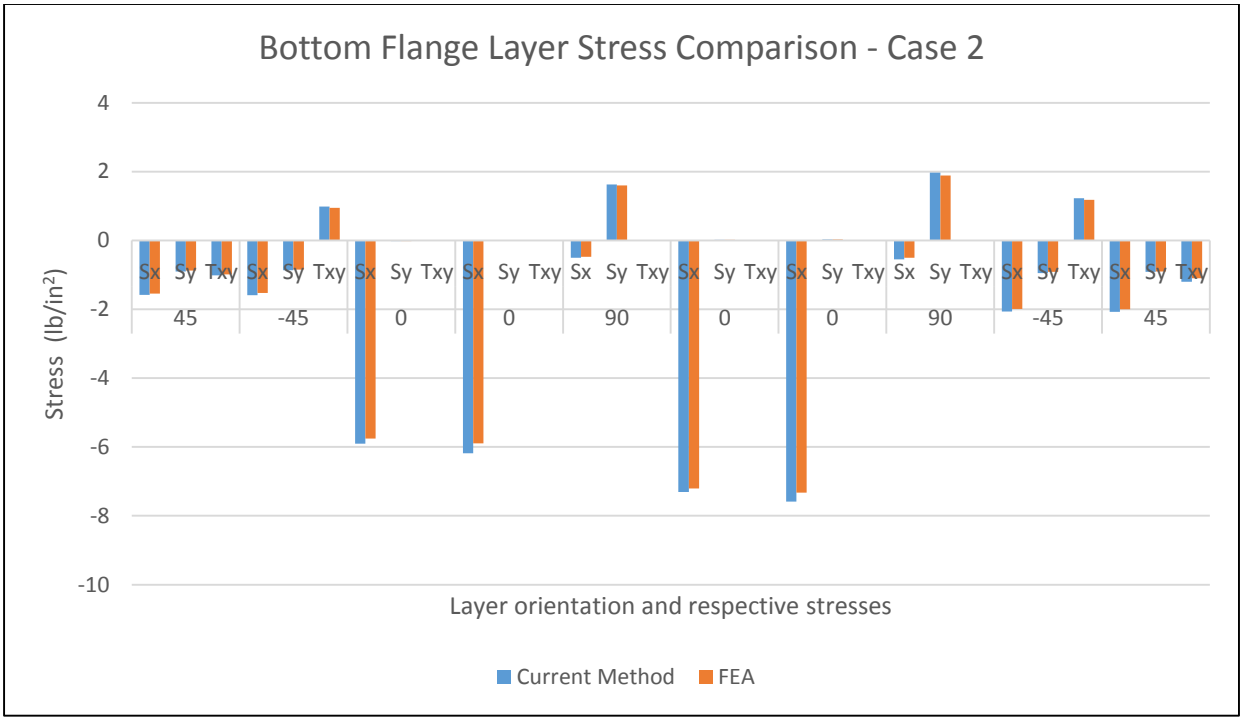

Graph 5-4: Comparison of Stresses in layers of bottom-flange sub-laminate for case 2.

Table 5-13 Bending Stiffness Stress Comparison for case 3– Top Flange

Case 3- Balance and Asymmetric – Top Flange $[\pm 45/0/90/0/90/\pm 45]_T$						
Ply #	Ply orientation	Property	Unit	Present Method	FEA	% Difference
1	+45	σ_x	lb/in^2	3.121	3.21	2.77
		σ_y	lb/in^2	1.605	1.711	6.20
		τ_{xy}	lb/in^2	1.888	1.942	2.78
2	-45	σ_x	lb/in^2	3.159	3.265	3.25
		σ_y	lb/in^2	1.671	1.821	8.24
		τ_{xy}	lb/in^2	-1.976	-1.985	0.45
3	0	σ_x	lb/in^2	10.881	11.312	3.81
		σ_y	lb/in^2	0.011	0.011	0.00
		τ_{xy}	lb/in^2	-0.009	-0.009	0.00
4	90	σ_x	lb/in^2	0.824	0.874	5.72
		σ_y	lb/in^2	-2.726	-2.895	5.84
		τ_{xy}	lb/in^2	-0.005	-0.005	0.00
5	0	σ_x	lb/in^2	9.988	10.243	2.49
		σ_y	lb/in^2	-0.018	-0.017	-5.88
		τ_{xy}	lb/in^2	0.005	0.005	0.00
6	90	σ_x	lb/in^2	0.748	0.801	6.62
		σ_y	lb/in^2	-2.825	-2.913	3.02
		τ_{xy}	lb/in^2	0.009	0.009	0.00
7	-45	σ_x	lb/in^2	2.402	2.564	6.32
		σ_y	lb/in^2	1.085	1.121	3.21
		τ_{xy}	lb/in^2	-1.393	-1.451	4.00
8	+45	σ_x	lb/in^2	2.44	2.64	7.58
		σ_y	lb/in^2	1.151	1.254	8.21
		τ_{xy}	lb/in^2	1.480	1.511	2.05

Table 5-14 Bending Stiffness Stress Comparison for Case 3– Bottom Flange

Case 3- Balance and Asymmetric – Bottom Flange $[\pm 45/0/90/0/90/\pm 45]_T$						
Ply #	Ply orientation	Property	Unit	Current Method	FEA	% Difference
1	+45	σ_x	lb/in^2	-1.687	-1.612	-4.65
		σ_y	lb/in^2	-0.998	-0.946	-5.50
		τ_{xy}	lb/in^2	-1.088	-1.073	-1.40
2	-45	σ_x	lb/in^2	-1.716	-1.651	-3.94
		σ_y	lb/in^2	-0.968	-0.913	-6.02
		τ_{xy}	lb/in^2	1.087	1.025	-6.05
3	0	σ_x	lb/in^2	-6.191	-5.982	-3.51
		σ_y	lb/in^2	-0.023	-0.021	-9.5
		τ_{xy}	lb/in^2	0	0	0
4	90	σ_x	lb/in^2	-0.505	-0.497	-1.61
		σ_y	lb/in^2	1.604	1.543	-3.95
		τ_{xy}	lb/in^2	0	0	0
5	0	σ_x	lb/in^2	-7.031	-6.696	-5.00
		σ_y	lb/in^2	0.029	0.025	-16.00
		τ_{xy}	lb/in^2	0	0	0
6	90	σ_x	lb/in^2	-0.558	-0.524	-6.49
		σ_y	lb/in^2	2.435	2.354	-3.44
		τ_{xy}	lb/in^2	0	0	0
7	-45	σ_x	lb/in^2	-1.903	-1.875	-1.49
		σ_y	lb/in^2	-0.795	-0.752	-5.72
		τ_{xy}	lb/in^2	1.093	1.078	-1.39
8	+45	σ_x	lb/in^2	-1.932	-1.852	-4.32
		σ_y	lb/in^2	-0.764	-0.711	-7.45
		τ_{xy}	lb/in^2	-1.092	-1.012	-7.91

Table 5-15 Bending Stiffness Stress Comparison for Case 4– Top Flange

Case 4- Unbalance and Asymmetric – Top Flange $[\pm 45/\text{-}60/15/30/0/\pm 45]_T$						
Ply #	Ply orientation	Property	Unit	Present Method	FEA	% Difference
1	+45	σ_x	lb/in^2	1.453	1.497	6.92
		σ_y	lb/in^2	-0.635	-0.701	2.00
		τ_{xy}	lb/in^2	0.109	0.107	13.10
2	-45	σ_x	lb/in^2	2.818	2.816	0.07
		σ_y	lb/in^2	0.794	0.487	8.01
		τ_{xy}	lb/in^2	-1.688	-1.501	3.53
3	-60	σ_x	lb/in^2	0.806	0.722	5.56
		σ_y	lb/in^2	-1.632	-2.225	6.34
		τ_{xy}	lb/in^2	0.251	0.521	11.32
4	15	σ_x	lb/in^2	8.611	8.851	2.63
		σ_y	lb/in^2	0.090	0.058	13.79
		τ_{xy}	lb/in^2	1.748	1.845	5.47
5	30	σ_x	lb/in^2	4.372	4.652	5.72
		σ_y	lb/in^2	0.504	0.564	9.04
		τ_{xy}	lb/in^2	1.648	1.754	6.16
6	0	σ_x	lb/in^2	10.016	10.783	6.41
		σ_y	lb/in^2	-0.275	-0.266	8.65
		τ_{xy}	lb/in^2	-0.168	-0.201	10.95
7	-45	σ_x	lb/in^2	2.713	3.103	5.22
		σ_y	lb/in^2	1.066	1.401	3.35
		τ_{xy}	lb/in^2	-1.769	-2.141	6.73
8	+45	σ_x	lb/in^2	1.199	1.465	6.76
		σ_y	lb/in^2	-0.385	-0.153	13.33
		τ_{xy}	lb/in^2	0.088	0.256	7.42

Table 5-16 Bending Stiffness Stress Comparison for Case 4– Bottom Flange

Case 4- Unbalance and Asymmetric – Bottom Flange $[\pm 45/\text{-}60/15/30/0/\pm 45]_T$						
Ply #	Ply orientation	Property	Unit	Current Method	FEA	% Difference
1	+45	σ_x	lb/in^2	-0.644	-0.443	-4.29
		σ_y	lb/in^2	0.385	0.625	-6.88
		τ_{xy}	lb/in^2	0.025	0.196	-4.59
2	-45	σ_x	lb/in^2	-1.547	-1.315	-4.41
		σ_y	lb/in^2	-0.475	-0.21	-6.67
		τ_{xy}	lb/in^2	0.955	0.719	-8.07
3	-60	σ_x	lb/in^2	-0.483	-0.412	4.37
		σ_y	lb/in^2	0.864	1.161	-1.29
		τ_{xy}	lb/in^2	-0.100	-0.223	-11.21
4	15	σ_x	lb/in^2	-5.258	-4.978	-5.77
		σ_y	lb/in^2	-0.057	-0.031	-9.68
		τ_{xy}	lb/in^2	-1.062	-1.047	-1.43
5	30	σ_x	lb/in^2	-3.107	-2.981	-5.37
		σ_y	lb/in^2	-0.370	-0.364	-8.24
		τ_{xy}	lb/in^2	-1.180	-1.121	-8.64
6	0	σ_x	lb/in^2	-7.549	-7.124	-6.71
		σ_y	lb/in^2	0.206	0.162	-6.79
		τ_{xy}	lb/in^2	0.118	0.121	-2.50
7	-45	σ_x	lb/in^2	-2.119	-2.102	-9.47
		σ_y	lb/in^2	-0.790	-1.011	-1.88
		τ_{xy}	lb/in^2	1.349	1.482	-3.38
8	+45	σ_x	lb/in^2	-1.113	-1.187	-7.58
		σ_y	lb/in^2	0.258	0.015	-6.67
		τ_{xy}	lb/in^2	-0.169	-0.324	0.93

Table 5-17 Bending Stiffness Stress Comparison for case 4 – Web

Case 4- Balance and Symmetric – Web $[\pm 45]_s$						
Ply #	Ply orientation	Property	Unit	Current Method	FEA	% Difference
1	+45	σ_x	lb/in^2	-0.237	-0.234	-1.28
		σ_y	lb/in^2	-0.012	-0.011	-9.09
		τ_{xy}	lb/in^2	-0.116	-0.115	-0.87
2	-45	σ_x	lb/in^2	-0.236	-0.231	-2.60
		σ_y	lb/in^2	0.041	0.038	-7.89
		τ_{xy}	lb/in^2	0.072	0.068	-5.88
3	-45	σ_x	lb/in^2	-0.513	-0.526	2.09
		σ_y	lb/in^2	-0.081	-0.079	-3.80
		τ_{xy}	lb/in^2	0.256	0.247	-4.05
4	+45	σ_x	lb/in^2	-0.374	-0.324	-16.05
		σ_y	lb/in^2	0.006	0.005	-20.00
		τ_{xy}	lb/in^2	-0.142	-0.137	-3.65

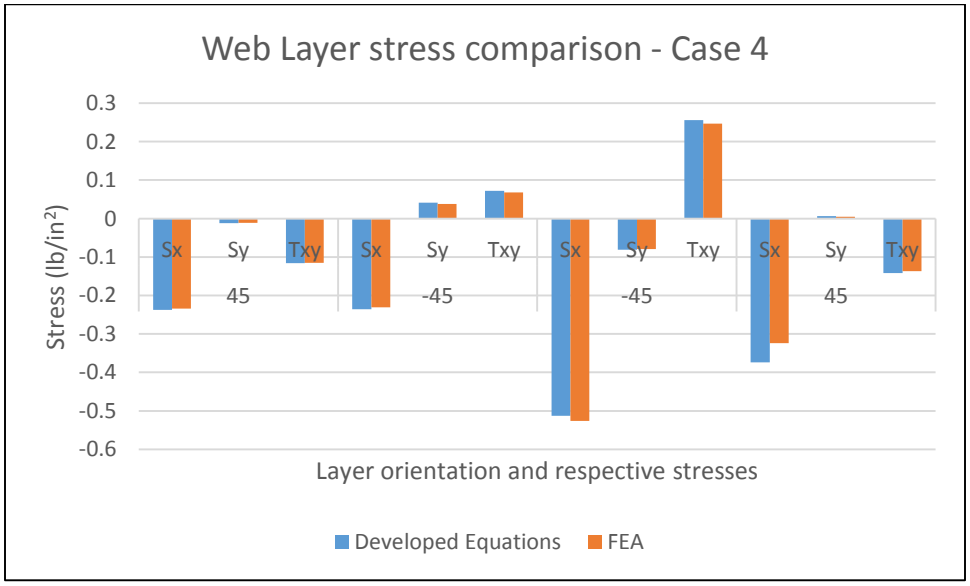

Graph 5-5: Comparison stresses in layers of web sub-laminate case 4.

5.5 Results Comparison for Thermal Moments

The results for temperature induced moments are listed in this section. Moments were applied in similar manner as explained in the validation sections of chapter 4. The moments generated by temperature gradient on sections will be compared in this section, different cases and conditions are listed in Table 5.17.

Table 5-18 Result comparison cases for thermal analysis

Case	Description	Layup for Top and Bottom Flange	Layup for Web	ΔT Top Flange (°F)	ΔT Bottom Flange (°F)	ΔT Web (°F)
1	Balanced and Symmetric	$[\pm 45/\ 0/\ 90\ ]_S$	$[\pm 45]_S$	70	0	0
3	Balanced and Symmetric	$[\pm 45/\ 0/\ 90\ ]_S$	$[\pm 45]_S$	30	120	0

The temperature induced moments were used to find the stresses in the layers of sub-laminates/sections by using method explained in Sections 3.4.5 and 3.4.6 of this document. The calculated stresses were compared with the stresses from finite element analysis. To find stresses from finite element analysis, temperature induced moments were inputted as mechanical loads on the same beam and stress values for each layer of sub-laminates were extracted.

5.5.1 Thermal moment comparison

Table 5-19 Thermal moment comparison – Case 1

Thermal Case – 1							
Property	Unit	FEA (M_y^{cT})	Present Method (M_y^{cT})	% Diff.	FEA (M_z^{cT})	Present Method (M_z^{cT})	% Diff.
Moment	lb-in	15.27	16.08	4.9	-28.81	-29.51	2.4

Table 5-20 Thermal Stress Comparison for Case 1 – Top Flange

Case 1- Balance and Symmetric – Top Flange ($\Delta T = 70$) $[\pm 45/\ 0/\ 90\ ]_S$						
Ply #	Ply orientation	Property	Unit	Present Method	FEA	% Difference
1	+45	σ_x	lb/in^2	503.67	515.23	2.24
		σ_y	lb/in^2	271.25	280.12	3.17
		τ_{xy}	lb/in^2	315.77	326.28	3.22
2	-45	σ_x	lb/in^2	505.21	520.31	2.90
		σ_y	lb/in^2	262.14	286.34	8.45
		τ_{xy}	lb/in^2	-309.33	-302.15	-2.38
3	0	σ_x	lb/in^2	1894	1947.15	2.73
		σ_y	lb/in^2	2.01	2.12	5.66
		τ_{xy}	lb/in^2	0.71	0.91	22.22
4	90	σ_x	lb/in^2	152.39	160.21	4.88
		σ_y	lb/in^2	-502.51	-480.57	-4.57
		τ_{xy}	lb/in^2	0.34	0.38	10.53
5	90	σ_x	lb/in^2	161.07	170.61	5.59
		σ_y	lb/in^2	-577.36	-544.39	-6.06
		τ_{xy}	lb/in^2	-0.34	-0.31	-9.68
6	0	σ_x	lb/in^2	2141.3	2210.2	3.12
		σ_y	lb/in^2	-5.22	-4.73	-10.64
		τ_{xy}	lb/in^2	-0.71	-0.62	-16.67
7	-45	σ_x	lb/in^2	586.39	612.34	4.24
		σ_y	lb/in^2	279.37	304.23	8.17
		τ_{xy}	lb/in^2	-352.08	-340.25	-3.48
8	+45	σ_x	lb/in^2	587.94	605.81	2.95
		σ_y	lb/in^2	270.26	284.51	5.01
		τ_{xy}	lb/in^2	503.67	515.23	2.24

Table 5-21 Thermal Stress Comparison for Case 1 – Bottom Flange

Case 1- Balance and Symmetric – Bottom Flange (ΔT = 0) $[\pm 45/\ 0/\ 90\ ]_S$						
Ply #	Ply orientation	Property	Unit	Present Method	FEA	% Difference
1	+45	σ_x	lb/in^2	-559.42	-532.64	-5.03
		σ_y	lb/in^2	-256.11	-248.15	-3.21
		τ_{xy}	lb/in^2	-328.36	-324.67	-1.14
2	-45	σ_x	lb/in^2	-557.88	-535.27	-4.22
		σ_y	lb/in^2	-265.23	-247.31	-7.25
		τ_{xy}	lb/in^2	334.81	336.31	0.36
3	0	σ_x	lb/in^2	-2035.8	-1986.3	-2.49
		σ_y	lb/in^2	5.14	4.85	-5.15
		τ_{xy}	lb/in^2	0.73	0.66	-6.06
4	90	σ_x	lb/in^2	-152.88	-142.57	-7.23
		σ_y	lb/in^2	549.15	536.36	-2.38
		τ_{xy}	lb/in^2	0.34	0.41	15.00
5	90	σ_x	lb/in^2	-144.22	-128.64	-12.10
		σ_y	lb/in^2	474.32	456.23	-3.96
		τ_{xy}	lb/in^2	-0.34	-0.4	15.00
6	0	σ_x	lb/in^2	-1789.11	-1687.52	-6.02
		σ_y	lb/in^2	-2.12	-2.05	-2.44
		τ_{xy}	lb/in^2	-0.73	-0.67	-4.48
7	-45	σ_x	lb/in^2	-476.69	-455.64	-4.62
		σ_y	lb/in^2	-247.99	-229.37	-8.12
		τ_{xy}	lb/in^2	292.05	304.12	3.97
8	+45	σ_x	lb/in^2	-475.15	-468.64	-1.39
		σ_y	lb/in^2	-257.11	-260.12	1.11
		τ_{xy}	lb/in^2	-559.42	-532.64	-5.03

Table 5-22 Thermal Stress Comparison for Case 1 – Web

Case 4- Balance and Symmetric – Web $[\pm 45]_S$						
Ply #	Ply orientation	Property	Unit	Present Method	FEA	% Difference
1	+45	σ_x	lb/in^2	247.38	257.42	3.90
		σ_y	lb/in^2	2.47	2.35	-5.10
		τ_{xy}	lb/in^2	104.37	112.35	7.10
2	-45	σ_x	lb/in^2	247.26	260.12	4.94
		σ_y	lb/in^2	-8.64	-7.86	-9.92
		τ_{xy}	lb/in^2	-95.05	-88.6	-7.27
3	-45	σ_x	lb/in^2	306.15	316.56	3.28
		σ_y	lb/in^2	17.28	19.01	9.10
		τ_{xy}	lb/in^2	-134.16	-140.25	4.34
4	+45	σ_x	lb/in^2	276.65	290.34	4.71
		σ_y	lb/in^2	-1.23	-1.22	-2.5
		τ_{xy}	lb/in^2	109.95	124.13	11.42

Table 5-23 Thermal moment comparison – Case 2

Thermal Case – 2							
Property	Unit	FEA (M_y^{cT})	Present Method (M_y^{cT})	% Diff.	FEA (M_z^{cT})	Present Method (M_z^{cT})	% Diff.
Moment	lb-in	20.766	18.03	-15.17	39.67	37.57	-5.59

Table 5-24 Thermal Stress Comparison for Case 2– Top Flange

Case 2- Balance and Symmetric – (Top Flange $\Delta T = 30$) (Bottom Flange $\Delta T = 120$) $[\pm 45/\ 0/\ 90\ ]_S$						
Ply #	Ply orientation	Property	Unit	Present Method	FEA	% Difference
1	+45	σ_x	lb/in^2	503.21	514.21	2.14
		σ_y	lb/in^2	184.34	195.17	5.55
		τ_{xy}	lb/in^2	272.57	287.53	5.20
2	-45	σ_x	lb/in^2	498.5	514.1	3.03
		σ_y	lb/in^2	212.15	227.48	6.74
		τ_{xy}	lb/in^2	-292.23	-301.21	2.98
3	0	σ_x	lb/in^2	1761.6	1875.54	6.08
		σ_y	lb/in^2	-12.14	-11.24	-6.76
		τ_{xy}	lb/in^2	-2.13	-2.24	6.25
4	90	σ_x	lb/in^2	120.83	132.45	8.77
		σ_y	lb/in^2	-484.81	-462.51	-4.82
		τ_{xy}	lb/in^2	-1.05	-1.12	6.25
5	90	σ_x	lb/in^2	94.34	104.43	9.66
		σ_y	lb/in^2	-256.47	-248.73	-3.11
		τ_{xy}	lb/in^2	1.05	1.11	4.55
6	0	σ_x	lb/in^2	1008.8	1124.82	10.31
		σ_y	lb/in^2	9.91	8.74	-13.27
		τ_{xy}	lb/in^2	2.13	2.21	4.98
7	-45	σ_x	lb/in^2	250.83	275.61	8.99
		σ_y	lb/in^2	159.57	165.32	3.48
		τ_{xy}	lb/in^2	-161.8	-174.52	7.29
8	+45	σ_x	lb/in^2	246.13	265.23	7.20
		σ_y	lb/in^2	187.38	196.5	4.64
		τ_{xy}	lb/in^2	503.21	514.21	2.14

Table 5-25 Stress Comparison for thermal Case 2 – Bottom Flange

Case 2- Balance and Asymmetric – (Top Flange $\Delta T = 30$) (Bottom Flange $\Delta T = 120$) $[\pm 45/\ 0/\ 90\ ]_S$						
Ply #	Ply orientation	Property	Unit	Present Method	FEA	% Difference
1	+45	σ_x	lb/in^2	84.56	93.52	9.58
		σ_y	lb/in^2	-23.34	-24.23	3.67
		τ_{xy}	lb/in^2	18.91	17.56	-7.69
2	-45	σ_x	lb/in^2	79.85	82.34	3.02
		σ_y	lb/in^2	4.47	5.02	10.96
		τ_{xy}	lb/in^2	-38.56	-36.74	-4.95
3	0	σ_x	lb/in^2	213.78	224.31	4.69
		σ_y	lb/in^2	-10.82	-11.24	3.74
		τ_{xy}	lb/in^2	-2.1	-2.21	4.98
4	90	σ_x	lb/in^2	0.61	0.62	-1.61
		σ_y	lb/in^2	-70.66	-75.34	6.21
		τ_{xy}	lb/in^2	-1.05	-1.1	4.55
5	90	σ_x	lb/in^2	-25.87	-26.38	1.93
		σ_y	lb/in^2	157.68	174.35	9.56
		τ_{xy}	lb/in^2	1.05	1.12	6.25
6	0	σ_x	lb/in^2	-539.02	-564.21	4.46
		σ_y	lb/in^2	11.07	12.19	9.19
		τ_{xy}	lb/in^2	2.1	2.31	9.09
7	-45	σ_x	lb/in^2	-167.82	-157.85	-6.32
		σ_y	lb/in^2	-48.11	-51.29	6.20
		τ_{xy}	lb/in^2	91.87	102.34	10.23
8	+45	σ_x	lb/in^2	-172.53	-185.64	7.06
		σ_y	lb/in^2	-20.3	-19.74	-2.84
		τ_{xy}	lb/in^2	84.56	93.52	9.58

Table 5-26 Thermal Stress Comparison for Case 2 – Web

Case 2- Balance and Asymmetric – (Top Flange $\Delta T = 30$) (Bottom Flange $\Delta T = 90$) $[\pm 45/0/90/0/90/\pm 45]_T$						
Ply #	Ply orientation	Property	Unit	Present Method	FEA	% Difference
1	+45	σ_x	lb/in^2	-408.87	-389.62	-4.94
		σ_y	lb/in^2	-7.53	-6.83	-9.29
		τ_{xy}	lb/in^2	-178.34	-167.82	-6.27
2	-45	σ_x	lb/in^2	-408.52	-419.54	2.63
		σ_y	lb/in^2	26.35	27.65	4.70
		τ_{xy}	lb/in^2	149.93	160.21	6.42
3	-45	σ_x	lb/in^2	-498.17	-513.13	2.92
		σ_y	lb/in^2	3.76	4.21	10.69
		τ_{xy}	lb/in^2	-195.38	-211.39	7.57
4	+45	σ_x	lb/in^2	-588.17	-612.84	4.03
		σ_y	lb/in^2	-52.7	-57.72	7.7
		τ_{xy}	lb/in^2	269.25	282.29	4.62

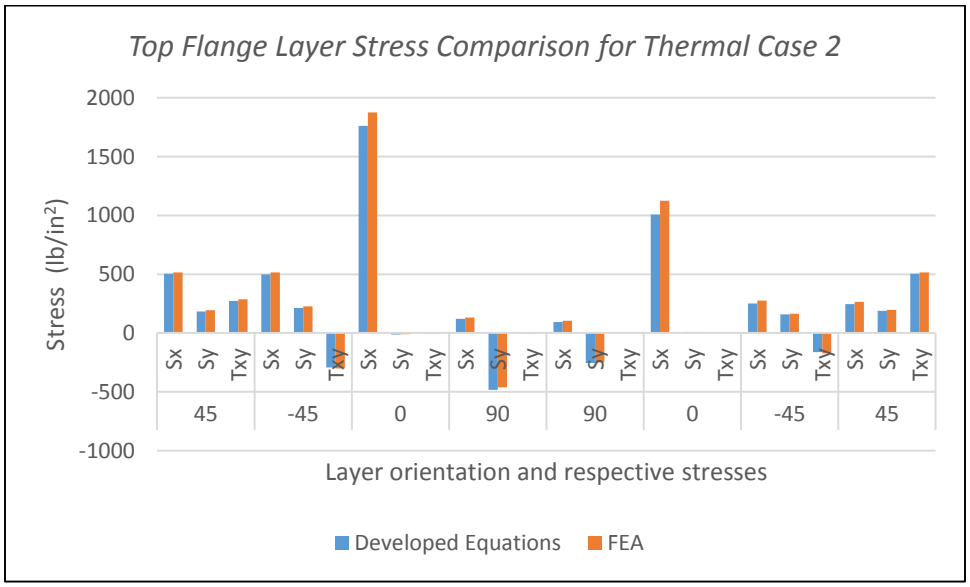

Graph 5-6: Comparison of Stresses in layers of top-flange for thermal case 2.

Chapter 6 CONCLUSION AND FUTURE WORK

An analytical method was developed to calculate centroid, equivalent axial stiffness, equivalent bending stiffness, and ply stresses due to mechanical axial and bending loading on a laminated composite beam of asymmetric Z cross-section. The method was extended to calculate the temperature induced moments about the centroid of the beam due to different temperature gradients on different sections of the beam. A finite element model was created to validate the equations, the results from finite element model were compared with the results obtained from analytical solution. To compare and validate the method, four parametrically different models were investigated for mechanical loading case, layup and ply orientation of the sub-laminates were the parameters varied in the models. To compare and validate the thermal model and equations, two parametrically different models were investigated, temperature gradients on the sections were the parameters for this case.

Following conclusions can be drawn from this research.

- Equivalent axial stiffness obtained from the finite element model were in excellent agreement with the analytical expressions for all four cases.
- The equivalent axial stiffness of balanced and symmetric (case 1) layup is almost equal to the axial stiffness of balanced and asymmetric (case 3), however the bending stiffness of the balanced and symmetric (case 1) is slightly greater than the balanced and asymmetric (case 3).
- The equivalent bending stiffness were validated by comparing curvatures and the curvatures in y and z directions obtained from the finite element model and analytical expressions showed excellent agreement with each other.
- The equivalent bending stiffness, of balanced and symmetric layup were greater than the equivalent bending stiffness of balanced and asymmetric, and unbalanced and asymmetric layups with same ply count.
- The temperature induced moments about the centroid, obtained from finite element model were in agreement with analytical expressions for all cases investigated.

- The temperature induced moments about the centroid, obtained from the analytical expressions can be substituted as mechanical loads at the centroid.
- The stresses in each ply of asymmetric Z-beam subjected to bending load at the centroid were in agreement with the stresses obtained analytically for all mechanical and thermal loading cases investigated in the research.
- The 0^0 ply above the mid-plane of top flange sub-laminate for balanced and symmetric case 1, exhibited maximum axial stress compared to 0^0 plies of all other cases, for same applied load.

The present method is a closed form analytical model which can be used in designing stage and can also be used for optimization, by inserting analytical equations in a programming software and varying the parameters.

The current method can be extended to find the shear center and to calculate the torsional and warping stiffness of this open section asymmetric Z-beam.

Appendix A

METHOD TO CALCULATE RADIUS OF CURVATURE FROM FINITE ELEMENT ANALYSIS

[16]

Basic geometrical techniques can be used to find the curvature of a curved beam, the beam can be treated as a line. Any three points on a line can be selected to determine the curvature of the line from the finite element model under bending. Let Points A, B, and C in Figure A.1 represent three arbitrary points on the line in finite element model with the following coordinates (x_1,y_1), (x_2,y_2), and (x_3,y_3) respectively.

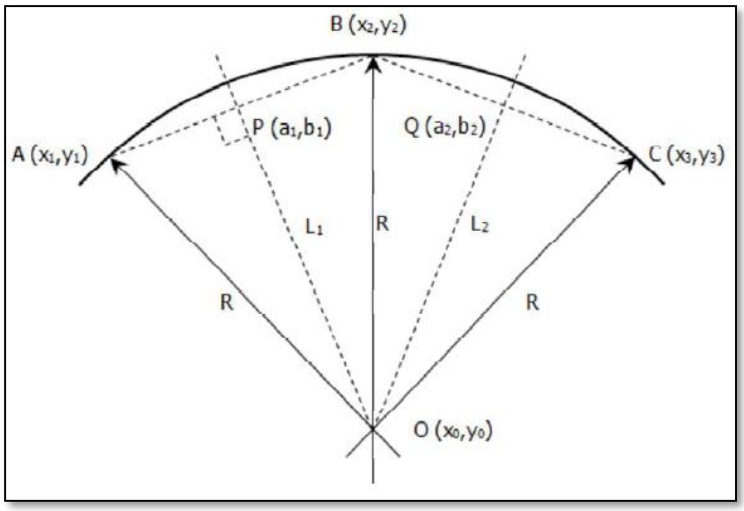

Figure A.1 Three reference points on curved line or beam.

The center of the curvature is represented by point O with coordinates (x, y). Using the co-ordinates of points A and B the slope and center point of line AB can be defined as

Slope of Line AB,

$$S_{AB} = \frac{y_2 - y_1}{x_2 - x_1}$$

Center Point P,

$$P_{(a_1,b_1)} = \left(\frac{x_1 + x_2}{2}, \frac{y_1 + y_2}{2}\right)$$

The equation of the line L1, which is perpendicular to line AB at point P can be expressed as.

$$S_{L1}x - y = S_{L1}a_1 - b_1$$

Where,

$$S_{L1} = -\frac{1}{Slope\ of\ line\ AB} = -\frac{1}{S_{AB}}$$

Similarly, using the same procedure the equation of line L2, perpendicular to line BC at point Q, can be expressed as.

$$S_{L1}x - y = S_{L1}a_1 - b_1$$

Where,

$$S_{L2} = -\frac{1}{Slope\ of\ line\ BC} = -\frac{1}{S_{BC}}$$

$$N_{(a_2,b_2)} = \left(\frac{x_2 + x_3}{2}, \frac{y_2 + y_3}{2}\right)$$

Line L1 and L2 intersect at the center of the curve and the coordinates of point O can be obtained by solving the equation of lines L1 and L2. The coordinates of center O can be expressed as.

$$x_0 = \frac{S_{L1}a_1 - S_{L2}a_2 - b_1 + b_2}{S_{L1} - S_{L2}}$$

$$y_0 = \frac{S_{L1}S_{L2}(a_1 - a_2) - S_{L1}b_1 + S_{L2}b_2}{S_{L1} - S_{L2}}$$

The distance from the center point O to any of the points A, B, and C is the radius of the curvature of the curve ABC. The radius of curvature can be expressed as,

$$R = \sqrt{(x_0 + x_1)^2 + (y_0 + y_1)^2} = \sqrt{(x_0 + x_2)^2 + (y_0 + y_2)^2} = \sqrt{(x_0 + x_3)^2 + (y_0 + y_3)^2}$$

$$\kappa = \frac{1}{R}$$

The above equations were programmed in excel and the curvatures were obtained by extracting displacement data from finite element analysis results.

Appendix B

ANSYS INPUT FILE FOR FINITE ELEMENT MODEL AND ANALYSIS

ANSYS INPUT CODE

Balanced and symmetric laminate, with mechanical and thermal loads and boundary conditions.

```
!Composite Z-Beam
!Initial analysis
finish
/clear,start
/FILNAM, Z beam
/TITLE, Comp z beam
/UNITS,BIN
/PREP7
!PArameters
tply=0.005
b1=0.5
b2=0.7
w=1.0
L=10
yc=0.0831
zc=-0.0732
!--------------------
!Material Propoerties
!--------------------
MP,EX,1,19.3e6
MP,EY,1,1.62e6
MP,EZ,1,1.62e6
MP,PRXY,1,0.28
MP,PRYZ,1,0.28
MP,PRXZ,1,0.28
MP,GXY,1,1.02e6
```

```
MP,GYZ,1,1.02e6
MP,GXZ,1,1.02e6
MP,CTEX,1,2.0e-6
MP,CTEY,1,15e-6
MP,CTEZ,1,15e-6
!-------------
!Element Types
!-------------
ET,1,SOLID185
ET,2,MASS21
ET,3,BEAM188
KEYOPT,3,1,0
KEYOPT,3,3,2
KEYOPT,1,3,1
KEYOPT,1,8,1
!-------------
! co-ordinates
!-------------
/triad,lbot
/VIEW,1,-1
/ANG,1
/REP,FAST
!------------
!Modeling
!------------
!Defining Keypoints
K,1,0,-0.49,0.5
K,2,0,0.01,0.5
k,3,0,0.01,0.54
```

```
k,4,0,-0.49,0.54
k,5,10,-0.49,0.5
k,6,10,0.01,0.5
k,7,10,0.01,0.54
k,8,10,-0.49,0.54
k,9,0,-0.01,0.5
k,10,0,-0.01,-0.5
k,11,0,0.01,-0.5
k,12,10,-0.01,0.5
k,13,10,-0.01,-0.5
k,14,10,0.01,-0.5
k,15,0,-0.01,-0.54
k,16,0,0.69,-0.54
k,17,0,0.69,-0.5
k,18,10,-0.01,-0.54
k,19,10,0.69,-0.54
k,20,10,0.69,-0.5
!Volumes
V,1,2,3,4,5,6,7,8
V,9,10,11,2,12,13,14,6
V,10,15,16,17,13,18,19,20
!------------
!Section Data
!------------
R,1
SECTYPE,13,BEAM,CSOLID,LINK
SECDATA,1,8,2
! Top flange
SECTYPE,1,SHELL,,TFlange
```

SECDATA,0.005,1,45,3

SECDATA,0.005,1,-45,3

SECDATA,0.005,1,0,3

SECDATA,0.005,1,90,3

SECDATA,0.005,1,90,3

SECDATA,0.005,1,0,3

SECDATA,0.005,1,-45,3

SECDATA,0.005,1,45,3

! Bottom flange

SECTYPE,2,SHELL,,BFlange

SECDATA,0.005,1,45,3

SECDATA,0.005,1,-45,3

SECDATA,0.005,1,0,3

SECDATA,0.005,1,90,3

SECDATA,0.005,1,90,3

SECDATA,0.005,1,0,3

SECDATA,0.005,1,-45,3

SECDATA,0.005,1,45,3

! Web

SECTYPE,3,SHELL,,Web

SECDATA,0.005,1,45,3

SECDATA,0.005,1,-45,3

SECDATA,0.005,1,-45,3

SECDATA,0.005,1,45,3

!Local co-ordinate sys

csys,0

Local,11,0,0,0,0,0,-90,0

csys,0

```
!-------
!Meshing
!-------
!orientation
VEORIENT,1,LINE,12
VEORIENT,2,LINE,20
VEORIENT,3,LINE,32
LSEL,S,LENGTH,,L
LESIZE,ALL,0.08,,,
LSEL,S,LENGTH,,4*tply
LESIZE,ALL,tply,,,
LSEL,S,LENGTH,,w
LESIZE,ALL,0.01,,,
LSEL,S,LENGTH,,b1
LESIZE,ALL,0.025,,,
LSEL,S,LENGTH,,b2
LESIZE,ALL,0.025,,,
LSEL,S,LENGTH,,tply
LESIZE,ALL,,,1
!Mesh attributes
VSEL,S,volu,,1
VATT,1,1,1,0,1
VSEL,S,volu,,2
VATT,1,1,1,11,3
VSEL,S,volu,,3
VATT,1,1,1,0,1
ALLSEL
VMESH,ALL
save,Z_BAlSyM_TEMP,db
```

```
!----------------------------------------
!Analysis Specific modeling and conditions
!----------------------------------------
!-----------------
!Thermal Analysis
!-----------------
/PREP7
TOFFSt,460
MP,REFT,1,0
SELTOL,1e-6
!Centroidal keypoints
csys,0
numstr,kp,300
k,,0,0.yc,zc
KSEL,S,KP,,300
KATT,1,1,2,0
KMESH,ALL
csys,0
k,400,l,yc,zc
KSEL,S,KP,,400
KATT,1,1,2,0
KMESH,ALL
nsel,s,,,88580
d,all,uy,0
d,all,uz,0
nsel,s,loc,x,l
CERIG,88580,all,UXYZ
```

```
!BC at origin
nsel,s,,,88579
D,all,all,0
nsel,s,loc,x,0
CERIG,88579,all,all
vsel,s,volu,,1
!applied in GUI
MPTEMP,1,0
UIMP,1,REFT,,,0
!Solution
ALLSEL
/SOLU
SOLVE
!-------------------
Mechanical Analysis
!-------------------
/prep7
SELTOL,1e-6
!Moment beam
k,400,L+0.01,yc,zc
k,401,L-0.01,yc,zc
l,400,401
lsel,s,LINE,,35
LESIZE,35,,,4
LATT,1,1,3,,,,13
LMESH,ALL
!Force on the centroidal node
nsel,s,,,88581
F,all,Fz,5
```

```
nsel,s,,88580
F,all,Fz,-5
!Connecting slave nodes to centroid node
NSEL,S,LOC,X,10
CERIG,88583,all,all
!BC at origin
nsel,s,,88579
D,all,all,0
nsel,s,loc,x,0
CERIG,88579,all,all
!Solution
ALLSEL
/SOLU
SOLVE
!----------------------
!Thermal--->Mechanical
!----------------------
/prep7
SELTOL,1e-6
!Force on the centroidal node
nsel,s,,88581
F,all,Fz,1878.5
F,all,Fy,901.5
nsel,s,,88580
F,all,Fz,-1878.5
F,all,Fy,-901.5
```

```
!Connecting slave nodes to centroid node
NSEL,S,LOC,X,10
!RBE3,1,ALL,ALL
CERIG,88583,all,all
!BC at origin
nsel,s,,,88579
D,all,all,0
nsel,s,loc,x,0
CERIG,88579,all,all
!Solution
ALLSEL
/SOLU
SOLVE
!----------------
!Post processing
!----------------
!Axial Dispacment
!At location (l/2)
allsel
nsel,s,loc,x,l/2
nsel,r,loc,y,0
nsel,r,loc,z,0
!Bending displacements
!SET 1 at x,0,0
!At location (l/2.5)
allsel
nsel,s,loc,x,l/2.5
nsel,r,loc,y,0
nsel,r,loc,z,0
```

```
!At location (l/1.5)
nsel,s,loc,x,6.64
nsel,r,loc,y,0
nsel,r,loc,z,0
nplot
!At location (l/1.25)
nsel,s,loc,x,l/1.25
nsel,r,loc,y,0
nsel,r,loc,z,0
nplot
```

Appendix C

MATLAB CODE FOR ANALYTICAL SOLUTION

Mechanical Loading Case

The following code is for balanced and symmetric (case 1) for applied mechanical moment.

```
clear all
clc
E1=10e6;E2=10e6;
v12=0.3;
tp=0.005;
G12=3.7e6;
Iso= 10e6;
[S] =[1/E1 -v12/E1 0; -v12/E1 1/E2 0; 0 0 1/G12];
[Q]= inv(S);
% The laminate is (+-45,0,90)s
%Q Bar for 45 deg
theta=45*pi/180;
m=cos(-theta);
n=sin(-theta);
[Ts45]= [m^2 n^2 2*m*n; n^2 m^2 (-m*n*2); -m*n m*n (m^2-n^2)];
m=cos(theta);
n=sin(theta);
[Te45]=[m^2    n^2  m*n;
       n^2    m^2  -m*n;
       -2*m*n  2*m*n  m^2-n^2];
q_45=Ts45*Q*Te45;
 %Q Bar for -45
theta=-45*pi/180;
m=cos(-theta);
n=sin(-theta);
Tsn45= [m^2 n^2 2*m*n; n^2 m^2 (-m*n*2); -m*n m*n (m^2-n^2)];
m=cos(theta);
n=sin(theta);
Ten45=[m^2    n^2  m*n;
       n^2    m^2  -m*n;
       -2*m*n  2*m*n  m^2-n^2];
q_n45=Tsn45*Q*Ten45;
%Q Bar for 0 deg
   q_0=Q;
 %Q Bar for 90 deg
theta=pi/2;
m=cos(-theta);
n=sin(-theta);
[Ts90]=[m^2    n^2  2*m*n;
       n^2    m^2  -2*m*n;
       -m*n    m*n   m^2-n^2;];
m=cos(theta);
n=sin(theta);
Te90=[m^2    n^2  m*n;
       n^2    m^2  -m*n;
       -2*m*n  2*m*n  m^2-n^2];
   q_90=Ts90*Q*Te90;
   %[+-45/0/90]s
   h0=-4*tp;h1=-3*tp;h2=-2*tp;h3=-tp;h4=0;h5=tp;h6=2*tp;h7=3*tp;h8=4*tp;
   A= 2*(q_90*tp+q_0*tp+q_n45*tp+q_45*tp);
```

```
   B= (0.5)*(q_45*(h1^2-h0^2)+q_n45*(h2^2-h1^2)+q_0*(h3^2-h2^2)+q_90*(h4^2-
h3^2)+q_90*(h5^2-h4^2)+q_0*(h6^2-h5^2)+q_n45*(h7^2-h6^2)+q_45*(h8^2-h7^2));
   D=(1/3)*(q_45*(h1^3-h0^3)+q_n45*(h2^3-h1^3)+q_0*(h3^3-h2^3)+q_90*(h4^3-
h3^3)+q_90*(h5^3-h4^3)+q_0*(h6^3-h5^3)+q_n45*(h7^3-h6^3)+q_45*(h8^3-h7^3));
   ABD = [ A B; B D];
   abd = inv(ABD);
   a11= abd(1,1);b11= abd(1,4); b16= abd(1,6); d11= abd(4,4); d16= abd(4,6);
d66= abd(6,6);
   a= (a11-((b16^2)/d66)); b= (b11-((b16*d16)/d66)); d = (d11-((d16^2)/d66));
   abds= [ a b;b d];
   ABDS= inv(abds);
   Aff = ABDS(1,1);
   Bff= 0;
   Dff= ABDS(2,2);
% Calculating A matrices for web
   %[+-45]s
   hw0=-2*tp;hw1=-1*tp;hw2=0*tp;hw3=tp;hw4=2*tp;
   Aw= 2*(q_n45*tp+q_45*tp);
   Bw= (0.5)*(q_45*(hw1^2-hw0^2)+q_n45*(hw2^2-hw1^2)+q_n45*(hw3^2-
hw2^2)+q_45*(hw4^2-hw3^2));
   Dw=(1/3)*(q_45*(hw1^3-hw0^3)+q_n45*(hw2^3-hw1^3)+q_n45*(hw3^3-
hw2^3)+q_45*(hw4^3-hw3^3));
   ABDW= [Aw Bw; Bw Dw];
   abdw = inv(ABDW);
   a11w= abdw(1,1);b11w= abdw(1,4); b16w= abdw(1,6); d11w= abdw(4,4); d16w=
abdw(4,6); d66w= abdw(6,6);
   aw= (a11w-((b16w^2)/d66w)); bw= (b11w-((b16w*d16w)/d66w)); dw = (d11w-
((d16w^2)/d66w));
   abdsw= [ aw bw;bw dw];
   ABDSw= inv(abdsw);
   Aww = ABDSw(1,1);
   Bww = 0;
   Dww = ABDSw(2,2);
   % Centroid
   wf1=0.5;wf2=0.7;ww=1;
   hf1=0.04;hf2=0.04;hw=0.02;
   zcf1=(hf2+ww+(hf1/2));zcf2=(hf2/2);zcw=(hf2+(ww/2));
   ycf1=(wf1/2);ycf2=((wf1-hw)+(wf2/2));ycw=(wf1-(hw/2));
   Zc= (wf1*zcf1*Aff+ wf2*zcf2*Aff + ww*zcw*Aww)/(wf1*Aff+wf2*Aff+ww*Aww)
   Yc= (wf1*ycf1*Aff+ wf2*ycf2*Aff + ww*ycw*Aww)/(wf1*Aff+wf2*Aff+ww*Aww)
   y= Yc-wf1+hw/2
   z=-(hf2+ww/2-Zc)
   % Axial Stiffness of the Beam
   AxStiff= (wf1*Aff) + (wf2*Aff) + (ww*Aww)
   % Axial FEA

   % Stiffness
   yw= -y;
   zw= -z;
   yf1= -(y-(hw/2)+(wf1/2));
   yf2= ((wf2/2)-(hw/2)-y);
   zf1= (zw+(ww/2)+(hf1/2));
   zf2=-((ww/2)-zw+(hf2/2));
   Dx=
(wf1*Dff)+(wf1*Aff*(zf1^2))+(2*wf1*Bff*zf1)+(wf2*Dff)+(wf2*Aff*(zf2^2))+(2*wf
2*Bff*zf2)+(Aww*((zw^2)*ww+((ww^3)/12)))
```

```
   Dy= (Aff*(((yf1^2)*wf1)+ ((wf1^3)/12)))+(Aff*(((yf2^2)*wf2)+
((wf2^3)/12)))+(Dww*ww)+(Aww*(yw^2)*ww)
   Dxy= (wf1*(Aff*zf1)*yf1)+ (wf2*(Aff*zf2)*yf2)+ (Aww*zw*yw*ww)
   % Dxy cals
   Mz= 0.1;
   y=0.01;
   ex= 5.9059e-08 ;
   Dxyn= sqrt((Dx*Dy)-((Mz*Dx*y)/ex));
   % finding ex
   exx= (Mz*Dx*y)/(Dx*Dy-(Dxy^2));
   % Curvature
   mx= 0.1;
   kx = (mx*Dy)/(Dx*Dy-(Dxy^2))
   kz = (-mx*Dxy)/(Dx*Dy-(Dxy^2))

   my=0.1;
   kx_y = (-my*Dxy)/(Dx*Dy-(Dxy^2))
   kz_y = (my*Dx)/(Dx*Dy-(Dxy^2))

      % Stress in layers
   % Top flange
   Nx_f1 = ((Aff*zf1*kx)+(Aff*yf1*kz)+(0*kx));
   Mx_f1 = ((0*zf1*kx)+(0*yf1*kz)+(Dff*kx));
   Mxy_f1 = -(1/d66)*((b16)*Nx_f1+(d61)*Mx_f1);
   N_f1 = [Nx_f1; 0; 0];
   M_f1 = [Mx_f1; 0; Mxy_f1];
  STN = abd*[N_f1; M_f1];
  e_0 = [STN(1,1); STN(2,1); STN(3,1)]
  k = [STN(4,1); STN(5,1); STN(6,1)]
  % Stress
  %45
  exy_45= e_0+((4*tp)*k);
  STRxy_45= (q_45*exy_45)
  % -45
  exy_n45= e_0+((3*tp)*k);
  STRxy_n45 = (q_n45*exy_n45)
  % 0 top and bottom
  exy_0_top= e_0+((2*tp)*k);
  STRxy_0= (q_0*exy_0_top)
  % 90
   exy_90_top= e_0+((tp)*k);
  STRxy_90= (q_90*exy_90_top)
     %45
  exy_45u= e_0+((-4*tp)*k);
  STRxy_45u= (q_45*exy_45u)
  % -45
  exy_n45u= e_0+((-3*tp)*k);
  STRxy_n45u = (q_n45*exy_n45u)
  % 0 top and bottom
  exy_0_topu= e_0+((-2*tp)*k);
  STRxy_0u= (q_0*exy_0_topu)
  % 90
   exy_90_topu= e_0+((-tp)*k);
  STRxy_90u= (q_90*exy_90_topu)

   % Bottom flange
```

```
 Nx_f2 = ((Aff*zf2*kx)+(Aff*yf2*kz)+(0*kx));
 Mx_f2 = ((0*zf2*kx)+(0*yf2*kz)+(Dff*kx));
 N_f2 = [Nx_f2; 0; 0];
 M_f2 = [Mx_f2; 0; 0];
STN2 = abd*[N_f2; M_f2];
e_02 = [STN2(1,1); STN2(2,1); STN2(3,1)]
k2 = [STN2(4,1); STN2(5,1); STN2(6,1)]
% Stress
%45
exy_452= e_02+((4*tp)*k2);
STRxy_45_2= (q_45*exy_452)
% -45
exy_n452= e_02+((3*tp)*k2);
STRxy_n45_2 = (q_n45*exy_n452)
% 0 top and bottom
exy_0_top2= e_02+((2*tp)*k2);
STRxy_0_2= (q_0*exy_0_top2)
% 90
 exy_90_top2= e_02+((tp)*k2);
STRxy_90_2= (q_90*exy_90_top2)
   %45
exy_45u2= e_02+((-4*tp)*k2);
STRxy_45u_2= (q_45*exy_45u2)
% -45
exy_n45u2= e_02+((-3*tp)*k2);
STRxy_n45u_2 = (q_n45*exy_n45u2)
% 0 top and bottom
exy_0_topu2= e_02+((-2*tp)*k2);
STRxy_0u_2= (q_0*exy_0_topu2)
% 90
 exy_90_topu2= e_02+((-tp)*k2);
STRxy_90u_2= (q_90*exy_90_topu2)

% Web Stresses
   % Stress in layers
   % B term will be present in ubal case
% Web
 Nx_w = ((Aww*zw*kx)+(Aww*yw*kz)+(0*kx));
 Mx_w = ((0*zw*kx)+(0*yw*kz)+(Dww*kx));
 N_w = [Nx_w; 0; 0];
 M_w = [Mx_w; 0; 0];
STNw = abdw*[N_w; M_w];
e_0w = [STNw(1,1); STNw(2,1); STNw(3,1)]
kw = [STNw(4,1); STNw(5,1); STNw(6,1)]
% Stress
%45
exy_45w= e_0w+((2*tp)*kw);
STRxy_45w= (q_45*exy_45w)
% -45
exy_n45w= e_0w+((tp)*kw);
STRxy_n45w = (q_n45*exy_n45w)
   %45
exy_45uw= e_0w+((-tp)*kw);
STRxy_45uw= (q_45*exy_45uw)
% -45
exy_n45uw= e_0w+((-2*tp)*kw);
STRxy_n45uw = (q_n45*exy_n45uw)
```

Thermal Code

The following code is for thermal loading case 1.

```
clear all
E1=10e6;E2=10e6;
v12=0.3;
tp=0.005;
G12=3.7e6;
Nx = 00;
DT = 70;
DTB= 0;
M = [0; 0; 0];
N = [0; 0; 0];
   alp= [13e-6; 15e-6; 0];
[S] =[1/E1 -v12/E1 0; -v12/E1 1/E2 0; 0 0 1/G12];
[Q]= inv(S);
%Q Bar for 45 deg
theta=45*pi/180;
m=cos(-theta);
n=sin(-theta);
[Ts45]= [m^2 n^2 2*m*n; n^2 m^2 (-m*n*2); -m*n m*n (m^2-n^2)];
m=cos(theta);
n=sin(theta);
[Te45]=[m^2    n^2  m*n;
       n^2    m^2  -m*n;
       -2*m*n  2*m*n  m^2-n^2];
q_45=Ts45*Q*Te45;
%thrermal 45
m=cos(-theta);
n=sin(-theta);
T=[m^2    n^2  m*n;
       n^2    m^2  -m*n;
       -2*m*n  2*m*n  m^2-n^2];
alp45xy= T*alp;
Nt_45= q_45*(T*alp);
 %Q Bar for -45
theta=-45*pi/180;
m=cos(-theta);
n=sin(-theta);
Tsn45= [m^2 n^2 2*m*n; n^2 m^2 (-m*n*2); -m*n m*n (m^2-n^2)];
m=cos(theta);
n=sin(theta);
Ten45=[m^2    n^2  m*n;
       n^2    m^2  -m*n;
       -2*m*n  2*m*n  m^2-n^2];
q_n45=Tsn45*Q*Ten45;
%thrermal -45
m=cos(-theta);
n=sin(-theta);
T=[m^2    n^2  m*n;
       n^2    m^2  -m*n;
       -2*m*n  2*m*n  m^2-n^2];
alpn45xy= T*alp;
```

```
Nt_n45= q_n45*(T*alp);
%Q Bar for 0 deg
theta=0;
   q_0=Q;
   %threrмal 0
m=cos(-theta);
n=sin(-theta);
T=[m^2    n^2  m*n;
       n^2    m^2  -m*n;
       -2*m*n  2*m*n  m^2-n^2];
alp0xy= T*alp;
Nt_0= q_0*(T*alp);
 %Q Bar for 90 deg
theta=pi/2;
m=cos(-theta);
n=sin(-theta);
[Ts90]=[m^2    n^2  2*m*n;
       n^2    m^2  -2*m*n;
       -m*n    m*n   m^2-n^2;];
m=cos(theta);
n=sin(theta);
Te90=[m^2    n^2  m*n;
       n^2    m^2  -m*n;
       -2*m*n  2*m*n  m^2-n^2];
   q_90=Ts90*Q*Te90;
   %threrмal 90
m=cos(-theta);
n=sin(-theta);
T=[m^2    n^2  m*n;
       n^2    m^2  -m*n;
       -2*m*n  2*m*n  m^2-n^2];
alp90xy= T*alp;
Nt_90= q_90*(T*alp);
   %[+-45/0/90]s
   h0=-4*tp;h1=-3*tp;h2=-2*tp;h3=-tp;h4=0;h5=tp;h6=2*tp;h7=3*tp;h8=4*tp;
   A= 2*(q_90*tp+q_0*tp+q_n45*tp+q_45*tp);
   B= (0.5)*(q_45*(h1^2-h0^2)+q_n45*(h2^2-h1^2)+q_0*(h3^2-h2^2)+q_90*(h4^2-
h3^2)+q_90*(h5^2-h4^2)+q_0*(h6^2-h5^2)+q_n45*(h7^2-h6^2)+q_45*(h8^2-h7^2));
   D=(1/3)*(q_45*(h1^3-h0^3)+q_n45*(h2^3-h1^3)+q_0*(h3^3-h2^3)+q_90*(h4^3-
h3^3)+q_90*(h5^3-h4^3)+q_0*(h6^3-h5^3)+q_n45*(h7^3-h6^3)+q_45*(h8^3-h7^3));
   ABD = [ A B; B D];
   abd = inv(ABD);
   a11= abd(1,1);b11= abd(1,4); b16= abd(1,6); d11= abd(4,4); d16= abd(4,6);
d66= abd(6,6);
   a= (a11-((b16^2)/d66)); b= (b11-((b16*d16)/d66)); d = (d11-((d16^2)/d66));
   abds= [ a b;b d];
   ABDS= inv(abds);
   Aff = ABDS(1,1);
   Bff= 0;
   Dff= ABDS(2,2);
   NT=
(DT*(Nt_90*tp+Nt_0*tp+Nt_n45*tp+Nt_45*tp+Nt_90*tp+Nt_0*tp+Nt_n45*tp+Nt_45*tp)
)
   N_bar = N+NT;
   Nxtf1= NT(1,1);
   % thermal bottom flange
```

```
     NTB=
(DTB*(Nt_90*tp+Nt_0*tp+Nt_n45*tp+Nt_45*tp+Nt_90*tp+Nt_0*tp+Nt_n45*tp+Nt_45*tp
));
   N_bar_B = N+NTB;
   Nxtf2= NTB(1,1);

   % Calculating A matrices for web
   %[+-45]s
   hw0=-2*tp;hw1=-1*tp;hw2=0*tp;hw3=tp;hw4=2*tp;
   Aw= 2*(q_n45*tp+q_45*tp);
   Bw= (0.5)*(q_45*(hw1^2-hw0^2)+q_n45*(hw2^2-hw1^2)+q_n45*(hw3^2-
hw2^2)+q_45*(hw4^2-hw3^2));
   Dw=(1/3)*(q_45*(hw1^3-hw0^3)+q_n45*(hw2^3-hw1^3)+q_n45*(hw3^3-
hw2^3)+q_45*(hw4^3-hw3^3));
   ABDW= [Aw Bw; Bw Dw];
   abdw = inv(ABDW);
   a11w= abdw(1,1);b11w= abdw(1,4); b16w= abdw(1,6); d11w= abdw(4,4); d16w=
abdw(4,6); d66w= abdw(6,6);
   aw= (a11w-((b16w^2)/d66w)); bw= (b11w-((b16w*d16w)/d66w)); dw = (d11w-
((d16w^2)/d66w));
   abdsw= [ aw bw;bw dw];
   ABDSw= inv(abdsw);
   Aww = ABDSw(1,1);
   Bww = 0;
   Dww = ABDSw(2,2);
   NTw= (DT*(Nt_n45*tp+Nt_45*tp+Nt_n45*tp+Nt_45*tp));
   Nxtw= NTw(1,1);
   %moments
      % Centroid
   wf1=0.5;wf2=0.7;ww=1;
   hf1=0.04;hf2=0.04;hw=0.02;
   zcf1=(hf2+ww+(hf1/2));zcf2=(hf2/2);zcw=(hf2+(ww/2));
   ycf1=(wf1/2);ycf2=((wf1-hw)+(wf2/2));ycw=(wf1-(hw/2));
   Zc= (wf1*zcf1*Aff+ wf2*zcf2*Aff + ww*zcw*Aww)/(wf1*Aff+wf2*Aff+ww*Aww);
   Yc= (wf1*ycf1*Aff+ wf2*ycf2*Aff + ww*ycw*Aww)/(wf1*Aff+wf2*Aff+ww*Aww);
   y= Yc-wf1+hw/2;
   z=-(hf2+ww/2-Zc);
   % Stiffness
   yw= -y;
   zw= -z;
   yf1= -(y-(hw/2)+(wf1/2));
   yf2= ((wf2/2)-(hw/2)-y);
   zf1= (zw+(ww/2)+(hf1/2));
   zf2=-((ww/2)-zw+(hf2/2));
   Dx=
(wf1*Dff)+(wf1*Aff*(zf1^2))+(2*wf1*Bff*zf1)+(wf2*Dff)+(wf2*Aff*(zf2^2))+(2*wf
2*Bff*zf2)+(Aww*((zw^2)*ww+((ww^3)/12)));
   Dy= (Aff*(((yf1^2)*wf1)+ ((wf1^3)/12)))+(Aff*(((yf2^2)*wf2)+
((wf2^3)/12)))+(Dww*ww)+(Aww*(yw^2)*ww);
   Dxy= (wf1*(Aff*zf1)*yf1)+ (wf2*(Aff*zf2)*yf2);
   NxT= Nxtf1*wf1 + Nxtf1*wf2 + Nxtw*ww;
   My= -(Nxtf1*yf1*wf1)+(Nxtf2*yf2*wf2*0)
   Mx= -(Nxtf1*zf1*wf1)+(Nxtf2*yf2*wf2*0)
   % Curvature
   mx= My;
   my= Mx;
   kx = ((mx*Dy)-(my*Dxy))/(Dx*Dy-(Dxy^2))
```

```
 ky = ((-mx*Dxy)+(my*Dx))/(Dx*Dy-(Dxy^2))
 % Stress in layers
 % Top flange
 Nx_f1 = ((Aff*zf1*kx)+(Aff*yf1*ky)+(0*kx));
 Mx_f1 = ((0*zf1*kx)+(0*yf1*ky)+(Dff*kx));
 Mxy_f1 = -(1/d66)*((b16)*Nx_f1+(d61)*Mx_f1);
 N_f1 = [Nx_f1; 0; 0];
 M_f1 = [Mx_f1; 0; Mxy_f1];
STN = abd*[N_f1; M_f1];
e_0 = [STN(1,1); STN(2,1); STN(3,1)]
k = [STN(4,1); STN(5,1); STN(6,1)]
% Stress
%45
exy_45= e_0+((4*tp)*k);
STRxy_45= (q_45*exy_45)
% -45
exy_n45= e_0+((3*tp)*k);
STRxy_n45 = (q_n45*exy_n45)
% 0 top and bottom
exy_0_top= e_0+((2*tp)*k);
STRxy_0= (q_0*exy_0_top)
% 90
 exy_90_top= e_0+((tp)*k);
STRxy_90= (q_90*exy_90_top)
   %45
exy_45u= e_0+((-4*tp)*k);
STRxy_45u= (q_45*exy_45u)
% -45
exy_n45u= e_0+((-3*tp)*k);
STRxy_n45u = (q_n45*exy_n45u)
% 0 top and bottom
exy_0_topu= e_0+((-2*tp)*k);
STRxy_0u= (q_0*exy_0_topu)
% 90
 exy_90_topu= e_0+((-tp)*k);
STRxy_90u= (q_90*exy_90_topu)

 % Bottom flange
 Nx_f2 = ((Aff*zf2*kx)+(Aff*yf2*ky)+(0*kx));
 Mx_f2 = ((0*zf2*kx)+(0*yf2*ky)+(Dff*kx));
 N_f2 = [Nx_f2; 0; 0];
 M_f2 = [Mx_f2; 0; 0];
STN2 = abd*[N_f2; M_f2];
e_02 = [STN2(1,1); STN2(2,1); STN2(3,1)]
k2 = [STN2(4,1); STN2(5,1); STN2(6,1)]
% Stress
%45
exy_452= e_02+((4*tp)*k2);
STRxy_45_2= (q_45*exy_452)
% -45
exy_n452= e_02+((3*tp)*k2);
STRxy_n45_2 = (q_n45*exy_n452)
% 0 top and bottom
exy_0_top2= e_02+((2*tp)*k2);
STRxy_0_2= (q_0*exy_0_top2)
% 90
 exy_90_top2= e_02+((tp)*k2);
```

```
STRxy_90_2= (q_90*exy_90_top2)
   %45
exy_45u2= e_02+((-4*tp)*k2);
STRxy_45u_2= (q_45*exy_45u2)
% -45
exy_n45u2= e_02+((-3*tp)*k2);
STRxy_n45u_2 = (q_n45*exy_n45u2)
% 0 top and bottom
exy_0_topu2= e_02+((-2*tp)*k2);
STRxy_0u_2= (q_0*exy_0_topu2)
% 90
 exy_90_topu2= e_02+((-tp)*k2);
STRxy_90u_2= (q_90*exy_90_topu2)

% Web Stresses
   % Stress in layers
   % B term will be present in ubal case
% Web
 Nx_w = ((Aww*zw*kx)+(Aww*yw*ky)+(0*kx));
 Mx_w = ((0*zw*kx)+(0*yw*ky)+(Dww*kx));
 N_w = [Nx_w; 0; 0];
 M_w = [Mx_w; 0; 0];
STNw = abdw*[N_w; M_w];
e_0w = [STNw(1,1); STNw(2,1); STNw(3,1)]
kw = [STNw(4,1); STNw(5,1); STNw(6,1)]
% Stress
%45
exy_45w= e_0w+((2*tp)*kw);
STRxy_45w= (q_45*exy_45w)
% -45
exy_n45w= e_0w+((tp)*kw);
STRxy_n45w = (q_n45*exy_n45w)
   %45
exy_45uw= e_0w+((-tp)*kw);
STRxy_45uw= (q_45*exy_45uw)
% -45
exy_n45uw= e_0w+((-2*tp)*kw);
STRxy_n45uw = (q_n45*exy_n45uw)
```

REFERENCES

[1] Craddock, J. N., and Yen, S. C., "The bending stiffness of laminated composite material Ibeams",
Composite Engineering Vol. 3 No.11, 1993, pp. 1025–1038.

[2] Lee, J., "Center of Gravity and Shear Center of Thin Walled Open Section Composite Beams", Composite Structures, Vol. 52, 2011, pp 255-260.

[3] Parambil, J.C., Chan, W.S., Lawrence, K.L., Sanghai, V., "Stress Analysis of Composite I-Beam by Non –Conventional Method", Proceedings of the American Society for Composites 26th Technical Conference, paper No.1027, 2011.

[4] Sanghai, V. and Chan, W.S., "Torsional Analysis of a Composite I-Beam", Proceedings of the American Society for Composites 28th Technical Conference, 2013.

[5] Gupta R. K., Venkatesh A. and Rao K. P., "Finite Element Analysis of Laminated Anisotropic Thin-Walled Open-Section Beams", Department of Aerospace Engineering, Indian Institute of Science, 1985.

[6] Ramesh Chandra and Inderjit Chopra, "Experimental and Theoretical Analysis of Composite I-Beams with Elastic Couplings", AIAA Journal, Vol. 29, NO. 12, December 1991, pp 2197-2206

[7] J. C .Massa and Ever J. Barbero," A strength of Material Formulation for thin walled composite beams with Torsion", Journal of Composite Materials, Vol. 32, No 17/1998 pp 1560-1594.

[8] Jung, S. N., and Lee, J. Y., "Closed-form analysis of thin-walled composite I-beams considering non-classical effects.", Composite Structures Vol.60, 2003, pp. 9–17.

[9] Chan, W. S., and Chou, C. J., "Effects of Delamination and Ply Fiber Waviness on Effective Axial and Bending Stiffnesses in Composite Laminates", Composite Structures, Vol. 30, pp. 299-306.

[10] Chan, W. S. and Demirhan, K. C., "A Simple Closed Form Solution of Bending Stiffness of Laminated Composite Tubes", Journal of Reinforced Plastics and Composites, Vol.19 No. 3, 2001.

[11] Rojas, C. A., Syed, K. A., and Chan, W. S., "Structural Response of Composite Truss Beams", The 22nd Annual Technical Conference of American Society of Composites, Sept. 2007.

[12] Syed, K.A. and Chan, W.S., "Analysis of Hat-Sectioned Reinforced Composite Beams", Proceedings of American Society of Composites, Sept. 2006.

[13] Rios, G., "A Unified Analysis of Stiffener Reinforced Composite Beams with Arbitrary Cross-Section", The University of Texas at Arlington, 2009.

[14] Chan, W.S. Lecture Notes of Fundamentals of Composites, Department of Mechanical and Aerospace Engineering, University of Texas at Arlington, fall 2014.

[15] Megson, An Introduction to Aircraft Structure Analysis, Chapter 15, pp. 466-468.

[16] Wang. J. S. and Chan, W. S., "Effects of Defects on the Buckling Loads of Rodpack Laminates," Journal of American Helicopter Society, July 2000.